

Structuring and Shaping of Mechanically Robust and Functional Hydrogels toward Wearable and Implantable Applications

Xiao-Qiao Wang,* An-Quan Xie, Pengle Cao, Jian Yang, Wei Li Ong, Ke-Qin Zhang,* and Ghim Wei Ho*

Hydrogels possess unique features such as softness, wetness, responsiveness, and biocompatibility, making them highly suitable for biointegrated applications that have close interactions with living organisms. However, conventional man-made hydrogels are usually soft and brittle, making them inferior to the mechanically robust biological hydrogels. To ensure reliable and durable operation of biointegrated wearable and implantable devices, mechanical matching and shape adaptivity of hydrogels to tissues and organs are essential. Recent advances in polymer science and processing technologies have enabled mechanical engineering and shaping of hydrogels for various biointegrated applications. In this review, polymer network structuring strategies at micro/nanoscales for toughening hydrogels are summarized, and representative mechanical functionalities that exist in biological materials but are not easily achieved in synthetic hydrogels are further discussed. Three categories of processing technologies, namely, 3D printing, spinning, and coating for fabrication of tough hydrogel constructs with complex shapes are reviewed, and the corresponding hydrogel toughening strategies are also highlighted. These developments enable adaptive fabrication of mechanically robust and functional hydrogel devices, and promote application of hydrogels in the fields of biomedical engineering, bioelectronics, and soft robotics.

and liquid components endows hydrogels with unique features such as softness, wetness, responsiveness, tunable mechanical properties, permeability, and biocompatibility. Besides, hydrogels are an integral part of living organisms, and are the major components of animal bodies, constituting many of the tissues and organs.^[2,3] Therefore, hydrogels are especially suitable for application in wearable and implantable devices, including tissue scaffolds,^[3] tissue adhesives,^[4,5] on-skin electronics,^[6,7] implanted electronics,^[8,9] artificial muscles,^[10] and wearable and medical robots.^[11] In these biointegrated applications, hydrogels can directly interact with human bodies.

Mechanical properties of biological hydrogels are crucial for maintaining some of the key functionalities of human bodies.^[2] For example, skin is soft to touch but can rapidly stiffen under large strain to prevent injury from overloading of tensile strains,^[12] and also autonomously heal from wounds to restore its original mechanical properties,^[13] representing an important defense and healing capability of human bodies. Articular cartilage, a dense

connective tissue, has fracture energy of 10^2 – 10^3 J m⁻², and can absorb mechanical loads between bones to protect joints from damage in daily activities.^[14] Tendons are connective tissues attaching muscle to bone with fracture energy of 20–30 kJ m⁻².^[15] They experience relatively high stresses and act as biological springs that can stretch elastically, thus storing and releasing energy during locomotion and regulating mechanical performance of muscles. To achieve mechanical matching with those biological components, hydrogels are required to be tough and rich in mechanical functionalities, so as to maintain stable operation of biointegrated hydrogel devices. For example, a tissue engineering hydrogel scaffold works as a template for tissue regeneration by providing cells with chemical cues and mechanical supports.^[16] It has to be mechanically robust and possess the desired stiffness for cell differentiation and function. An on-skin soft hydrogel electronic device usually needs to be tough and stretchable, capable of bearing repetitive deformation, but it also has to be elastic, preventing hysteresis and degeneration of mechanical performance under cyclic stretching.^[17,18]

1. Introduction

Hydrogels are hydrophilic crosslinked polymer networks that can absorb large amounts of water.^[1,2] The coexistence of solid

X.-Q. Wang, A.-Q. Xie, P. Cao, J. Yang, K.-Q. Zhang
 National Engineering Laboratory for Modern Silk
 College of Textile and Clothing Engineering
 Soochow University
 Suzhou 215123, China
 E-mail: xqwang@suda.edu.cn; kqzhang@suda.edu.cn

W. L. Ong, G. W. Ho
 Department of Electrical and Computer Engineering
 National University of Singapore
 4 Engineering Drive 3, Singapore 117583, Singapore
 E-mail: elehw@nus.edu.sg

 The ORCID identification number(s) for the author(s) of this article can be found under <https://doi.org/10.1002/adma.202309952>

DOI: 10.1002/adma.202309952

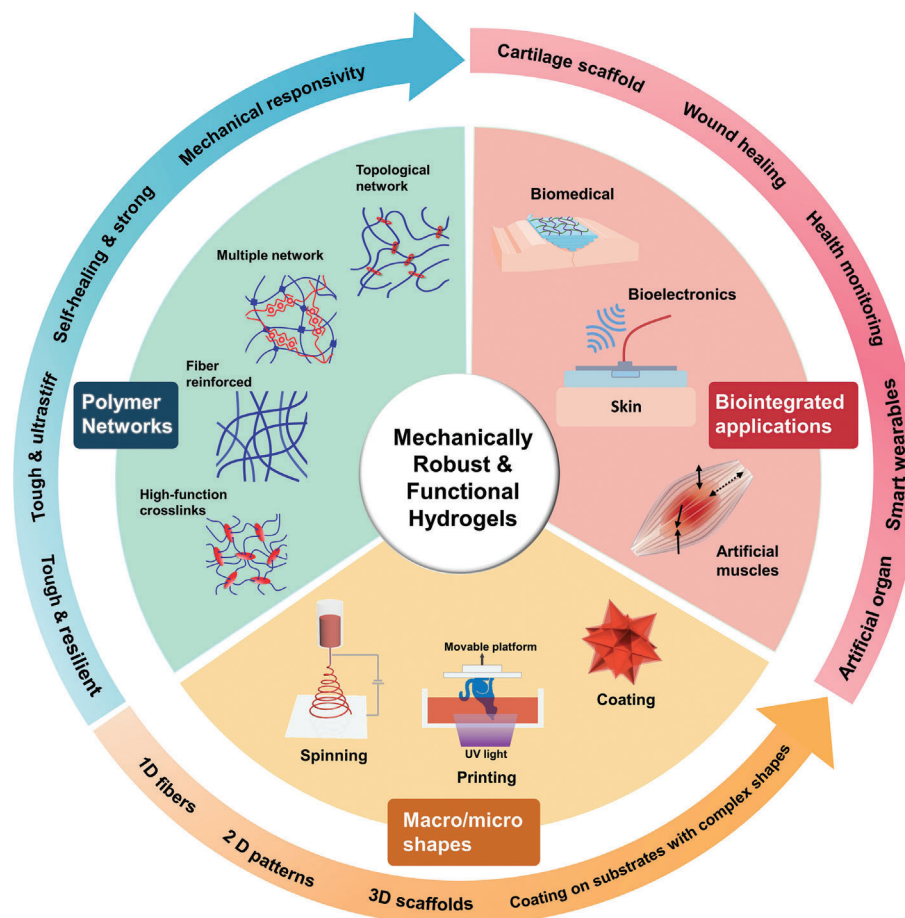


Figure 1. Overview of polymer network structuring strategies and shaping technologies for the fabrication of mechanically robust hydrogels and devices toward various biointegrated applications.

An artificial hydrogel muscle that performs stimulus-responsive actuation is expected to be mechanically strong and generate large deliverable force and high work density to drive movements of body parts.^[10,19,20] Conventional synthetic hydrogels composed of a single network of hydrophilic polymers are soft and brittle, and they usually fail at a tensile stress less than sub-MPa and strain less than 100%.^[21] To date, significant efforts have been made to improve mechanical strength of hydrogels, and the progress on mechanically robust hydrogels, such as tough hydrogels based on multimechanism design,^[22] tough hydrogels from noncovalent interactions,^[23] and hydrogels with extreme mechanical properties from unconventional polymer networks^[2] have been reviewed. However, an overview of various polymer networks used for making mechanically robust and functional hydrogels, and their adaptive shaping for wearable and implantable applications, is still absent in the field.

In this review, structuring and shaping of mechanically robust and functional hydrogels toward biointegrated applications are discussed (Figure 1). We first briefly summarize and analyze polymer network structuring principles for improving mechanical performance of hydrogels. Then we go into a deep discussion of the emerging special polymer networks that endow hydrogels with various unusual mechanical functionalities, which

are desirable for wearable and implantable applications. Next, we review three categories of representative prototyping techniques including 3D printing, spinning, and coating, which enable macro/microscale shaping of tough hydrogels and creation of various mechanically robust hydrogel constructs. Their processing compatibility with hydrogel toughening mechanisms is also discussed. Lastly, we review the most recent progress of functional hydrogel devices in biomedical, bioelectronic, and robotic applications, and conclude with a perspective discussion on the remaining challenges and opportunities. By highlighting these strategies of polymer network structuring and shaping for tough hydrogels and devices, we hope to provide new insights in understanding the key roles of mechanically functional hydrogels in biointegrated applications, and give materials and engineering guidelines for devising wearable and implantable hydrogel devices.

2. Polymer Structural Design and Mechanical Engineering of Hydrogels

Mechanical performance of hydrogels mainly depends on the polymer network structures. Conventional hydrogels composed of polymer networks crosslinked by permanent covalent bonds

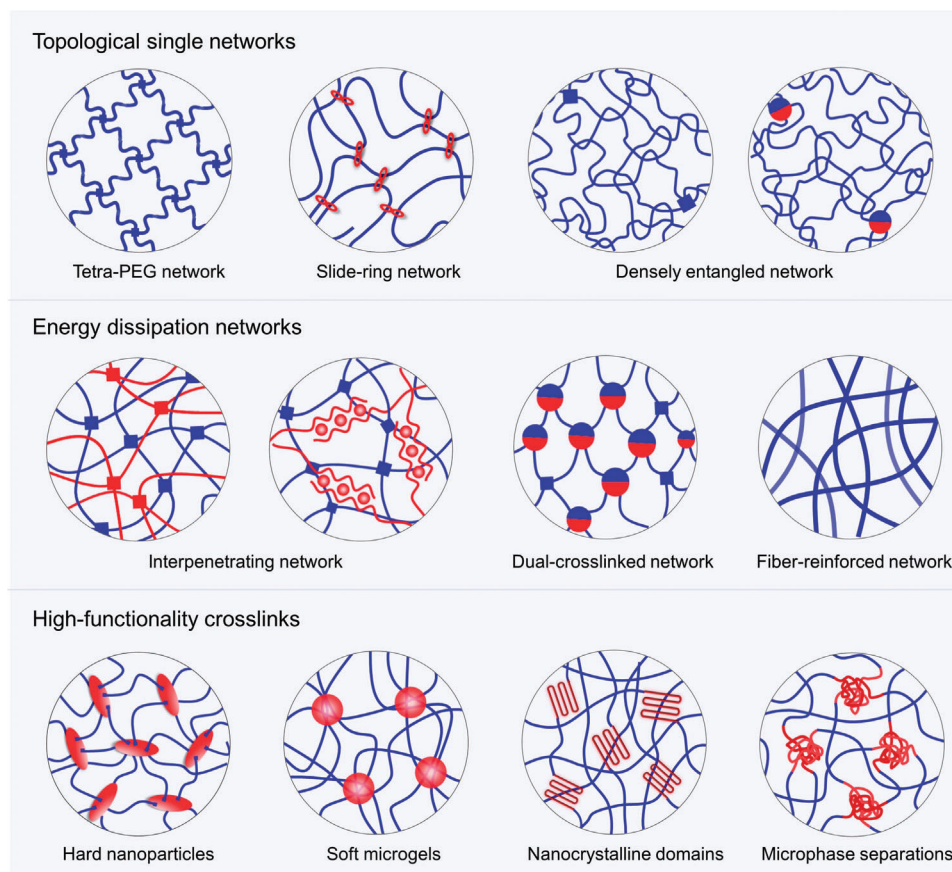


Figure 2. Schematic illustration of polymer network architectures used to make tough hydrogels including topological single networks with high homogeneity, energy dissipation networks, and polymer networks with high-functionality crosslinks.

are brittle. The poor mechanical behavior can be attributed to several factors such as i) irregular distribution of crosslinking points, ii) different polymer chain lengths between the crosslinking points, iii) high water content, and/or iv) lack of energy dissipation to prevent crack propagation.^[21,24] Owing to the difference in reactivity between monomers and crosslinkers, more densely crosslinked microgels are formed first and then connected by large chains, leading to irregular distribution of crosslinking points. At the same time, it is difficult to ensure that the polymer chains are crosslinked at equal intervals when using crosslinkers, thereby resulting in a wide range of chain lengths. The heterogeneous polymer structures produce defects that act as stress concentrators, and stress concentration happens easily in the shorter chains, inducing the formation of microcracks. Moreover, a lack of significant energy dissipation systems in the process zone^[22] will cause the microcracks to propagate easily among the networks, eventually leading to mechanical failure of hydrogels. Besides, high water content will also decrease crosslinking density, thereby reducing fracture energy as fewer chains are broken for crack propagation. Considering these critical influencing factors, there are two main approaches in the design of polymer networks for tough hydrogels: i) reducing heterogeneities in polymer networks by forming homogeneous hydrogels to evenly distribute mechanical load over a significant fraction of polymer chains, thereby presenting fewer sites for the formation of microcracks;

and ii) introducing one or more strategies to dissipate energy in order to resist crack propagation. In this section, various polymer network structuring methods for constructing tough hydrogels based mainly on these two approaches are evaluated and analyzed, which are of great importance for supporting practical applications of hydrogel devices. The engineering of remarkable mechanical functionalities desired for biointegrated applications are the primary focus, which are discussed in further detail.

2.1. Polymer Network Strategies for Toughening Hydrogels

As discussed above, the general principle for making tough hydrogels is to increase homogeneities of polymer networks to reduce stress concentration and microcrack formation in the short chains, and/or to introduce energy dissipation systems that prevent crack propagation. Accordingly, polymer networks based on such toughening mechanisms are rationally categorized and discussed (**Figure 2**), and mechanical performance of representative hydrogels are summarized in **Table 1**.

2.1.1. Homogenizing Polymer Networks to Enhance Toughness

Traditional hydrogels suffer from uneven polymer network structures, generally induced by poorly controlled crosslinking

Table 1. Typical examples of tough hydrogels with high mechanical performance based on different network structures

Material strategies		Tensile strain [%]	Tensile strength [MPa]	Young's modulus [MPa]	Toughness [MJ m ⁻³]	Fracture energy [J m ⁻²]	Water content [w%]	Strain rate [s ⁻¹]	Refs.	
Natural materials	Excised human back skin	54	21.6	83.3	3.6	–	70	0.012	[145]	
	Articular cartilage	80	10–30	10–100	–	800–1800	70	0.042	[146,147]	
	Tendon	10–30	40–70	120–660	–	20 000–30 000	70	–	[15,148]	
	Major ampullate silk	20–60	710–1650	1200–11500	100–360	–	–	–	[149]	
Topological single networks	Tetra-PEG hydrogel	700	0.2	–	–	–	90	–	[37]	
	Slide-ring hydrogel	1200–1400	1.5–5.5	–	6.6–22	2900–3600	–	0.125	[17]	
	Highly entangled PAAm	1000	0.3	–	1.6	–	75	–	[48]	
	Highly entangled PEG	590	0.46	0.68	0.85	1575	80	0.04	[50]	
	Highly entangled triblock copolymer	750	0.12	0.01	–	3000	95	0.05	[55]	
	Highly entangled PANa	5–2530	1–50	0.24–2050	1.7–17.8	–	10–40	0.033	[54]	
Interpenetrating networks	PAMPS–PAAm	1000–2000	1–10	0.1–1.0	–	100–1000	90	0.139	[21]	
	PAAm–alginate	1600	0.17	0.06	–	8700	86	0.033	[57]	
	B-DN	600	10	2	–	3000	42	0.14	[62]	
	Agar–HPAAm	5260	0.27	0.11	9.4	1000	–	0.028	[63]	
	PDGI–PAAm	2200	0.6	–	5.0	–	94	0.278	[64]	
	PAAm–CS	450	2.1	0.3	–	12 900	–	0.024	[66]	
	PVA–PAAm	200	2.5	5.0	–	14 000	62	0.033	[67]	
	C1/20-SM3 gel	550	13	21	55.5	23 400	30	0.083	[68]	
Chemically and physically dual-crosslinked networks	Poly(AAm-co-AAc)–Fe ³⁺	750	5.9	1.7	27.8	–	60–70	0.042	[78]	
	Poly(AAm-co-AMPS)–Zr ⁴⁺	215–1250	2.1–11.6	0.4–28.5	–	200–24200	33–74	0.139	[79]	
	Poly(VI-co-MAAc)	40–330	1.3–5.4	20–170	–	600–4500	50–60	0.139	[81]	
	DC cellulose	80	2.7	2	0.85	–	87	0.0007	[82]	
Physically dual-crosslinked networks	Ch–PAAc–Ag ⁺ gel	610	24.0	35	84.7	–	33	–	[85]	
	DP-hydrogel	1000	6.8	8	53	–	50	0.028	[86]	
	Poly(AAm-co-AAc)–Clay–Fe ³⁺	2110	3.5	0.64	49.1	–	–	0.083	[87]	
	PAAc–MXene–Fe ³⁺	3080	3.3	–	62.4	–	80	0.167	[88]	
	d-Gel	74–210	13.7–56.2	25.7–152	20–40	–	45	–	[89]	
Fiber reinforced networks	DCC–alginate	50–200	20	200–370	7–30	–	56	0.017	[90]	
	Wood hydrogel	15	36	310	–	–	65	–	[91]	
	ANF–PVA	70–325	1.4–5.0	1.9–9.1	–	2300–9200	70–92	0.002	[92]	
	Mechanically trained PVA	260	5.2	0.2	–	1250	84	0.3	[93]	
	Annealed BC–PVA	10	50	500	–	–	50	0.026	[94]	
	HA–PVA	1400–2900	11.5–23.5	–	175–210	131 000–170 000	70–95	–	[95]	
	Fiber-reinforced agarose	22–27	75–85	325–400	–	–	–	0.0016	[99]	
	PDMS fiber–PAAm	100	0.18–0.25	0.2	–	4100	60–70	0.02	[100]	
	PA–GF hydrogel composite	–	–	606	–	250 000	32	0.139	[101]	
		Nanoclay crosslinked PNIPAM	1030	0.3	0.026	–	–	90	0.048	[105]
Rigid nanoparticle based crosslinks	SiO ₂ -g-PBA crosslinked poly(AAm-co-LMA)	2060	1.4	53.4	8.7	–	75	0.139	[108]	
	VSNP crosslinked PAAm	1200–3400	0.07–0.3	0.04	–	–	70	0.111	[107]	
	Hybrid supramolecular composite	18	193	6000	22.8	–	–	0.0017	[109]	
	GO crosslinked PAAm	3400	0.39	0.03	4.7	–	80	0.083	[110]	
	HA–PEG gel	2600	7.3	0.72	138	6360	66	0.028	[111]	
		PNaAMPS microgel–PAAm	1300	2.5	0.22	14	–	85	0.139	[115]
		Alginate microgel–PAAm	1470	0.20	0.04	1.6	–	–	0.033	[116]
Soft microgel-based crosslinks	PAAm microgel–PAMPS	5500	0.9	–	22.0	157 000	60–80	–	[117]	
	PAAS microgel–PAAm	400	0.99	0.11	–	–	63	–	[118]	

(Continued)

Table 1. (Continued)

Material strategies		Tensile strain [%]	Tensile strength [MPa]	Young's modulus [MPa]	Toughness [MJ m ⁻³]	Fracture energy [J m ⁻²]	Water content [w%]	Strain rate [s ⁻¹]	Refs.
Nanocrystalline domain-based crosslinks	Freeze-thawed PVA	250–375	0.3–1.2	0.03–0.1	–	160–420	90	0.667	[122]
	Dry-annealed PVA	300–400	1–9	0.3–9	–	1000–9000	58–75	–	[123]
	Wet-annealed PVA	1360	11.2	2.7	82.3	25 390	55	0.017	[125]
	Solvent-exchange PVA	900	3.1	0.46	–	3720	75	0.049	[126]
	Salting-out PVA	300–2100	0.05–15	0.02–2.5	0.02–150	–	90	–	[128]
Microphase-based crosslinks	Poly(AAm-co-HMA)	2000	0.69	–	3.7	–	80	0.056	[130]
	PVA-C6	330	3.9	21.7	–	32 000	50	0.17	[131]
	Salting-out gelatin	417	4.3	0.76	–	–	50	0.028	[133]
	Poly(NaSS-co-MPTC)	150–1500	0.1–2.0	0.01–8	0.1–7	1000–4000	50–70	0.139	[139]
	Poly(DMAA-co-MAAc)	400	1.6	28	–	9300	70	0.083	[140]
	Poly(MAAm-co-MAAc)	200–620	1.2–8.3	2.3–217.3	2.0–27.9	2900–23 500	50–70	0.139	[141]
	Gelatin/poly(MAAc-co-AAc)	400	10	7.5	–	–	35–45	0.14	[143]
PNAGA	600–1400	0.16–1.1	0.05–0.15	–	200–1200	70–90	–	[144]	

methods. If polymer networks with controlled crosslinking points and chain lengths are carefully synthesized, the resultant hydrogels with less structural defects can be endowed with enhanced mechanical properties. Therefore, many efforts have been made to develop hydrogels with a well-controlled homogeneous structure. In the following section, topological single networks including tetra-PEG networks, slide-ring networks, and highly entangled polymer networks for constructing tough hydrogels with high homogeneity are discussed.

Given that differences in length of polymer chains between crosslinking points tend to reduce mechanical properties, Sakai et al. created four-arm polyethylene glycol (PEG) hydrogels for the first time in 2008 by cross-end-coupling of A and B tetra-functional PEG macromers having complementary end groups.^[25] Topological defects such as entanglements and loops were found to be negligible in tetra-PEG hydrogels, owing to the impenetrable sphere-like behavior of the tetra-arm star polymer in the semidilute solution and symmetrical A–B type cross-end coupling.^[26] Extremely low heterogeneities of the networks were confirmed by characterizations such as small angle neutron scattering, static light scattering, infrared spectroscopy, and nuclear magnetic resonance.^[27,28] Therefore, tetra-PEG hydrogels were considered to have a nearly ideal single network with uniform chain length and evenly distributed crosslinking points, endowing them with high mechanical strength comparable to that of native articular cartilage.^[29] Various kinds of tetra-PEG hydrogels were subsequently developed,^[30] and the ends of tetra-PEG macromers were modified with reactive end-groups such as *N*-succinimidyl and amine,^[25,31,32] maleimide and thiol,^[33,34] and boronic acid and diol.^[35,36] The introduction of functional groups into tetra-PEG networks can further broaden their functionalities and applications.^[37–39] Tetra-PEG hydrogels possess many advantages such as high mechanical performance, biocompatibility, and an easy fabrication process, but further development of this kind of ideal polymer networks is impeded by the limited range of available monomers and polymers.

Slide-ring hydrogels reduce stress concentration by reconfiguring the polymer networks with slidable crosslinks.^[40–42] In slide-ring hydrogels, figure-of-eight crosslinking points (two covalently

crosslinked polymer rings) that interconnect two polymer chains can slide freely along the single polymer chain akin to pulleys, and the sliding range is bounded by bulky end groups. Sliding of the pulleys enables reconfiguration of polymer networks, and the tension in polymer chains interconnected by the pulleys can be equalized, making the slide-ring hydrogels highly stretchable and elastic. This pulley effect contributes to remarkable mechanical properties significantly different from those of conventional hydrogels with fixed junctions. Slide-ring hydrogels are mainly synthesized from cyclodextrin-based polyrotaxanes.^[43,44] Cyclodextrins (CDs) are cyclic oligosaccharides comprising six, seven, or eight glucose units that are named α -, β -, or γ -CDs, respectively. Compared to other cyclic molecules, CDs are readily available in large quantities with high purity, and can be modified with various functional groups.^[45–47] Ito first reported slide-ring gels composed of α -CDs and PEG, showing high stretchability of up to 24 times in length and a large volume change of up to 24 000 times in weight.^[42] Reducing the number of CDs on one PEG chain increases slidable range of the crosslinkers and thus extensibility of the slide-ring gels, and increasing the PEG concentration enhances the PEG–PEG interactions. In their recent publication, optimization of the PEG volume fraction and the coverage of CDs on PEG chains endowed the slide-ring hydrogel with strain-induced crystallization effect. The resulting hydrogel with PEG volume fraction of 38% exhibited J-shaped stress–strain response, suggesting its self-reinforcement behavior. The hydrogel was also highly stretchable with tensile strain of $\approx 1200\%$ and strong with tensile strength of ≈ 5.5 MPa, achieving toughness of up to 22 MJ m⁻³.^[17]

High crosslinker content in conventional hydrogels causes brittleness, as the networks are inhomogeneous and extension of the short-chain polymers is quite limited. Instead of using special polymers or complicated methods, Miyata and co-workers reported that free radical polymerization with a high monomer concentration and low crosslinker content produced tough and stretchable hydrogels, which contained a lot of physical crosslinking points from the entanglements of polymer chains and few covalent crosslinking points.^[48] They demonstrated that a polyacrylamide (PAAm) hydrogel prepared with high crosslinker

content (0.1 mol%) could slightly extend, while a PAAm hydrogel (75 wt% water content) prepared with high monomer concentration (5.0 mol L⁻¹) and low crosslinker content (0.005 mol%) had fracture strain close to 1000% and fracture stress close to 300 kPa. This principle for making tough hydrogels was also applied to other hydrophilic monomers.^[49–51] For example, Suo and co-workers recently reported highly entangled PAAm^[49] and PEG^[50] hydrogels with high toughness and elasticity. The densely entangled long-chain networks of PEG with sparse covalent crosslinks had water content of 80 wt%, fracture energy of 1575 J m⁻², and toughness of 0.854 MJ m⁻³. In these works, the influence of chain entanglements on the fracture of polymer networks was studied. When a densely entangled network with sparse covalent crosslinking points is stretched, the tension transmits along the chain and to many other chains through entanglements. However, once a chain breaks at a single covalent bond, the energy stored in many entangled long chains dissipates, leading to high toughness. The dense chain entanglements function as slip links, which stiffen but not embrittle the polymer network.^[52,53] The sparse crosslinks enable long polymer chains and toughen the polymer network. In addition to the above-mentioned hydrogels utilizing sparse covalent crosslinks to fasten entangled polymer chains, highly entangled hydrogels with physical crosslinks were also developed recently.^[54,55] ABA triblock copolymers at high concentration assembled into a hierarchically ordered hydrogel via a solvent-nonsolvent rapid-injection process, and the hydrophobic A-blocks aggregated into micellar domains, working as rigid crosslinking points in the highly entangled polymer network.^[55] By tuning the initial concentration of the copolymers, hydrogels with water content of 95 wt% exhibited a maximum elongation of ≈ 8.5 times and fracture energy of ≈ 3000 J m⁻².

2.1.2. Introducing Energy Dissipation Mechanisms

Besides homogenizing polymer networks, another approach to make tough hydrogels focuses on developing heterogeneity to produce an energy dissipation mechanism. When a crack forms in the hydrogel, the energy released is transmitted to the crack tip. Once the energy is sufficient to rupture polymer chains along the crack path, the crack will continue to propagate. By introducing an energy dissipation system to the network, energy at the crack tip will be diffused by this new system and becomes insufficient to support crack propagation, thereby toughening the hydrogel. Incorporating energy dissipation systems into polymer networks is crucial for devising tough hydrogels. Energy dissipation can be achieved by rupture of polymer chains, decrosslinking of physical crosslinks, and/or fracture and pullout of fibers. In this section, interpenetrating networks, dual-crosslinked networks, and fiber-reinforced networks developed for making tough hydrogels with such energy dissipating mechanisms are discussed.

Gong et al. first reported double network (DN) hydrogels in 2003, which consisted of two interpenetrating polymer networks. The first rigid, brittle network is tightly covalently crosslinked while the second soft, ductile network is loosely covalently crosslinked.^[56] Under stretching, the first network serves as sacrificial bonds that gradually fracture at a relatively low stress and dissipate energy, while the second network sustains stress by large extension and prevents macroscopic crack propagation

via viscous energy dissipation. This synergetic mechanism enables DN hydrogels to have high water content (≈ 90 wt%), high mechanical strength (tensile strength of 1–10 MPa), and high fracture toughness (fracture energy of 100–1000 J m⁻²).^[21] It should be noted that covalently crosslinked DN hydrogels developed in the early years of research had poor fatigue resistance, owing to irreversible rupture of the covalent networks for energy dissipation. To develop tough and fatigue resistant hydrogels, interpenetrating polymer networks with a physically crosslinked network have been widely explored, and decrosslinking of the physical networks serves to dissipate energy under mechanical loading. These physical crosslinks in tough hydrogels can usually be recovered after decrosslinking, potentially leading to antifatigue properties. As a remarkable example, Suo and co-workers fabricated interpenetrating polymer networks composed of covalently crosslinked polyacrylamide and ionically crosslinked alginate (86 wt% water content), which had fracture energy of ≈ 9000 J m⁻².^[57] Under stretching, the covalent network maintained the integrity of the matrix, enabling unzipping of the alginate network over a large strain region for persistent energy dissipation. Furthermore, the covalent network preserved the memory of the initial state, and therefore much of the deformation was reversed after releasing. The unzipped ionic crosslinks were healable by re-zipping so that the internal damage sustained during stretching could be largely recovered. Following this work, various reversible physical networks for energy dissipation were studied, including acidic ionic networks,^[58–60] alkaline ionic networks,^[61] hydrophobic interaction networks,^[62–64] hydrogen bonding networks,^[65] chain entanglement networks,^[66] and crystalline polymer networks.^[67,68] Therefore, a variety of covalent-physical or fully physical interpenetrating networks with high toughness were developed.^[69] In recent years, the DN concept has been extended to composite materials that employ metals, ceramics, and 3D printed frameworks as sacrificial bonds.^[70–72] Moreover, mechanical properties and functionalities of DN hydrogels have been largely enhanced by introducing additional functional components or tuning compositions of the two polymer networks. Tough DN hydrogels with various functions such as lubrication,^[73] tissue adhesion,^[74] self-healing,^[75] and self-growing^[76] have been successfully prepared. For example, mechanochemically active copolymers were incorporated into DN hydrogels, whose mechanical performance were enhanced when reactive strand extensions were triggered by force.^[77] Strand extension was provided by the sodium salts of bicyclo[6.2.0]decane (BCD) mechanophores, which released stored length through a force-coupled [2 + 2] cycloreversion. In the mechanoresponsive DN hydrogels, the covalently crosslinked copolymer network of BCD and 2-acrylamido-2-methylpropanesulfonic acid sodium salt (NaAMPS) acted as the first network. Upon being stretched to their nominal breaking point, reactive strand extensions of up to 40% occurred in the BCD–NaAMPS network, leading to hydrogels that exhibited 40% to 50% enhancement in stretchability and doubled tear energies compared to the control samples.

Simultaneously introducing two different crosslinking mechanisms into a single polymer network creates tough dual-crosslinked hydrogels. For example, in a dual-crosslinked hydrogel that combines chemical and physical crosslinks, noncovalent bonds with relatively low binding energies rupture to serve as

sacrificial bonds for energy dissipation while covalent bonds remain intact under deformation, thereby maintaining a tough and stable network. Zhou and co-workers reported a poly(acrylamide-co-acrylic acid) hydrogel reinforced by a secondary carboxylic-Fe³⁺ crosslink (60–70 wt% water content), and the coordination bonds served as reversible sacrificial bonds and ruptured to dissipate energies under stretching.^[78] Mechanical properties of the hydrogels could be easily tuned by the concentration of acrylic acid or Fe³⁺-loading solution, and high tensile strength (≈ 6 MPa), large elongation (>7 times), high toughness (≈ 27 MJ m⁻³), and good mechanical recovery of under ≈ 4 h self-recovery at room temperature were achieved. In a recent study, a weak poly(acrylamide-co-2-acrylamido-2-methyl-1-propane-sulfonic acid)(poly(AAm-co-AMPS)) chemical hydrogel was reinforced by strong sulfonate-Zr⁴⁺ metal-coordination interaction.^[79] The resultant dual-crosslinked hydrogel with water content of 33–74 wt% possessed high strength and toughness, which was tunable over 3–4 orders of magnitude by changing the composition and metal-to-ligand ratio. The physical crosslinks of sulfonate-Zr⁴⁺ coordination complexes were robust yet dynamic and could be broken up in alkaline solutions, thereby allowing reversible regulation of mechanical properties. Noncovalent crosslinking mechanisms including ionic coordination^[78,80] hydrogen bonding,^[81] crystallization,^[82,83] and dipole-dipole^[84] were developed in the design of chemically and physically dual-crosslinked hydrogels, which featured high fracture energy and recoverable mechanical properties after undergoing cyclic loading and unloading. In addition, physically dual-crosslinked networks with high mechanical performance were exploited, which were usually achieved by integrating ionic coordination interactions with another noncovalent crosslinking mechanism, such as electrostatic,^[85] hydrophobic,^[86] hydrogen bonding,^[87,88] and host-guest interactions.^[89]

In biological hydrogels, the gel matrices are usually reinforced with micro/nanofibers, and the resulting composites are strong and tough. For example, the articular cartilage is made up of stiff and strong collagen fibers embedded in a proteoglycan matrix, while the skeletal-muscle tissue contains highly oriented, densely packed myofibers composed of multinucleated muscle cells. Therefore, tough hydrogels with biomimetic fiber-reinforced structures have been developed by introducing fibers into polymer networks or generating fibrous structures in polymer networks.^[90–93] In these heterogeneous hydrogels, rigid fiber-based components increase the mechanical strength, while deformation, pulling out and fracture of the fibers under mechanical loading provide additional energy dissipation function, thereby increasing the overall toughness. It was reported that a crystallized PVA hydrogel reinforced by bacterial cellulose nanofibrous networks exhibited mechanical strength exceeding that of cartilages.^[94] The strength of supramolecular interactions in aligned hierarchical fibrous hydrogels could be tuned by controlled drying and prestretching, and their mechanical strength and elastic modulus were comparable to that of natural tendons.^[90] By utilizing a combined method of directional freezing and salting out, He and co-workers recently developed multilength-scale hierarchical PVA hydrogels with an aligned micro-nanofibrous network and molecular crystallization. The obtained hydrogels maintained high water content of 70–90 wt%, and had tensile strength of up to 23.5 MPa and fracture energy

of up to 170 kJ m⁻².^[95] Densification of the microfibrils and nanofibrils strengthened the hydrogel by increasing the material density, and pulling out and fracture of those fibrils toughened the hydrogel by increasing energy dissipation during fracture. In addition, the nanofibrils were toughened by high crystallinity induced by the salting out process. Besides the above-mentioned networks reinforced by micro/nanofiber-based components, fabric scaffolds^[96–99] or macroscale fibers^[100] were also incorporated into polymer networks to improve mechanical properties, such as polyampholyte-woven glass fiber fabric hydrogel composites,^[101] 3D printed fiber scaffold-reinforced hydrogels,^[96] and elastomer fiber-PAAm hydrogel composites.^[100]

2.1.3. Endowing Crosslinks with High Functionality

Compared with the first two categories of toughening strategies, which focus on designing the entire network to obtain hydrogels with high homogeneity or energy dissipation systems, the strategy discussed in this section concentrates on functionality design of the crosslinking points. In conventional hydrogels, crosslinking densities and chain distances between covalent crosslinking points can hardly be well controlled, and the crosslinking reaction does not produce a regular inter-crosslinking distance, leading to a broad distribution of chain lengths between the crosslinking points. In comparison, incorporating micro/nanomaterial-based crosslinkers into polymer networks to produce high-functionality crosslinks can improve control over the crosslinking densities and inter-crosslinking distances, thus facilitating better load redistribution within the networks to prevent microcrack formation. Moreover, detachment of physical interactions between crosslinkers and polymer chains, deformation/fracture of soft crosslinkers, or dissociation of dynamic crosslinkers can effectively dissipate energy to prevent crack propagation. In the following section, high-functionality crosslinks based on rigid nanoparticles, soft microgels, nanocrystalline domains, and microphase separations are discussed.

Haraguchi and Takehisa proposed a poly(*N*-isopropyl acrylamide)-clay (PNIPAM-clay) nanocomposite hydrogel with extraordinary mechanical properties.^[102] In the initial reaction solution containing monomers, initiators, and water-swallowable exfoliated inorganic clays, the clays were uniformly dispersed with regular neighboring clay-clay distance determined by the concentration, and the initiators were located near the clay surface through strong ionic interaction. Radical polymerization was then initiated thermally from the clay surface, with the uniformly distributed clays acting as crosslinkers, and therefore polymer chain distances between the crosslinking points were regular. The resulting composite hydrogel had elongation over 1000%. Accordingly, other nanocomposite hydrogels using crosslinkers such as clays,^[103–105] macromolecular microspheres,^[106] silica nanoparticles,^[107–109] graphene oxides,^[110] and MXene^[88] were designed. Recently, Zhu and co-workers selected densely methacrylate-grafted, highly rigid hyaluronic acid (HAMA) to construct the hard phase, and selected *o*-nitrobenzyl alcohol (NB)-terminated tetra-armed PEG for the soft phase. The resultant nanocomposite hydrogel composed of 65 \pm 2 wt% water exhibited ultrahigh toughness of 138 MJ m⁻³ and tensile strength of 15.31 MPa.^[111] The PEG networks possessed high structural

homogeneity, while strong interfacial bonding between the hard HAMA granules and the soft PEG matrix supported a very efficient load transfer between the two phases, which further reduced stress concentration and enhanced fracture strength and toughness. Additionally, in these nanocomposite hydrogels with rigid nanomaterial-based crosslinkers, detachment of physical interactions between the crosslinkers and polymer chains, such as desorption of polymer chains physically absorbed by the nanoparticles^[112] and decrosslinking of physical crosslinks between the nanoparticles and chains^[88] can dissipate energy and toughen hydrogels. Micro/nanogels were designed as high-functionality soft crosslinkers, and polymer chains bonded with uniformly distributed soft particles in polymer networks via covalent bonding^[113,114] or physical interpenetration.^[115–118] Gong and co-workers reported microgel-reinforced hydrogels, where densely crosslinked polyelectrolyte microgels of poly(2-acrylamido-2-methylpropanesulfonic sodium) (PNaAMPS) were incorporated into a sparsely crosslinked neutral PAAm matrix.^[119–121] In a microgel-reinforced hydrogel, PNaAMPS microgels acted as multifunctional physical crosslinkers that were highly entangled with PAAm chains, thus forming DN microgels in the composite network. Irreversible rupture of the polyelectrolyte networks in the DN microgels acted as sacrificial bonds for significant energy dissipation that toughened the hydrogel. Recently, Yan and co-workers developed a microgel-reinforced hydrogel (60–80 wt% water content) with the interpenetrating entanglements of poly(1-acrylamido-2-methylpropanesulfonic acid) (PAMPS) polymer chains in soft PAAm microgels, and the hydrogel displayed ultrahigh fracture energy of 157 kJ m⁻².^[117] They demonstrated that the deformable interpenetrating networks in soft microgels transformed the hydrogel from isotropic to anisotropic state under stretching, which effectively dissipated energy, alleviated stress concentration at the crack tip, and prevented crack propagation.

Instead of externally introducing micro/nanomaterials into hydrogels to produce high-functionality crosslinks, robust yet dynamic crosslinking domains can be generated within polymer networks by crystallization or microphase separations. On one hand, when hydrogels are subjected to mechanical loading, the microdomains act as robust crosslinking points, allowing the stress to disperse. On the other hand, disentanglement of the microdomains effectively dissipates energy before fracture of the hydrogels, serving as a continuous source of toughening. For example, PVA can form nanocrystalline domains to crosslink polymer networks through various methods, such as freezing–thawing,^[122] annealing,^[123–125] solvent exchanging,^[126] and salting out.^[127,128] Qiu and co-workers proposed a solvent exchange method for preparing tough and strong PVA hydrogels with homogeneous and high-density nanocrystalline domains.^[126] In the first step, PVA was dissolved in a good solvent (e.g., dimethyl sulfoxide), allowing complete dispersion of polymer powders in nonaggregated states, and maintaining extended conformations and interlaced networks. In the step of crosslinking, the gel was transferred to a poor solvent (i.e., water), which possesses relatively weak hydrogen bond accepting capability. Upon solvent displacement, the intermolecular hydrogen bonds between extended PVA chains were restored to form a tough and strong hydrogel. The hydrogel exhibited high transparency, suggesting a homogeneous network

structure. Moreover, high-density nanocrystalline domains in the hydrogel acted as dense crosslinks and energy dissipation domains, leading to extraordinary stiffness and toughness. Microphase separations can be induced by noncovalent interactions among polymer networks,^[129] including hydrophobic associations,^[130–133] electrostatic interactions,^[134–139] and hydrogen bonds.^[140–144] The produced microdomains are composed of polymer chains in strong physical interactions, acting as dynamic and reversible physical crosslinks in polymer networks, and thus dramatically improving mechanical performance of hydrogels. For example, alkyl side chains can usually form hydrophobic domains to crosslink polymer networks. Gao and co-workers prepared a hydrophobic association hydrogel using acrylamide as the main component and hexadecyl methacrylate as the hydrophobic segments.^[130] They demonstrated that a combined surfactant consisting of anionic surfactants (i.e., sodium dodecyl sulfate) and amphoteric surfactants (i.e., dodecyl dimethyl betaine) produced a relatively close arrangement of the hydrophobic segments to form mixed micelles in the polymer networks. At an optimal formulation, the hydrogel with water content of ≈80 wt% exhibited tensile strain of ≈2000% and toughness of 3.7 MJ m⁻³. Recently, water vapor-induced phase separation (wVIPS) of short alkyl side-modified PVA hydrogels was reported, and the phase separation states including phase size, contrast level, and distribution were largely affected by the relative humidity (RH) during the wVIPS process. Therefore, the hydrogels treated by high RH (≈98.3%) and low RH (≈16.2%) exhibited distinctly different mechanical performances.^[132] Microphase separations based on electrostatic interactions usually occurred in polyampholyte^[135] or polyion-complex hydrogels.^[138] Polyampholyte hydrogels poly(sodium p-styrenesulfonate-co-3-(methacryloylamino) propyl-trimethylammonium chloride) (poly(NaSS-co-MPTC)) with a bicontinuous phase-separated structure were reported.^[134] During dialysis of counterions from the gels, phase separation was driven by Coulombic and hydrophobic interactions. Under mechanical loading, successive fracture of ionic bonds, hard phases, and soft phases in the networks significantly dissipated mechanical energy and thus toughened the hydrogels. Hydrophobic side group stabilized hydrogen bonding^[140] or also known as cooperative hydrogen bonding^[144] is an effective pathway to develop microphase separation hydrogel. In a recent publication, the effect of the content of hydrophobic methyl side groups on the phase-separated structures and mechanical properties of gelatin/poly(methacrylic acid-co-acrylic acid) hydrogels was studied. With an increasing content of methacrylic acid, the hydrogel transformed from a crosslinked network to a bicontinuous phase-separated structure and to a phase-separated structure with wide size distribution. The hydrogel with a bicontinuous phase separation exhibited the best mechanical performance.^[143]

2.2. Engineering Mechanical Functions Adaptive for Biointegrated Applications

Moving beyond the polymer network strategies for toughening hydrogels, the key question is how to engineer specific mechanical functions in tough hydrogels for different biointegrated applications. Here, we highlight remarkable mechanical

functionalities, which are seen in biological materials, including high toughness and resilience, high toughness and stiffness, self-healing and high strength, and stimuli-responsive stiffening/softening. They are not easily achieved in synthetic hydrogels but are imperative for fabricating biointegrated functional hydrogel devices with mechanical adaptivity. The polymer network characteristics for each type of functional hydrogels are analyzed.

2.2.1. Tough Yet Resilient Hydrogels with Low Hysteresis

Mechanical resilience is important for the survival or reproduction of living organisms. For example, resilience enables muscles to withstand millions of repeated loadings without performance degeneration in their lifespan, which is essential for breathing, heart beating, and movement regulation of animals.^[150] Hydrogels employed in wearable and implantable devices also need to be mechanically tough yet resilient, so as to maintain stable device functions in cyclic and dynamic stretching. Building tough yet resilient hydrogels requires a design of tough network mechanisms that allow high stretching of polymer chains, as well as elastic crosslinked network mechanisms that enable full and fast recovery of mechanical properties without hysteresis from the large stretching. Commonly used energy dissipation mechanisms usually rely on covalent or physical sacrificial bonds, leading to hydrogels with irreversible deformation or hysteresis. So far, polymer networks have been synthesized to achieve either high toughness^[22] or high elasticity^[151] but rarely both.

The delicately designed tetra PEG hydrogels with covalently crosslinked networks were reported to withstand more than seven-folds of stretching without hysteresis, whereas their toughness were relatively low.^[37] Recently, research on polymer network topologies via novel crosslinking methods have been explored to deal with the conflict between toughness and elasticity.^[17,18,49,50,54,152–157] Reversible extension of a soft percolating network is targeted for achieving high elastic limit strain. Therefore, a coiled long-chain polymer network in physically entangled or loosely covalently crosslinked state is usually designed, and the bonding between the high-functionality crosslinks and the polymer chains needs to be strong enough to avoid irreversible rupture of crosslinking points or slipping of polymer chains within a large deformation range. Moreover, an energy dissipation design of the crosslinking points before fracture of the network can decrease stress concentration at the crack tip, thereby enhancing the overall toughness. For example, Cao and co-workers developed a PAAm hydrogel crosslinked by tandem-repeat proteins, which could be stretched up to 1100% strain with a hysteresis of <5% and a high fracture energy of $\approx 900 \text{ J m}^{-2}$.^[152] At an optimized concentration of tandem-repeat proteins as covalent crosslinkers, uniformly and randomly entangled PAAm polymer chains formed a percolating network. Upon stretching, elastic extension of the coiled PAAm polymer chains and reshaping of the polymer network contributed to high stretchability, while the polyprotein crosslinkers only started to unfold when the hydrogel approached its fracture limit, thereby allowing a high elastic deformation (**Figure 3a**). It was demonstrated that the polyprotein crosslinkers at the crack zone experienced large forces to trigger unfolding, and therefore resisted crack propa-

gation. Similarly, a PAAm hydrogel crosslinked by deformable helical peptides was tough and resilient, making it suitable for wearable sensors.^[153] Topological architectures with slidable crosslinking points or distributed polymer blocks were also reported. For instance, Ito and co-workers developed a slide-ring gel composed of α -CDs and PEG with high toughness and low hysteresis. The slidable crosslinkers enabled reorientation and crystallization of the PEG polymer chains under stretching, which produced a self-reinforcement effect.^[17] The self-reinforcement process was based on topological transformation of the polymer network without sacrificial bond effect, and therefore the hydrogel possessed both high toughness of 6.6 to 22 MJ m^{-3} and almost 100% rapid recovery of extension energy (**Figure 3b**). Hu and co-workers reported an architected polymer network composed of a soft polymer network entangled with millimeter-scale hard polymer blocks.^[154] Reversible extension of the soft polymer network at low strain enabled elastic limit strain of $\approx 200\%$, and at a crack tip in the architected network, the large strain in the soft matrix spread high stress over the entire hard phase, largely preventing crack propagation. Recently, Yan and co-workers prepared hysteresis-free and tough nanocomposite gels through in situ polymerization of acrylamide within nanochannels of covalent organic frameworks (COFs) or molecular sieves (MSs). The loosely covalently crosslinked polymers formed a long-chain network in a densely entangled state, and strong hydrogen interactions between COFs and interpenetrating polymer chains immobilized the chains that might slip under mechanical loading, which avoided energy dissipation. Upon stretching, the tension in the polymer chains could be transferred to many other chains through entanglements, and thus the composite network continuously absorbed and stored mechanical energy. Upon releasing, the energy was released. The optimized hydrogel with water content of $\approx 65 \text{ wt}\%$ exhibited rapid self-reinforcement properties under stretching, and 97% recovery of extension energy during 100 consecutive cycles of 2000% strain was observed. In addition, the rigid COFs decreased stress concentration at the crack tips, and a maximum crack propagation strain of 5800% of the gels was demonstrated.^[156]

2.2.2. Tough Yet Ultrastiff Hydrogels

The cartilage and tendon of animals are rather tough and hard to break, and are rather stiff with Young's modulus up to 100 MPa .^[15,146] Similarly, natural spider silks can have toughness of $\approx 350 \text{ MJ m}^{-3}$ and modulus up to 10 GPa .^[149] Although remarkable progress have been made in toughening hydrogels, it is still challenging to synthesize hydrogels simultaneously having high toughness and elastic modulus that can compete with these natural materials.^[158] Tough and stiff hydrogels need to be both deformation resistant and energy dissipative. Therefore, synchronously incorporating micro/nanostructure-based rigid components and sacrificial bond-based energy dissipation systems into polymer networks is expected to coordinatively stiffen and toughen hydrogels.

In this respect, energy dissipation fiber-reinforced hydrogels combine the attributes of a rigid fiber that provides stiffness and a soft hydrogel matrix that dissipates energy.^[90,98,101,159] Gong and co-workers reported that drying a highly swollen

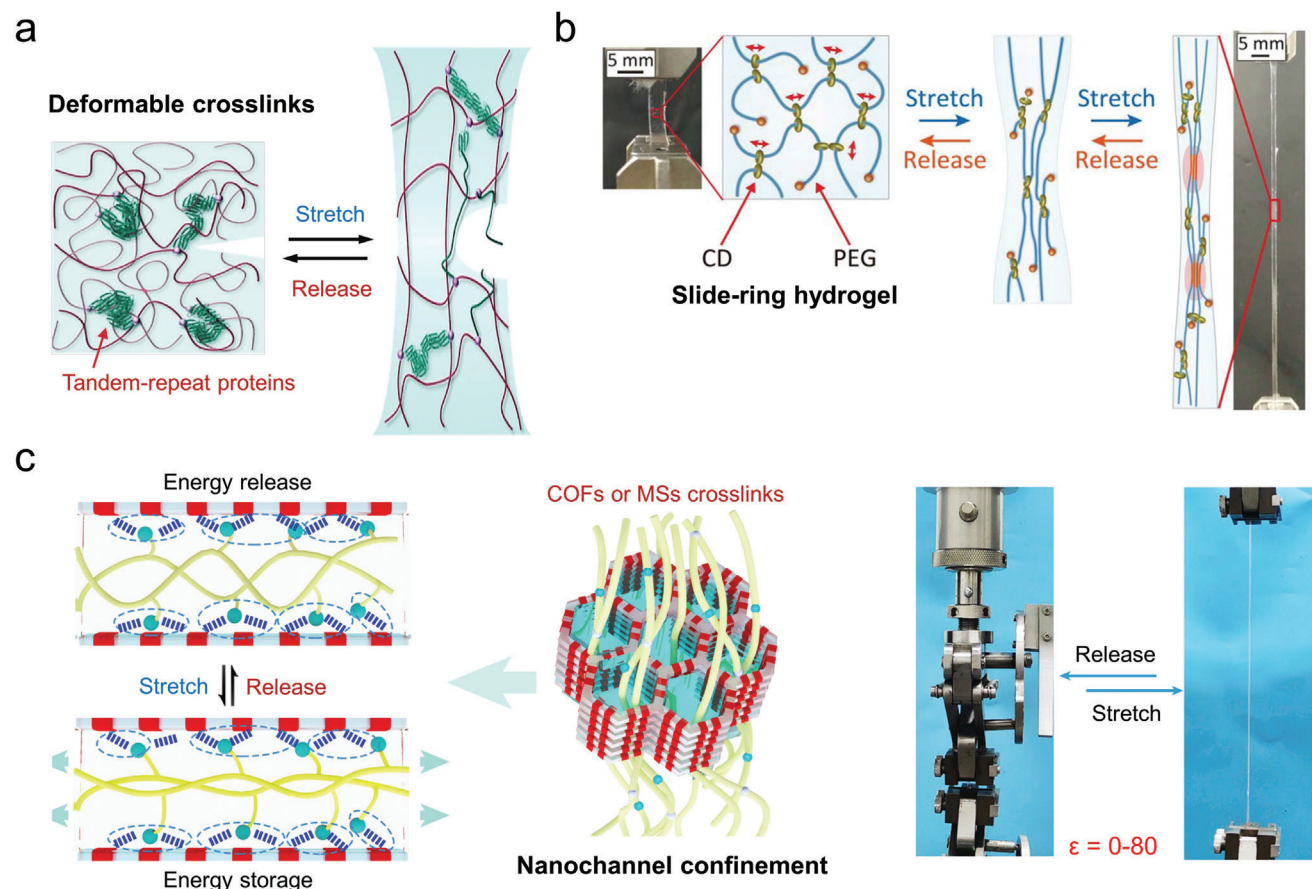
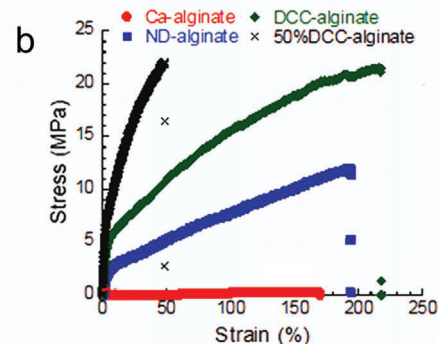
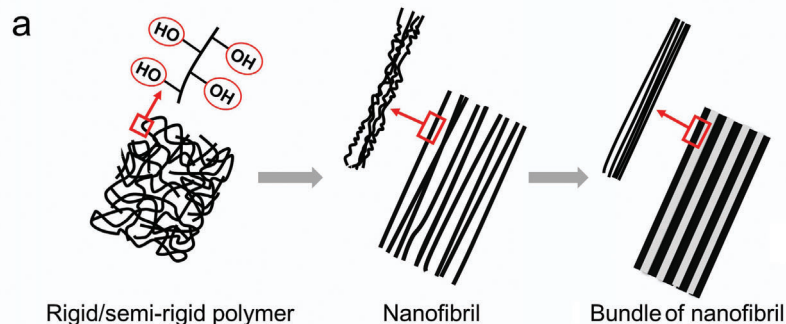


Figure 3. Typical examples of tough yet resilient hydrogels. a) A PAAm hydrogel consisting of random coiled polymer chains crosslinked by polyproteins, showing unfolding of the polyproteins before fracture. Reproduced with permission.^[152] Copyright 2020, Springer Nature. b) A slide-ring hydrogel that shows reversible PEG chain alignment during stretching and releasing. Reproduced with permission.^[17] Copyright 2021, American Association for the Advancement of Science (AAAS). c) A composite network of densely entangled polymer chains immobilized by COFs or MSs via hydrogen bonding interactions, exhibiting reversible deformation in an ultralarge strain range. Reproduced with permission.^[156] Copyright 2023, Springer Nature.

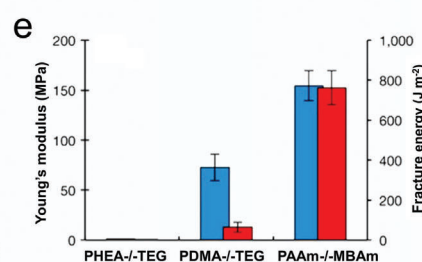
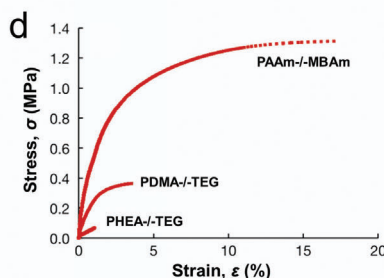
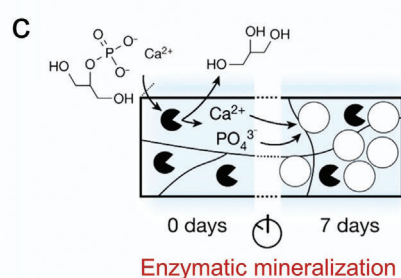
physical hydrogel in confined conditions produced an anisotropic hydrogel with aligned multiscale hierarchical fibrous structures, which were similar to those of collagen fibril structures in tendons and ligaments. During the confined drying process, sufficiently high tensile stress was applied to align the rigid/semirigid polymer chains (such as alginate and cellulose), and multiscale fibrous structures (from nano- to sub-micro- to microscale) spontaneously formed in the bulk hydrogel via physical associations (Figure 4a). The aligned hierarchical structures in the anisotropic hydrogel led to high stiffness due to the formation of fiber structures, and supramolecular interactions such as ionic and hydrogen bonds served as reversible sacrificial bonds to toughen the hydrogel. By controlling the degree of prestretching during the drying process, aligned fibrous structures and their internal supramolecular interactions could be well tuned. The aligned fibrous alginate hydrogel with 57 wt% water processed without prestretching (DCC–alginate) had Young's modulus of ≈ 203.3 MPa and toughness of ≈ 30.9 MJ m⁻³, whereas the hydrogel prestretched at 50% strain (50% DCC–alginate) had Young's modulus of ≈ 367.4 MPa and toughness of ≈ 7.0 MJ m⁻³ (Figure 4b). Mineralization of polymer networks has turned out to be another effective strategy for simultaneous stiffening and

toughening hydrogels.^[160–162] For example, Tiller and co-workers introduced a method of enzyme-induced mineralization to prepare highly mineralized hydrogels containing 50–90 wt% water, which had elastic modulus varying over four orders of magnitude and fracture energy more than 1000 J m⁻².^[163] Different polymer networks entrapped with alkaline phosphatase were prepared via photopolymerization, which were subsequently immersed in calcium 2-glycerol phosphate solution buffered to pH 9.8 with triethanolamine for mineralization. Slow calcification took place during the 7 days of immersion and inorganic calcium phosphates formed percolating networks inside the hydrogels, leading to much improved mechanical performance (Figure 4c,d). The 70 wt% mineralized PAAm hydrogel possessed a nano-sized inorganic network filled with spherical holes, and exhibited Young's modulus of 155 ± 15 MPa and fracture energy of up to 763 ± 85 J m⁻² in the same range as cartilage (Figure 4e). Besides, organic–inorganic composite hydrogels crosslinked by nanoparticles can be tough yet ultrastiff by sensibly combining soft and rigid phases within polymer networks.^[109,164] In the composite systems, the interfacial bonding between the soft polymer matrix and rigid nanoparticles needs to be strong enough to transfer load from the matrix to the nanoparticles. Therefore,

Aligned hierarchical fibrous structures



Rigid inorganic particle reinforcement



Robust yet dynamic crosslinks

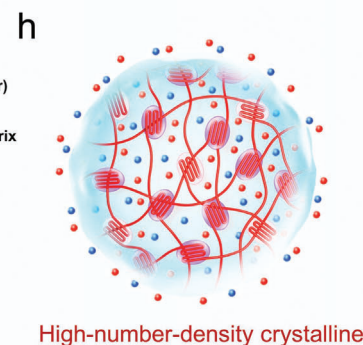
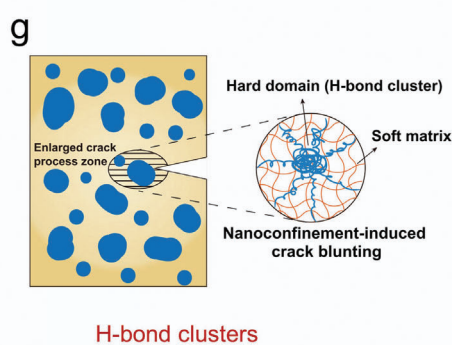
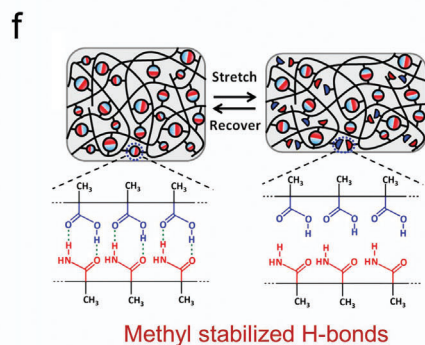


Figure 4. Typical examples of tough yet ultrastiff hydrogels. a) Schematic illustration for an anisotropic hydrogel with aligned multiscale hierarchical fibrous structures. b) Stress–strain curves of alginate hydrogels. Reproduced with permission.^[90] Copyright 2018, Wiley-VCH. c) Enzyme-induced bulk calcification of polymer networks for preparation of mineralized hydrogels and d) their stress–strain curves, e) Young's modulus (blue), and fracture energy (red). c–e) Reproduced with permission.^[163] Copyright 2017, Springer Nature. f) A poly(MAAM-co-MAAc) supramolecular hydrogel based on compact hydrogen bonds stabilized by hydrophobic motifs. Reproduced with permission.^[141] Copyright 2019, American Chemical Society. g) Crack-resistant behavior of a PDMAEA-Q/PMAA hydrogel composed of an ionically crosslinked network and abundant hydrogen-bond clusters. Reproduced with permission.^[165] Copyright 2023, Springer Nature. h) A PVA hydrogel containing high number densities of uniform crystalline domains. Reproduced with permission.^[166] Copyright 2023, Wiley-VCH.

delicate design of covalent^[164] or noncovalent^[109] interfacial bonding are usually required. As an example, a mixture solution of functionalized polymer-grafted silica nanoparticles (P1), a semicrystalline hydroxyethyl cellulose derivative (H1), and curcubit[8]uril (CB[8]) underwent aqueous self-assembly by host–guest interactions at the molecular level and nanofibril formation at colloidal-length scale, forming a supramolecular polymer-colloidal hydrogel (SPCH) that could be readily drawn into uni-

form fibers. The CB[8] acted as physical crosslinkers that created interfacial bonding between the colloidal particles and the hydrogel matrix with crystalline domains, which promoted the formation of nanoscale fibrils in the network. The resultant supramolecular fiber exhibited toughness of $22.8 \pm 10.3 \text{ MJ m}^{-3}$ and Young's modulus of $6.0 \pm 2.9 \text{ GPa}$, and its high damping capacity (low resilience) of $64.2 \pm 2.2\%$ holds great potential for energy dissipation and shock-absorbing applications.

Polymer networks with robust yet dynamic crosslinks such as robust hydrogen bonding and high-density crystalline domains were reported to be tough and stiff.^[125,140,141,165,166] Although hydrogen bonds between polymer chains are weak in an aqueous environment, they can be largely reinforced when shielded against the attack of water molecules by hydrophobic motifs, and therefore act as rigid components that largely enhance the stiffness of hydrogels. Wu and co-workers developed tough and ultrastiff supramolecular poly(methacrylamide-co-methacrylic acid) hydrogels with water content of ≈ 50 –70 wt%, showing fracture energy of 2.9–23.5 kJ m⁻² and Young's modulus of 2.3–217.3 MPa. The high stiffness was attributed to dense crosslinking and reduced segmental mobility caused by the compact hydrogen bonds between carboxylic acid and amide groups, which were stabilized by hydrophobic methyl motifs (Figure 4f). Moreover, the gel released from 100% tensile strain readily recovered to its original length after incubation in hot water (60 °C) for 3 min, and fully recovered its original mechanical properties after cooling back to room temperature owing to the reformation of dissociated hydrogen bonds.^[141] In another example, Wu and co-workers reported tough and strong poly(2-(dimethylamino)ethylacrylate) methyl chloride quarternary salt/poly(methylacrylic acid) (PDMAEA-Q/PMAA) hydrogel fibers. The hydrogen bonding among carboxylic acid groups stabilized by methyl motifs formed abundant hydrogen-bond clusters and cluster aggregates with the sizes of 8–28 nm, which were robust and acted as the rigid phase, and the interaction of positively charged PDMAEA-Q and negatively charged PMAA formed ionically crosslinked networks that were soft and ductile (Figure 4g). The resulting hydrogel microfibers with water content of 30 wt% were stiff with Young's modulus of 428 MPa, and tough with superhigh fracture energy of 187 kJ m⁻² due to energy dissipation of the hydrogen-bond clusters. Besides, moisture treatment allowed fast mechanical recovery of the hydrogels released from 100% cycled tensile strains.^[165] Recently, a solvent exchange assisted salting out strategy was developed to fabricate PVA sal-exogels with high density of nanocrystalline domains (Figure 4h).^[166] The process of solvent exchange produced a hydrogel network, and the following salting out process boosted its crystalline domains, increasing the crystallinity in the hydrogel to $\approx 20.7\%$. Under deformation, these high-density crystalline domains remained intact at small strains to prevent network deformation, but disentangled at larger strains for persistent energy dissipation, thus leading to a combination of excellent stiffness and toughness.

2.2.3. Self-Healing Strong Hydrogels

Self-healing is defined as the ability to heal macroscopic cracks such as cuts or scratches autonomously or under the effect of a stimulus, which is an inherent property of many biological materials.^[167] Self-healing is a highly desirable property for tough and robust hydrogel devices such as wearable devices and robots in the dynamic and real-world environments, as it extends their lifespan and reduces the environmental burden of polymer waste and electronic waste. The capability to self-heal in hydrogels is enabled by polymer networks crosslinked by dynamic covalent or noncovalent bonds.^[168] Achieving efficient self-healing in hy-

drogels with tensile strength in the range of MPa is still a significant challenge, because networks with short-lived reversible bonds that enable efficient self-healing are usually weak, while networks with long-lived strong covalent bonds restrict the motion of chains and reduce self-healing efficiency. In the following section, polymer networks with multiple dynamic bonds such as a combination of dynamic covalent bonds with noncovalent bonds,^[169–172] cooperative hydrogen bonds,^[144,173,174] coordination and hydrogen bonds,^[175,176] and electrostatic and hydrophobic interactions^[62,136,177] are introduced, which are utilized to make hydrogels with high strength and excellent self-healing properties.

Dynamic covalent bonds such as imine bonds, acylhydrazone bonds, disulfide bonds, boronate ester bonds, as well as Diels–Alder reactions have been used to create self-healing in hydrogels.^[178–179] Self-healing chemical hydrogels based on a single kind of dynamic covalent bonds generally exhibit Young's modulus and fracture stress in the Pa to kPa range.^[168] Integrating dynamic covalent bonds with other noncovalent bonds represents an attractive approach for improving mechanical and self-healing properties of hydrogels in a synergistic way. For example, Chen and co-workers integrated acylhydrazone bonds and Pluronic F127 micelle crosslinking two kinds of dynamic crosslinks in one system, and prepared self-healable hydrogels (85 wt% water content) with toughness of 14.1 MJ m⁻³ and ultralarge tensile strain of up to 11700%.^[169] Energy dissipation occurred from simultaneous decomposition of the PF127 micelles and chain sliding facilitated by reconfiguration of the acylhydrazone bonds. Meanwhile, this unique combination and dynamics led to excellent self-healing performance. After 24 h healing at room temperature, the hydrogel recovered 85% of its original tensile strength (247 kPa). In another representative example, Connal and co-workers proposed a molecular design strategy based on dynamic imine bonds and acid-ether hydrogen bonds.^[171] Copolymers of methacrylic acid, oligo(ethylene glycol) methacrylate, and 4-hydroxybenzaldehyde formed a poly(MAA₁₁₃-co-BA₃₇-OEGMA₅₀) hydrogel. MAA chains formed hydrogen bonds with OEGMA chains, while the BA groups introduced hydrophobicity to stabilize the hydrogen bonds. The copolymers were then crosslinked by ethylenediamine (EDA) to form dynamic imine bonds in the network. Those synergetic interactions enabled the damaged hydrogel to recover 84% of its original tensile strength (2.7 MPa) after only 50 min of self-healing at 25 °C.

High-strength hydrogels with self-healing capability based on cooperative hydrogen bonds were also developed. For example, Liu and co-workers developed a high-strength supramolecular PNAGA hydrogel with water content of 70 wt%, in which dual-amide in one side group of NAGA amplified the hydrogen bonding interactions between amino acids and resulted in strong physical crosslinking in the hydrogel.^[144] Moreover, temperature sensitivity of the hydrogen bonds enabled 80% recovery of tensile strength (1.3 MPa) after the damaged hydrogel healed at 90 °C for 3 h. Besides, synergetic interactions of multiple noncovalent bonds were utilized to make self-healable strong hydrogels. For example, in a physically crosslinked polyacrylic acid–cellulose nanofibril–Fe³⁺ (PAAc–CNF–Fe³⁺) hydrogel, carboxylated CNFs and PAAc chains formed hydrogen bonding interaction, and dual ionic coordination bonds between Fe³⁺ and carboxylic groups from PAAc and carboxylated CNFs further reinforced the

Table 2. Typical examples of self-healable hydrogels with high strength based on multiple dynamic bonds

Hydrogels	Post-healing strength [MPa]	Posthealing elongation [%]	Strength recovery [%]	Healing time	Water content [w%]	Healing methods	Dynamic bonds	Refs.
Pluronic F127 micelle-PEO	0.25	10 650	85	24 h	85	Room temperature	Acylhydrazone bonds and hydrophobic interactions	[169]
Poly(MAA ₁₁₃ -co-BA ₃₇ -OEGMA ₅₀)-EDA	1.1	120	34	10 min	–	Heating at 25 °C	Imine bonds and hydrogen bonds stabilized by hydrophobic interactions	[171]
	2.0	330	63	30 min				
	2.7	500	87	50 min				
PNAGA	1.3	380	80	3 h	70	90 °C water bath	Cooperative hydrogen bonds	[144]
PAMPS-DMAA	0.48	900	80	24 h	20–50	Heating at 23 °C	Cooperative hydrogen bonds	[173]
PVA-TA	1.5	200	40	1 h	40	Room temperature under water	Hydrogen bonds and crystallization	[174]
PAAm/PAAc-Fe ³⁺ /NaCl	0.6	400	50	12 h	48	80–100% relative humidity	Hydrogen bonds, coordination interactions and hydrophobic interactions	[176]
	1.1	550	90	24 h				
CS-PAAc-Fe ³⁺ /NaCl ⁺	1.4	700	38	24 h	–	70 °C heating	Coordination interactions and chain entanglements	[75]
	1.1	550	90	24 h				
PAAc-CNF-Fe ³⁺	0.7	800	51	3 h	–	Heating at 25 °C	Multiple coordination interactions and hydrogen bonds	[175]
	1.1	1100	85	12 h				
	1.2	1500	88	24 h				
PMPTC-PNaSS	2.2	630	60	12 h	50	Saline solution treatment	Electrostatic interactions	[137]
PAAc-CTAB	0.8	600	42	15 min	28	Surfactant treatment and 80 °C heating	Electrostatic and hydrophobic interactions	[177]
	1.5	700	79	1 h				
B-DN	2.3	100	20	1 h	42	DMF treatment and 60 °C heating	Electrostatic and hydrophobic interactions	[62]
Poly(urea-IL-SPMA)-3d	0.6	220	43	5 h	50	Room temperature and 60% RH	Electrostatic interactions and hydrogen bonds	[180]
	1.0	450	70	15 h				
	1.2	650	85	24 h				
PDDA/PEI-PSS/PAAc	0.4	1000	31	2 h	42	Incubated in water at room temperature	Electrostatic and hydrophobic interactions, hydrogen bonds	[136]
	0.7	1700	55	6 h				
	1.2	2430	95	14 h				

network.^[175] After 12 h healing at 25 °C, the damaged hydrogel exhibited 85% healing efficiency (recovery of tensile strength), and the tensile strength reached 1.1 MPa. Sun and co-workers reported that mixing positively charged polyelectrolyte mixtures of poly(diallyldimethylammonium chloride) (PDDA)/branched poly(ethylenimine) (PEI) with negatively charged polyelectrolyte mixtures of poly(sodium 4-styrenesulfonate) (PSS)/poly(acrylic acid) (PAAc) produced a self-healable tough hydrogel with water content of 42 wt%. The polyelectrolyte complex hydrogel exhibited high mechanical performance owing to multiple noncovalent interactions including electrostatic, hydrogen bonding, and hydrophobic interactions, and the damaged hydrogel almost fully restored its original mechanical properties after incubation in wa-

ter for 14 h at room temperature.^[176] It should be noted that water contents of the abovementioned hydrogels were mostly below 70 wt%. Reducing water contents to a moderate level is a prerequisite for preparing mechanically strong and self-healable hydrogels. Representative self-healing strong hydrogels and their performance are summarized and compared in **Table 2** and **Figure 5**, respectively.

2.2.4. Fast Stimuli-Responsive Stiffening/Softening Hydrogels

Inspired by a sea cucumber that rapidly increases the stiffness of its inner dermis upon exposure to a stimulus,^[181] researchers

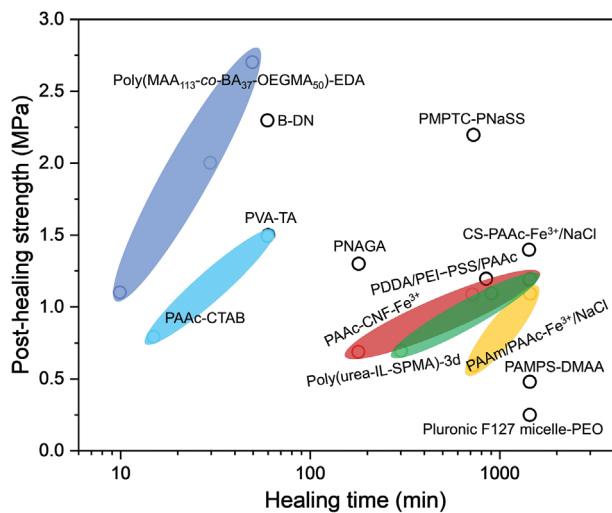


Figure 5. Posthealing strength versus healing time of typical self-healable strong hydrogels. Materials include the PNAGA gel,^[144] Pluronic F127 micelle-PEO gel,^[169] poly(MAA₁₁₃-co-BA₃₇-OEGMA₅₀)-EDA gels,^[171] PAMPS-DMAA gel,^[173] PVA-TA gel,^[174] PAAc-CNF-Fe³⁺ gels,^[175] PAAm/PAAc-Fe³⁺/NaCl gels,^[176] CS-PAAc-Fe³⁺/NaCl gel,^[75] PMPTC-PNaSS gel,^[137] PAAc-CTAB gels,^[177] B-DN gel,^[62] poly(urea-IL-SPMA)-3d gels,^[180] and PDDA/PEI-PSS/PAAc gel.^[136]

attempt to develop mechanically adaptive hydrogels with dynamically changeable stiffness.^[182] Development of stiffness adaptive hydrogels provides opportunities for devising smart wearables and robots. For example, a thermal stiffening hydrogel is soft at room temperature, being wearable without restricting body motions, but exhibits fast stiffening upon activation by frictional heat, therefore protecting the body against friction and heat in an accident.^[183,184] Stimulus-responsive softening and shape changing of a hydrogel microrobot allow it to pass through narrow and confined spaces without suffering mechanical damage to its own body and surrounding soft tissues.^[185] Mechanical properties of hydrogels strongly depend on the crosslinking density, the polymer chain interactions, and the volume fraction. Therefore, physical or chemical stimuli can stiffen or soften a responsive hydrogel by tuning these factors.^[182] In this section, smart hydrogels with mechanical properties responsive to thermal, light, and mechanical stress are discussed. These stimuli have been extensively investigated in the past few years and offer the advantage of easy and rapid manipulation without the need for additional reagents.

Among various environmental stimuli, temperature is the most widely used trigger that can induce gel stiffening or softening. A thermal stiffening hydrogel can instantly self-strengthen with a rapid increase in Young's modulus upon heating, which is highly desirable for load-bearing and self-protection applications at high temperatures. The most studied thermal stiffening hydrogels are based on lower critical solution temperature (LCST)-type polymers such as PNIPAm.^[186] Upon heating above the phase transition temperature (T_c), PNIPAm chains undergo coil-to-globule transition and aggregate to form a rich-polymer percolating framework that largely increase gel stiffness. During phase transition, the coil-to-globule transition at the molecular level usually causes a macroscopic volume shrinkage of hydrogels, i.e., volume phase transition,^[187,188] and thermal stiff-

ening hydrogels based on volume phase transition generally experience a large change in water content and slow recovery speeds. To prevent macroscopic volume contraction of LCST-type hydrogels, hydrophilic polymers are often incorporated to serve as molecular scaffolds to retain the released water at the micro-mesoscales.^[114,189–191] For instance, Guo and co-workers grafted hydrophilic poly(*N,N*-dimethylacrylamide) (PDMA) side chains on a PNIPAm network, and the obtained hydrogel with optimized composition was capable of thermal responsive microphase separation with significant toughening effect under isochoric conditions.^[189] Above T_c , PNIPAm chains collapsed and formed a concentrated load bearing phase, while the swelling of hydrophilic PDMA side chains prevented water from being squeezed out and maintained high water content of 83 wt%. The resulting network topology could be pictured as stiff collapsed PNIPAm domains embedded within a soft and highly hydrated matrix, therefore giving rise to a large increase of elastic modulus. Meanwhile, deformation of the rich PNIPAm phase led to significant energy dissipation and high fracture energy of ≈ 1000 J m⁻². Besides the LCST-type hydrogels, other microphase separation hydrogels have also demonstrated similar thermal stiffening behaviors. As a typical example, Gong and co-workers reported that a poly(acrylic acid)/calcium acetate hydrogel exhibited super-rapid and significant hikes in stiffness by 1800-fold when the temperature increased from 25 to 70 °C, while the volume of the hydrogel was almost unchanged. In the composite hydrogel, the PAAc carboxyl side groups formed dynamic complexes with acetate ions and Ca²⁺ (PAAc-COO⁻...Ca²⁺...⁻OOCCH₃). The hydrophobic acetate moieties dehydrated above 32 °C, which greatly stabilized the ionic bonds among Ca²⁺, the carboxylates, and PAAc side groups. Such a cooperative change of hydrophobic and coordination interaction induced change of the polymer network from a homogeneous state into a polymer dense and sparse phase. Remarkable microphase separation of the hydrogel at 70 °C achieved a significant thermal stiffening behavior, and the Young's modulus reached above 100 MPa (Figure 6a). It is worth mentioning that the thermal stiffening behavior happened very quickly, as the transfer of water was within the polymer network during the phase separation process.^[183] The aforementioned thermal responsive reconfiguration of polymer networks involve enhanced noncovalent interactions and demonstrate the stiffening effect, whereas dissociation of various noncovalent interactions, such as hydrogen bonds,^[141,185,192,193] hydrophobic interactions,^[194,195] and ionic bonds^[138] lead to thermal softening effect. As an example, copolymers of acrylonitrile (AN), AAm, and PEG3kDMA (synthesized from PEG3k and methacryloyl chloride) formed a physically dual-crosslinked hydrogel, containing strong hydrophobic dipole-dipole interactions and weak hydrophilic hydrogen bonds. The hydrogel exhibited reversible softening and stiffening without volume change when subjected to heating (37 °C) and cooling (25 °C), which was attributed to the disassociation/association of dipole-dipole interactions and hydrogen bonds.^[185] The thermal softening temperature could be increased by increasing the content of AN, as the hydrophobic crystalline regions from cyano dipole pairings were less vulnerable to heat.

Photoresponsiveness of hydrogels is usually based on a variation in the degree of crosslinking, which can be triggered by photoreactions, such as cleavage, addition, and

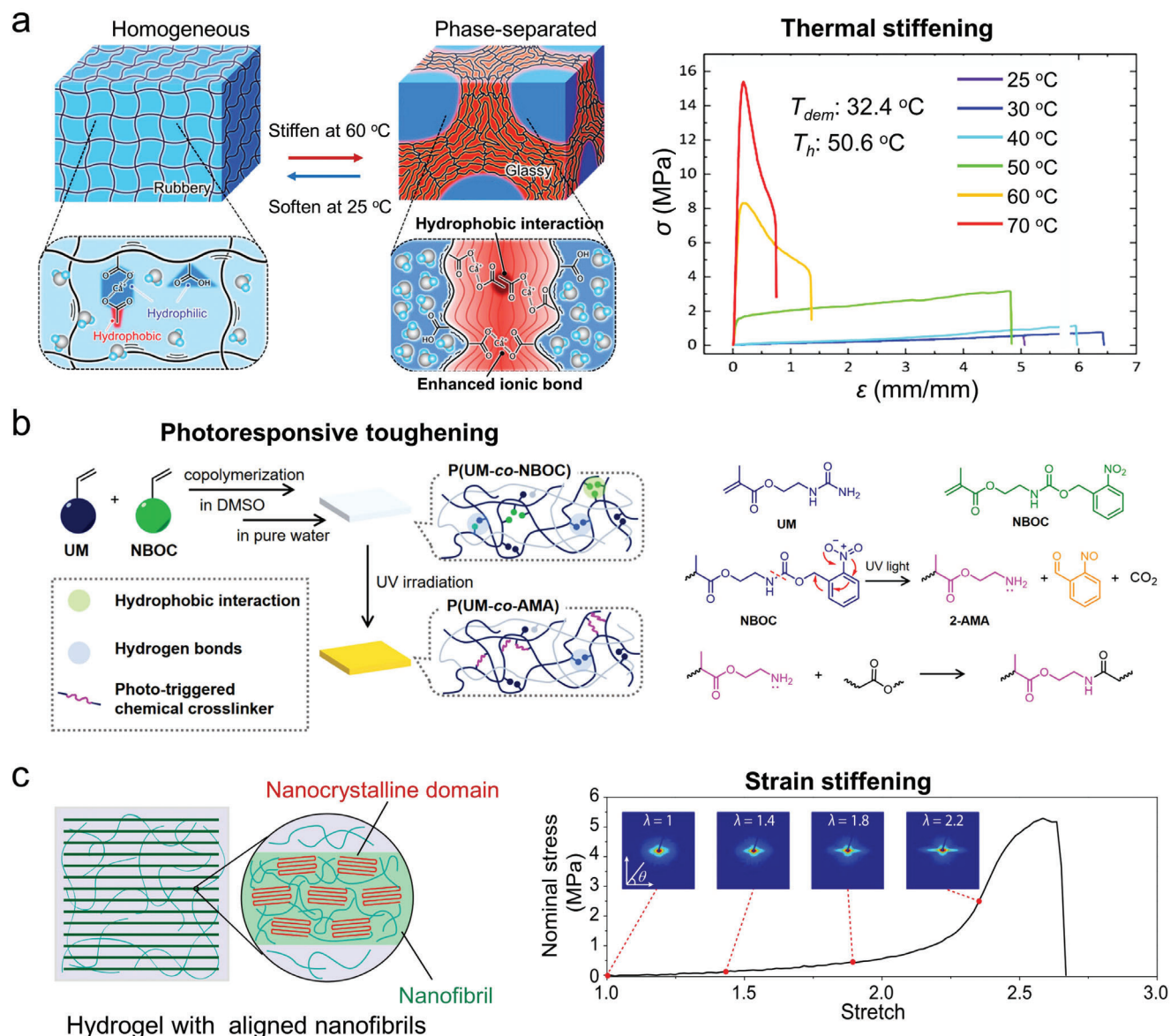


Figure 6. Stimuli-responsive stiffening/softening hydrogels. a) Schematic illustration for the thermal stiffening mechanism of a poly(acrylic acid)/calcium acetate hydrogel and its stress–strain curves at different temperatures. Reproduced with permission.^[183] Copyright 2019, Wiley-VCH. b) Schematic illustration for UV irradiation induced conversion of a poly(UM-co-NBOC) physical hydrogel to a poly(UM-co-AMA) chemical hydrogel and chemical reactions that occur in the polymer network. Reproduced with permission.^[198] American Chemical Society. c) Schematic illustration for a PVA hydrogel with aligned nanofibrillar architectures and its nominal stress versus stretch curve and corresponding SAXS patterns at different stretches. Reproduced with permission.^[93] Copyright 2019, National Academy of Sciences.

isomerization.^[196,197] The commonly employed photoresponsive compounds are nitrobenzyl ester, anthracene, coumarin, azobenzene, and spiropyran derivatives. Nitrobenzyl ester derivatives are the most widely applied photolabile group, and can serve as cleavage-type functional groups in photoresponsive hydrogels. For example, a physical hydrogel was prepared by copolymerization of hydrophilic monomers, 2-ureidoethyl methacrylate (UM), and photoresponsive hydrophobic monomers, 2-nitrobenzyl oxycarbonylaminoethyl methacrylate (NBOC) at high concentrations. The hydrophobic interactions of NBOC acted as dynamic crosslinks, and thus the physical hydrogel was soft and

highly stretchable. Upon UV irradiation, NBOC was irreversibly split with the formation of hydrophilic 2-aminoethyl methacrylate (AMA) and the release of 2-nitrobenzaldehyde and CO₂. Therefore, the original physical crosslinks by hydrophobic interactions of NBOC were destroyed. Meanwhile, the chemical reaction between the amino groups of AMA and the ester bonds of UM led to the formation of new chemical crosslinks (Figure 6b). Such a photoswitching of physical gels to chemical gels enabled a dramatic increase in Young's modulus.^[198] Compared with irreversible photocleavage reactions, photoaddition^[199,200] and isomerization reactions^[201,202] in hydrogels allow for reversible

modulation of mechanical properties by light. For instance, coumari is a well-known light-sensitive molecule that can undergo a [2 + 2] photodimerization under irradiation at 365 nm and decouple with the irradiation of 254 nm light. Sun and co-workers fabricated supramolecular hydrogels via host–guest interactions between coumarin and γ -cyclodextrin. Upon irradiation of 365 nm light, photodimerization of coumari occurred in γ -CD, and thus the host–guest interactions converted to COU–COU covalent interactions. Such a conversion of weak host–guest physical crosslinks to strong chemical crosslinks in hydrogels induced a storage modulus increase of 1.6 MPa. Moreover, the host–guest interactions could be restored when the COU–COU covalent interactions decoupled at 254 nm light irradiation.^[199] In addition to devising photoreactions of molecules belonging to the architecture of polymer networks, photomodulation of mechanical properties of hydrogels can also be achieved by introducing photothermal fillers into thermoresponsive polymer networks. For example, a small amount of graphene oxide was added into an interpenetrating network of chemically crosslinked polyacrylamide and physically crosslinked gelatin. The obtained composite hydrogel with water content of 76 wt% had high mechanical toughness (strength > 400 kPa and fracture strain > 500%), owing to the double network with the sacrificial gelatin network and GO bridging to dissipate energy. Under NIR light irradiation, the temperature quickly increased and caused melting of the thermoresponsive gelatin network, and therefore led to modulus decrease of the hydrogel.^[203]

Similar to the majority of biological tissues, the skin becomes stiff when the applied strain or stress increases, which effectively prevents damage. This strain-stiffening behavior is attributed to the hierarchical structure of skin, in which stiff collagen fibers resist deformation and an interwoven elastin network ensures elastic recoil.^[204,205] Conventional covalent hydrogels composed of flexible polymer chains rarely exhibit strain-stiffening effect, as the chains usually rupture to relieve stress before they get straightened thus causing strain softening. To mimic the biological strain-stiffening behaviors, synthetic hydrogels with modulus-contrast hierarchical structures, such as semiflexible polymer networks,^[206–208] nanofibrillar architectures,^[93,209,210] and polymer networks with high-functionality crosslinks^[118,211,212] have been developed. As a remarkable example, Rowan and co-workers developed hydrogels with semiflexible polymer networks based on polyisocyanopeptides (PICs) grafted with oligo(ethylene glycol) (OEG) side chains.^[206] PICs displayed a helical architecture stabilized by intramolecular hydrogen bonds along the polymer backbone. Owing to the thermoresponsive property of OEG, the modified PIC chains bundled together to generate a transparent hydrogel at an extremely low concentration (0.006 wt%). In a PIC-based hydrogel, the semiflexible network could be conceptualized as an interconnected structure of filaments, regulated by stiffness of the polymers and the bundling process. Under stretching, the filaments will orientate along the stretching direction, thereby leading to a strain stiffening response. PIC-based semiflexible networks usually have mechanical strength in the kPa range which is comparable to soft tissues. To achieve muscle-like high mechanical performance, Zhao and co-workers proposed a strategy of mechanical training to fabricate aligned nanofibrillar architectures in PVA hydrogels.^[93] After 5 cycles of freezing and

thawing process, a microphase separated PVA hydrogel was prepared, which consisted of high concentration of polymer chains in the form of nanofibrils crosslinked by nanocrystalline domains and low concentration of amorphous polymer chains. Subsequently, the freeze-thawed PVA hydrogel was exposed to repeated prestretching in water, which enabled gradual alignment of nanofibrils with aligned nanocrystalline domains. The PVA hydrogel with aligned nanofibrillar architectures (84 wt% water content) exhibited a J-shaped stress–strain response in the direction parallel to the aligned nanofibrils with a fracture stress of 5.2 MPa, suggesting a strain-stiffening behavior (Figure 6c). In situ small angle X-ray scanning measurements under stretching suggested that amorphous polymer chains between the adjacent nanocrystalline domains in the nanofibrils were stretched, and sliding between nanofibrils may also occur. Recently, mechanically strong hydrogels with rigid crosslinking domains were proposed to mimic nonlinear mechanical properties of skins. A circular array of PAAc hydrogels was produced in a sparsely crosslinked PAAm hydrogel matrix by photopolymerization with a photomask, forming an architected polymer network composed of a soft PAAm matrix and stiff blocks of PAAm/PAAc interpenetrating networks.^[213] It was demonstrated that the soft matrix was first straightened under stretching and the stiff domains evolved from circle to spindle as the strain increased. This sequential response resulted in an immense strain-stiffening behavior. The patterned hydrogel showed high strength of 1.20 MPa while maintaining a low initial Young's modulus of 31.0 kPa. Additionally, the tough slide-ring hydrogel discussed in the previous section also exhibited strain-stiffening properties, which was attributed to the strain-induced crystallization effect.^[17]

3. Macro/Microscale Shaping of Mechanically Robust Hydrogels

The significant improvement of mechanical properties based on micro/nanoscale structural engineering has largely broadened the application scope of hydrogels in the last two decades. For emerging biointegrated applications, it is highly desirable to fabricate mechanically robust hydrogels with well-defined shapes and spatially controlled structures. For example, hydrogels with spatially resolved structures can support and direct the growth of cells.^[214] Microminiaturization and precise structuring of conductive hydrogels promote deployment of hydrogels in integrated soft sensor devices and improve their response speeds and sensitivities. Moreover, soft robotic applications require tough hydrogels with customizable shapes and structures. Recent technological advances in hydrogel microfabrication, such as 3D printing,^[215] photolithography,^[216] and microfluidics^[217] have led to the production of hydrogel constructs with precise microstructures. Nevertheless, the conflict between mechanical performance and processability remains a major challenge in hydrogels. The fabrication of tough hydrogels usually requires careful structure optimization through a multistep and time-consuming preparation process, which impedes their deployment for rapid shaping and microstructuring. Development of robust biointegrated hydrogel devices urgently needs processable hydrogels with high mechanical performance. In this section, we review the emerging advances in shaping and microfabrication of tough hydrogels. Three techniques, namely, 3D printing, spinning, and

coating, and the corresponding mechanical performance exhibited by the fabricated hydrogel constructs are discussed.

3.1. 3D Printing

The fabrication of mechanically robust hydrogels with 3D structures mainly employs extrusion- and lithography-based printing,^[218–220] and different printing methods have their own specific requirements for hydrogel inks to achieve printability and shape fidelity. Extrusion-based printing is the most commonly used printing technique for hydrogel materials. Shear-thinning behavior and rapid, reversible sol–gel transition are key factors in defining printability and shape fidelity in extrusion printing. Inks for extrusion usually have a viscosity of 6–30 × 10⁷ mPa s, and show both flow and shape-retention properties, i.e., the shear-thinning.^[221] Shear-thinning occurs under the shearing force, resulting in a sol state of the ink with storage modulus (G') < loss modulus (G'') and ease of extruding. After extrusion, the ink rapidly recovers to the gel state ($G' > G''$) as the shear rate drops, thereby contributing to retention of the printed shape. For lithography-based printing approaches that depend on spatially controlled light irradiation, including stereolithography (SLA) and digital light processing (DLP), inks usually consist of photocrosslinkable hydrogel precursors with a low viscosity of 0.25–1 × 10³ mPa s.^[222] The low viscosity allows for easy moving of printed parts in the ink and facilitates removal of the unreacted ink from pores or narrow negative features within a print. Besides, fast photocrosslinking reaction spatially controlled by light irradiation is the key factor that determines the printability and structural stability postprinting, and therefore hydrogel precursors used for lithography-based printing need to be designed with appropriate photoinitiators. In addition to the abovementioned ink properties required for different printing techniques, hydrogel toughening mechanisms that are compatible with the processing procedures need to be suitably implemented, such as devising inherent high-strength hydrogels or further enhancing hydrogel prints after printing.

Tough interpenetrating networks are usually applied in extrusion-based printing. The hydrogel inks are usually designed with moderate rheology for printing, followed by photoinduced polymerization^[58,223–225] or further enhancement of polymer networks via other strategies.^[226,227] Our group reported manufacturing of 3D tough freeform architectures with interpenetrating networks, during which alginate–Ca²⁺ acted as rheological modifiers in hydrogel inks. Addition of alginate–Ca²⁺ transformed a water-like monomer ink into a viscoelastic hydrogel, and mechanically reversible ionic crosslinking of the hydrogel featured fast and responsive association/dissociation, leading to a desired shear-thinning behavior (Figure 7a).^[228] Compared with fragile PAAm hydrogels, tough PAAm–alginate prints were able to tolerate crushing tests (Figure 7b). Extrusion-based printing of tough hydrogel constructs with different interpenetrating networks, such as jammed microgel–PAM networks,^[224] PVA–CS double physical networks,^[226] and phenol-modified alginate based covalent and physical networks^[225] were reported. Tough supramolecular hydrogel prints containing microdomains composed of polymer chains with strong physical interactions such as hydrogen bonds^[229,230] and electrostatic interactions,^[231,232] were fabricated

by extrusion printing. For example, Liu and co-workers printed diverse PNAGA hydrogel based 3D structures by utilizing the thermoplasticity of hydrogen bonding networks. The hydrogel ink consisted of low-strength PNAGA, NAGA monomer, and photoinitiator, which was a gel state at room temperature. Before printing, the ink was heated to 80 °C, which was 10 °C lower than the gel–sol transition temperature. When air pressure was applied to the ink, the gel–sol transition would occur enabling smooth extrusion, and the reformed hydrogel deposited on the platform at room temperature could well retain its printed shape (Figure 7c). After UV irradiation induced polymerization of the NAGA monomers, 3D-printed PNAGA hydrogel constructs were obtained, which exhibited excellent mechanical strength owing to the strong hydrogen bonds among dual amide motifs (Figure 7d).^[229] In addition, a few 3D tough hydrogel architectures based on macroscale heterogeneous hydrogel structures were fabricated via lithography-based printing.^[96,233–235] Tang and co-workers reported a heterogeneous hydrogel consisting of a stiff hydrogel skeleton by stereolithography and a soft hydrogel matrix by casting, and the two polymer networks entangled topologically (Figure 7e). When the heterogeneous hydrogel was stretched, the compliance of the soft matrix diffused the stress in the stiff skeleton (Figure 7f). Upon rupture, the energy stored in the entire hydrogel structure was dissipated. This stress deconcentration led to high toughness. The heterogeneous hydrogel ruptured at a large stretch and had toughness of 4599 ± 545 J m⁻², much higher than that of the homogeneous stiff hydrogel (710 ± 19 J m⁻²) and the soft hydrogel (186 ± 41 J m⁻²). A heterogeneous hydrogel construct in the shape of a human heart valve could bear cyclic pressure without failure up to 50 000 times.^[233] DLP-based multimaterial printing was reported to fabricate complex heterogeneous 3D structures consisting of acrylamide–PEGDA hydrogels covalently bonded with diverse UV curable polymers.^[235] The rigid polymer structures increased the material stiffness with reasonably good stretchability, and mechanical properties of the hydrogel composites could be further tuned by adjusting the geometries of their rigid skeletons. Gradient stiffness was achieved in a lattice structure-reinforced hydrogel by reducing the rod diameter from bottom to top (Figure 7g).

3.2. Spinning

Hydrogel spinning techniques have been developed to fabricate fiber-based constructs, which feature light weight, high length-to-diameter ratio, high deformability, good weavability and knittability for biointegrated applications.^[236,237] Nevertheless, the fabrication of hydrogel fibers is still challenging owing to the infeasibility to obtain spinning dopes by dissolving or melting crosslinked hydrogels. Benefiting from the progress in fiber manufacturing techniques recently, mechanically robust hydrogel fibers have been fabricated by utilizing newly established hydrogel spinning strategies, including draw spinning,^[109,164,165,238–245] wet spinning,^[246–251] microchannel integrated spinning,^[54,252–255] and electrospinning.^[256–261] Dilute hydrophilic polymer solution or monomer precursor solution were used as spinning dope, and rational filamentation and toughening strategies were employed. Dilute hydrophilic polymer solution with well-designed components was usually utilized as spinning dope in a draw

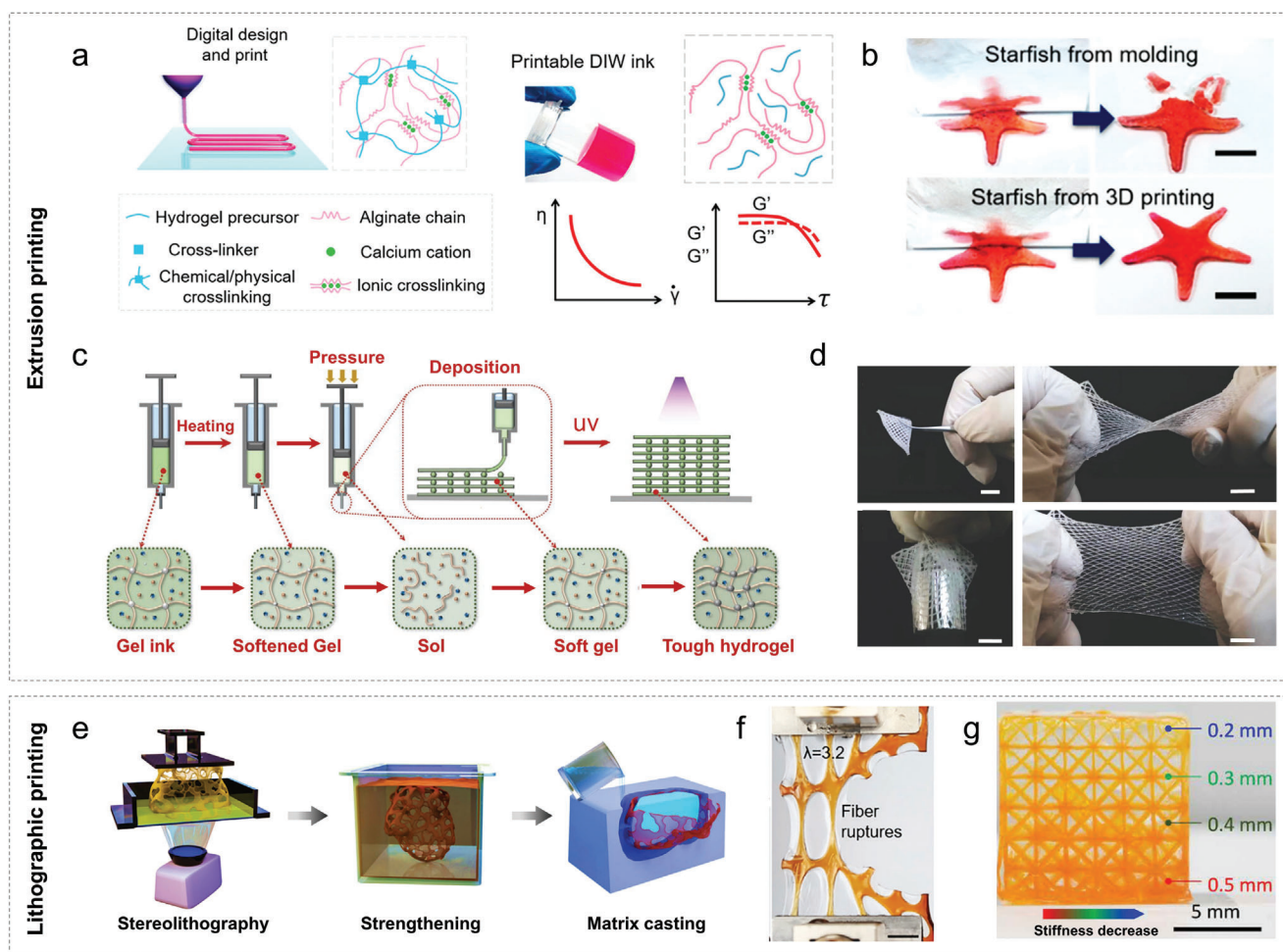


Figure 7. 3D printing of mechanically robust hydrogel constructs. a) Extrusion-based printing of tough hydrogel architectures with interpenetrating networks by using alginate- Ca^{2+} as a rheological modifier. b) Crushing tests on a PAAm starfish hydrogel (top) and a PAAm-alginate starfish hydrogel print (bottom). (a,b) Reproduced with permission.^[228] Copyright 2019, American Chemical Society. c) Extrusion-based printing of supramolecular PNAGA hydrogel constructs by utilizing thermoplastic hydrogen bonding networks and d) printed robust hydrogel webs. (c,d) Reproduced with permission.^[229] Copyright 2021, Wiley-VCH. e) Fabrication of tough heterogeneous hydrogels consisting of a stiff hydrogel skeleton by stereolithography and a soft hydrogel matrix by casting and f) a fracture image of a heterogeneous hydrogel. (e,f) Reproduced with permission.^[233] Copyright 2021, Elsevier. g) A rigid lattice structure-reinforced hydrogel with gradient stiffness. Reproduced with permission.^[235] Copyright 2021, AAAS.

spinning and electrospinning process. Liu and co-workers prepared hydrogel dope composed of PAAc crosslinked by vinyl-functionalized silica nanoparticles, which could be directly drawn into fibers using a steel rod, and the obtained fibers were further reinforced by adding ions and inserting twist (Figure 8a). The resultant hydrogel fibers were covalently crosslinked by silica nanoparticles and reinforced by coordination interaction and twisting, generating mechanical strength, modulus, and toughness comparable to that of natural spider silk.^[164] By utilizing the electrospinning technique, Zhao and co-workers attempted to fabricate tough and strong nanofibrous hydrogels that mimic the bouligand structure of the natural hydrogel in the lobster underbelly.^[256] Five layers of aligned nanofibrous PVA films prepared by electrospinning were assembled into a helicoidal architecture, in which each layer was rotated by a certain degree relative to the adjacent one. After electrospinning, the multilayered bouligand-type nanofibrous PVA was welded in a high-humidity

environment to produce strong interfaces between the adjacent layers, followed by a dry annealing process to introduce substantial nanocrystalline domains in the nanofibers. The high crystallinity and strong interface led to high mechanical performance of the nanofibrous hydrogel, and the bouligand structure further enhanced nominal strength up to 8.4 MPa. Conventional industry used wet spinning technique based on nonsolvent-induced phase separation can hardly prepare covalently crosslinked hydrogel. UV curing is usually introduced in recent development of continuous wet spinning of hydrogel fibers containing covalent networks. To fabricate tough double network hydrogel fibers with chemical and physical crosslinks, spinning dope containing poly(ethylene glycol) diacrylate, 2-hydroxyethyl acrylate (HEA), alginate, and photoinitiator were spun into a CaCl_2 coagulation bath under a UV light, forming a double network hydrogel fiber consisting of a covalently crosslinked poly(PEGDA-co-HEA) network and an ionically crosslinked alginate- Ca^{2+} network.^[247] The

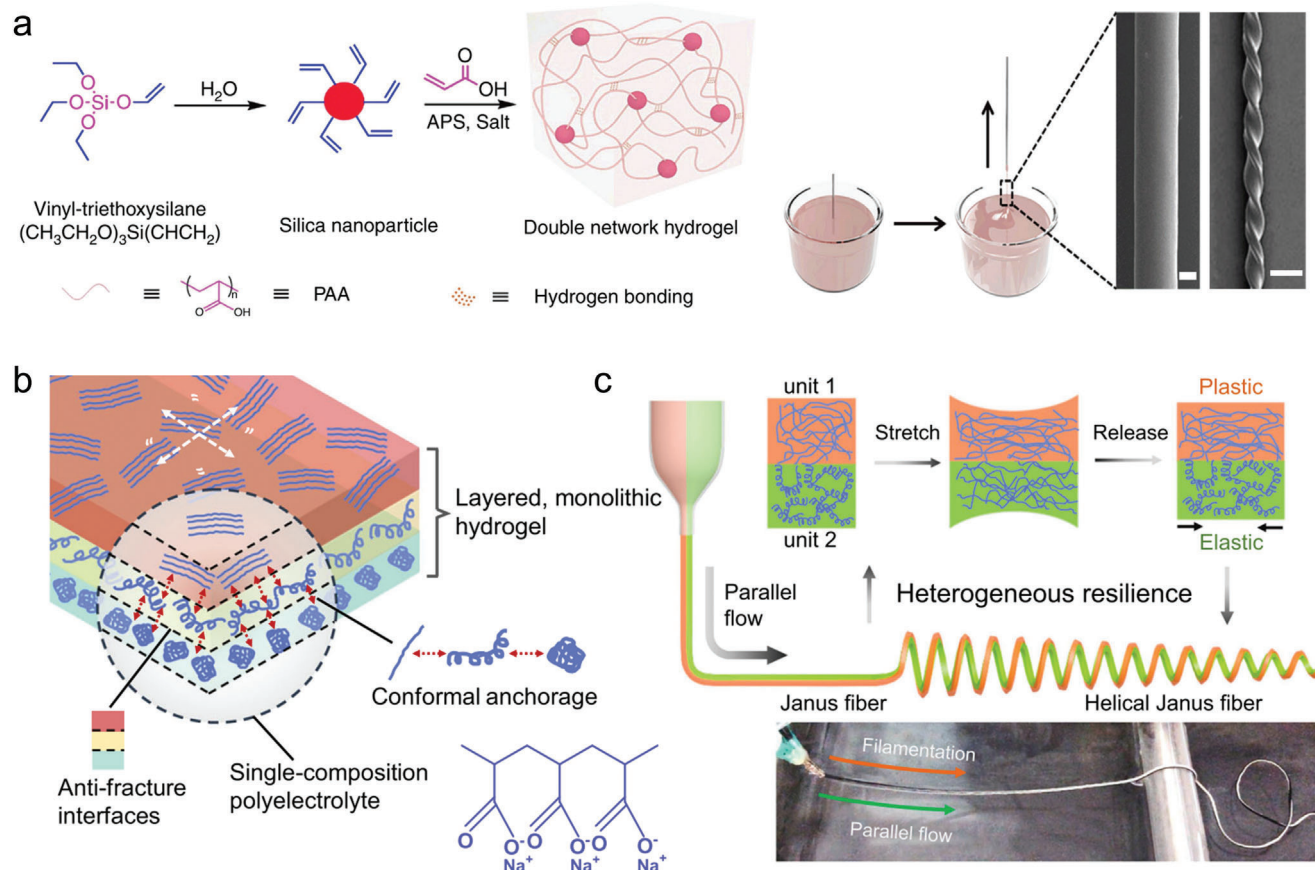


Figure 8. Spinning of mechanically robust hydrogel fibers. a) Draw spinning of PAAc hydrogel fibers crosslinked by vinyl-functionalized silica nanoparticles. Reproduced with permission.^[164] Copyright 2019, Springer Nature. b) Schematic of layered, monolithic PANa-based hydrogel fibers of varied macromolecule conformations. c) Microchannel-integrated spinning of PANa-based Janus fibers followed by a strain programming process for the fabrication of helical fibers. (b,c) Reproduced with permission.^[54] Copyright 2022, Springer Nature.

prepared hydrogel fiber with water content partially replaced by glycerin was highly stretchable and resilient, and exhibited antifreezing capability and air stability. Compared with the usual single-fiber structures prepared by draw spinning or wet spinning, microchannel-integrated spinning enables preparation of multicomponent and mutimaterial fibers. In this respect, our group recently reported microchannel-integrated spinning of sodium polyacrylate (PANa) hydrogel fibers with mechanical properties determined by the macromolecule conformation of PANa. Polymorphic structures such as fibers, ribbons, Janus fibers, multilayered fibers, and core-shell fibers were prepared by changing the geometry of the microchannels. Diameter controllable helical fibers could be fabricated by strain programming of the Janus fibers consisting of two kinds of microfibrillar units with mismatched mechanical resilience (Figure 8b,c).^[54] Table 3 summarizes representative mechanically robust hydrogel fibers fabricated via various spinning techniques.

3.3. Coating

Hydrogel coatings on medical devices can endow the coated bulk devices with new functions such as drug delivery, lubricity, anti-

biofouling, and conductivity.^[262] Coating hydrogels on substrates with complex shapes is challenging due to the poor processibility of hydrogels and their precursor monomer solution. In addition, strong adhesion to the substrate is required to prevent delamination of hydrogel coatings under cyclic swelling or repeated sliding against the surroundings. The adhesion of hydrogels to other substrates by simple attachment is usually low owing to the presence of abundant water at the interface. Robust hydrogel coating requires high toughness of the hydrogel matrix, as well as strong interfacial interaction between the hydrogel and the target substrate,^[263,264] which can be achieved by utilizing mechanisms such as covalent bonding,^[263,265,267] interfacial interpenetration,^[268–271] and polymer connection.^[272–275] The commonly used covalent bonds are based on functional silanes, such as 3-(trimethoxysilyl) propyl methacrylate (TMSPMA) and (3-aminopropyl) triethoxysilane (APTES). The alkoxy groups at one end hydrolyze into silanol groups in an aqueous environment and condense with hydroxyl groups on the substrate to form siloxane bonds, and the other end vinyl groups of TMSPMA are able to copolymerize with vinyl groups in hydrogel coating precursors. For APTES, the other amino end groups can condense with carboxyl groups in hydrogels containing alginate or hyaluronan by EDC–Sulfo–NHS chemistry. Zhao and

Table 3. Mechanically robust hydrogel fibers prepared based on different spinning techniques and reinforcing strategies

Spinning methods	Hydrogels	Fiber forms	Reinforcing factors	Mechanical properties	Stretching speeds	Refs.
Draw spinning	Ion-doped SiO ₂ -PAAc	Twisted core-sheath fiber	Covalent crosslinking by SiO ₂ , coordination complex and twist	Tensile strength = 895 MPa; tensile strain = 44%; Young's modulus = 28.7 GPa; toughness = 214 MJ m ⁻³ .	Strain rate = 0.278 s ⁻¹	[164]
	MPAH	Core-sheath fiber	Reversible polymer chain alignment	Tensile strength = 5.6 MPa; tensile strain = 1180%; toughness = 26.8 MJ m ⁻³ .	Stretching rate = 100 mm min ⁻¹	[238]
	Poly(AAm-co-AAc)-Fe ³⁺ with glycerol	Fiber	Coordination complex	Tensile strength = 1.2 MPa; tensile strain = 500%; Young's modulus = 0.27 MPa.	Stretching rate = 10 mm min ⁻¹	[239]
	Poly(DMAAc-co-OEGMA)-clay with glycerol	Fiber	Noncovalent crosslinking by clay and postdrawing	Tensile strength = 7.2 MPa; tensile strain = 164%; Young's modulus = 16.1 MPa.	Strain rate = 0.083 s ⁻¹	[240]
	PDMAEA-Q /PMAA	Fiber	Hydrogen bond clusters	Tensile strength = 11.6 MPa; tensile strain = 219%; Young's modulus = 428 MPa; toughness = 19.8 MJ m ⁻³ .	Strain rate = 0.02 s ⁻¹	[165]
Wet spinning	ABA triblock copolymer	Fiber	Hydrophobic interaction and strain programmed crystallization	Tensile strength = 15.5–146.2 MPa; tensile strain = 170–900%; Young's modulus = 353–608.2 MPa; toughness = 103.2–121.2 MJ m ⁻³ .	Strain rate = 0.05 s ⁻¹	[246]
	Poly(PEGDA-co-HEA)-alginate with glycerol	Fiber	Covalently ionically crosslinked double network	Tensile strength = 0.2 MPa; tensile strain = 400%.	Stretching rate = 25 mm min ⁻¹	[247]
	PNA@PMA	Core-sheath fiber	Hydrogen bonding	Tensile strength = 2.25 MPa; tensile strain = 840%.	Stretching rate = 50 mm min ⁻¹	[248]
	HPIFs-CaCl ₂	Fiber	Coordination complex	Tensile strength = 2.5 MPa; tensile strain = 215%.	Stretching rate = 20 mm min ⁻¹	[251]
Microchannel-integrated spinning	Poly(PEGDA-co-AAm)@alginate	Core-sheath fiber	Core-sheath dimension	Tensile strength = 0.3–0.79 MPa; tensile strain = 35–63%; Young's modulus = 0.61–2.58 MPa.	Strain rate = 0.003 s ⁻¹	[252]
	PAMPS-PAAm-TEG	Fiber	Hydrogen bonding	Tensile strength = 5.6 MPa; tensile strain = 159%.	Stretching rate = 200 mm min ⁻¹	[255]
	PANa-based multicomponent hydrogel	Fiber; ribbon; core-sheath; Janus and helical fiber	Aggregated macromolecule conformation	Tensile strength = 1–50 MPa; tensile strain = 5–2530%; Young's modulus = 0.24–2050 MPa; toughness = 1.7–17.8 MJ m ⁻³ .	Strain rate = 0.033 s ⁻¹	[54]
Electrospinning	PVA	Bouligand-type fibrous film	High crystallinity and bouligand-type alignment	Tensile strength = 8.4 MPa; tensile strain = 640%.	Stretching rate = 300 mm min ⁻¹	[256]
	ANF-PVA	Fibrous film	Crystallinity and hydrogen bonding	Tensile strength = 3.3–5.5 MPa; tensile strain = 30–90%; Young's modulus = 10.7–15.4 MPa.	Strain rate = 0.005 s ⁻¹	[257]
	Multiurea linkage segmented PUU	Fibrous film	Hydrogen bonding and hydrophobic interaction	Tensile strength = 2.5 MPa; tensile strain = 370%.	Stretching rate = 50 mm min ⁻¹	[261]

co-workers first reported tough bonding of hydrogels on diverse nonporous solid materials by covalently anchoring tough dissipative hydrogels onto the substrates.^[263] The chemical anchorage resulted in high intrinsic work of adhesion and significant energy dissipation of bulk double network hydrogel during detach-

ment, leading to interfacial toughness over 1000 J m⁻². Recently, to improve the processibility of covalent bonding-based hydrogel coatings, polymer-based hydrogel coating precursor were developed.^[266,276] As an example, a viscous hydrogel paint was proposed, which consisted of copolymers of hydrogel monomers

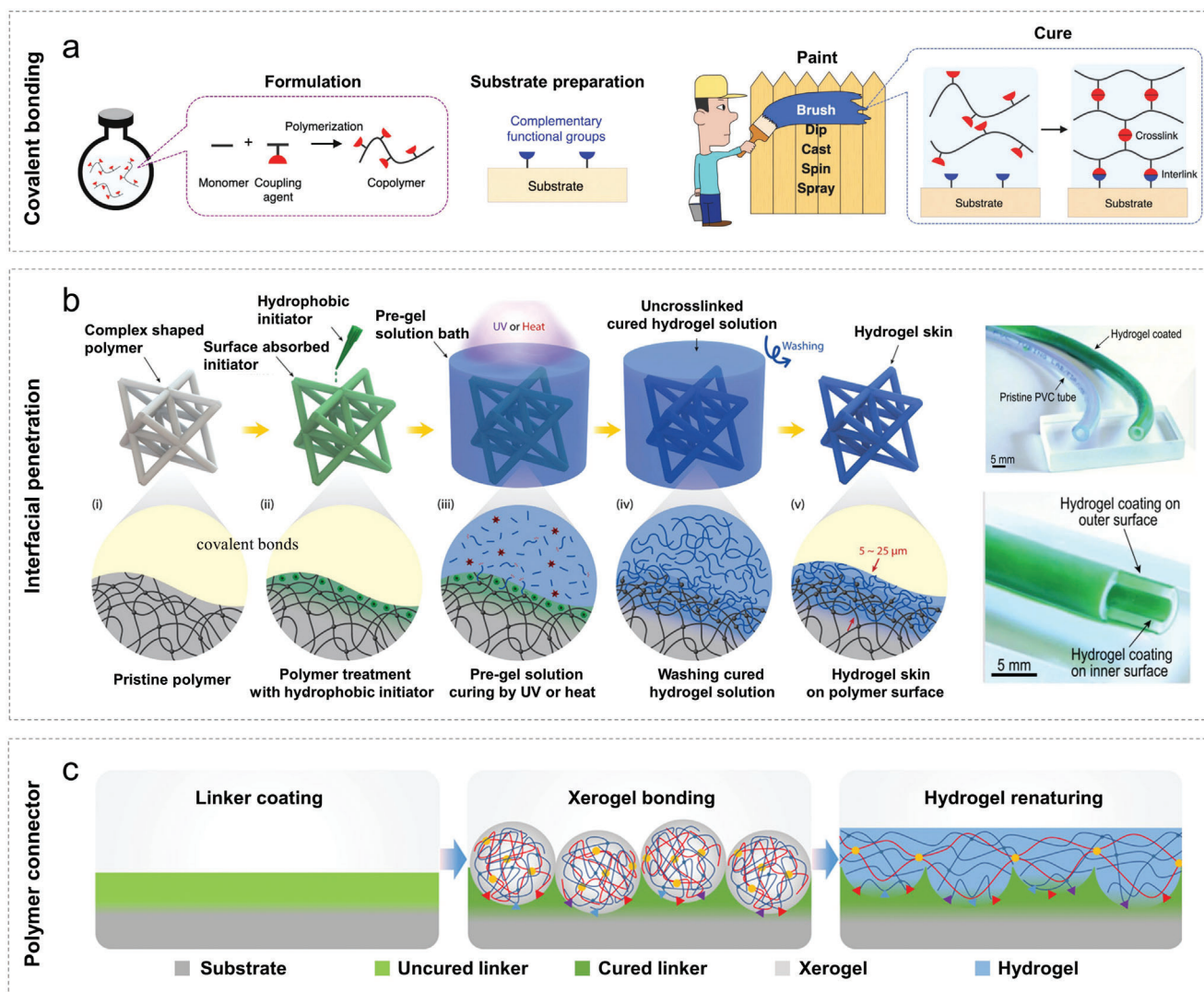


Figure 9. Hydrogel coatings. a) A viscous copolymer paint consisting of hydrogel monomers and TMSPMA, and condensation based reactions of the paint that crosslink the hydrogel and bond the hydrogel coating and the substrate. Reproduced with permission.^[266] Copyright 2019, Wiley-VCH. b) Hydrogel skins formed on complex polymer substrates via hydrophilic initiators induced polymerization and hydrophobic initiators induced interpenetrations. Reproduced with permission.^[268] Copyright 2018, Wiley-VCH. c) Adhering dehydrated xerogel particles to a surface with a polymer connector layer, followed by formation of a hydrogel coating after rehydration of the xerogel particles. Reproduced with permission.^[275] Copyright 2021, AAAS.

and TMSPMA. The condensation of silanol groups in hydrolyzed TMSPMA molecules crosslinked copolymer chains in the paint, producing a hydrogel coating, and their condensation with hydroxyl groups on the target substrate formed siloxane bonds that interlinked the hydrogel coating to the substrate (Figure 9a).^[266] Interpenetration between two polymer networks at the hydrogel–solid interface can be formed when the substrate surface is permeable to the polymer chains of hydrogels or bonding agents. Notably, most polymer substrates are hydrophobic. When a polymer substrate with absorbed hydrophobic initiators such as benzophenone and benzoyl peroxide was immersed in a hydrogel monomer solution, the hydrophobic initiators served as grafting agents for the hydrogel polymers to crosslink with the substrate polymer chains. Meanwhile, hydrophilic initiators induced the polymerization of monomers above the substrate into a hydro-

gel coating. This surface initiation method led to hydrogel–solid interfacial bonding via polymer entanglements at the molecular level (Figure 9b).^[268] It was demonstrated that the interpenetration of the substrate and hydrogel chains led to a significant increase in mechanical robustness of the hydrogel coating, analogous to double network tough hydrogels. Besides, introducing a polymer layer easily bonded to the solid surface as a connector between the hydrogel and the solid substrate is another effective strategy for preparing robust hydrogel coatings. Polymers such as epoxy,^[275] cyanoacrylate,^[272] polydopamine,^[273] and cellulose acetate^[274] were developed as connector layers. For example, uncured fluidic epoxy resin was sprayed on the surface of a specific substrate followed by an immediate coverage of xerogel particles. A hydrogel layer was formed after the xerogel particles were re-natured in the presence of water. The epoxy cured together with

the xerogel particles, and the resultant “key-lock” structures enhanced the stability of the hydrogel coating (Figure 9c).^[275]

4. Toward Wearable and Implantable Applications

The intrinsic features of hydrogels such as softness, wetness, and biocompatibility make them especially suitable for applications that are in close contact with biological organisms. As discussed above, the exploitation of new polymer networks and processing techniques enables the development of mechanically robust and functional hydrogels with customizable shapes, leading to their deployment in biointegrated applications. In this part, we provide a discussion on the recent progress of biointegrated hydrogel devices in biomedical, bioelectronic, artificial muscle, and soft robotic applications, and the mechanical functionality and shape adaptivity of hydrogels in different application scenarios are highlighted.

4.1. Biomedical

Tissue engineering combines cells, scaffolds, and growth factors to construct functional artificial tissues or organs.^[3] Facile tunability in chemical compositions and physical properties makes hydrogels suitable for application as bioactive scaffolds that provide chemical cues and mechanical supports for tissue regeneration. Tough hydrogels can provide superior mechanical properties comparable to that of natural tissues such as the cartilages, skins, and vessels, and hold great potential in the construction of acellular or cell-laden scaffolds for cartilage tissue engineering.^[277,278] The mechanical properties, biocompatibility, bioactivity, and biodegradability of tough hydrogels are usually studied for those applications. A DN hydrogel composed of poly(2-acrylamido-2-methylpropanesulfonic acid) and poly(*N,N'*-dimethyl acrylamide) (PAMPS/PDMAAm) was developed as a promising material for making articular cartilage scaffolds, which exhibited high mechanical strength and wear resistance comparable to that of clinically available ultrahigh molecular weight polyethylene.^[279,280] The experimental results revealed that the PAMPS/PDMAAm hydrogel was bioactive and induced cell infiltration in the muscle tissue without any toxic effects for 6 weeks. Moreover, type 2 collagen, aggrecan, and SOX9 mRNAs were highly expressed in the chondrogenic ATDC5 cells cultured on the gel surface, indicating a spontaneous regeneration of the articular cartilage.^[281] 3D printing is particularly useful for tissue engineering applications, as it can generate biomimetic architectures with customized complex macro/microstructures and with direction-dependent properties.^[282,283] Biomaterialized tough hydrogels were synthesized by a one-step visible-light-mediated nano-biomineralization strategy via a rational design of a phosphate source and ruthenium photochemistry, which allowed for facile fabrication of tough hydrogel architectures via 3D printing.^[284–287] The biomaterialized tough hydrogels exhibited high bioactivity and good adhesion to bone mesenchymal stem cells, and the expression of vital osteogenic markers alkaline phosphatase were increased by a factor of 1.2 to 3 on the biomaterialized tough hydrogels compared to blank hydrogels without biomineralization (Figure 10a). This enhance-

ment was attributed to the high elastic modulus (≈ 800 kPa) and improved bioactivity via biomineralization, and the 3D architectures provided improved tissue breathability and nutrition delivery, beneficial for skin repair and bone regeneration. It is noted that the existing tough hydrogels with high strength and toughness are primarily applied for acellular scaffolds, as their stiff sub-micrometer- or nanosized gel networks usually suffer from limited supply of oxygen and nutrients, which inhibits the proliferation and differentiation of encapsulated cells. 3D printed hydrogels have shown great potential to overcome this problem by forming macropores within scaffolds.^[58,288–291] As an example, a bilayer biohybrid gradient hydrogel scaffold with transforming growth factor β 1 loaded on the top layer and β -tricalciumphosphate incorporated on the bottom layer was fabricated by thermal-assisted extrusion printing technique.^[290] The biohybrid hydrogel scaffold featured highly interconnected porosity, desirable mechanical properties, and excellent biocompatibility, facilitating the attachment, spreading, and chondrogenic and osteogenic differentiation of human bone marrow stem cells in vitro (Figure 10b).

Tissue adhesives are widely used for wound management and tissue repair.^[4,5,292–294] In addition to excellent biocompatibility and strong adhesion to the surface of tissues, tissue adhesives are required to be mechanically tough to withstand dynamic movements. As a remarkable example, a two-layer tough adhesive hydrogel consisting of an adhesive surface and a dissipative matrix was designed, which adhered strongly to porcine skin, cartilage, heart, artery, and liver.^[264] The adhesive layer such as chitosan that contains positively charged primary amine groups, could adhere to the tissue surface via electrostatic attractions, enabling amine groups to bind covalently with carboxylic acid groups from the PAAm–alginate DN hydrogel matrix and the tissue surface. Therefore, the two-layer hydrogel adhesive integrated high adhesion energy with high matrix toughness simultaneously. The hydrogel adhesive was compliant and conformed closely to the geometry of the myocardium, capable of bearing tens of thousands of inflation–deflation cycles, and no leakage was observed under strains up to 100% (Figure 10c). Recently, a dry double-sided tape (DST) made from a combination of a biopolymer (gelatin or chitosan) and crosslinked poly(acrylic acid) grafted with *N*-hydroxysuccinimide ester (PAAc-NHS ester) was designed to enable fast adhesion of wet tissues and devices.^[267] The PAAc-NHS ester facilitated quick hydration and swelling of the DST to dry the wet surfaces of various tissues under gentle pressure of ≈ 1 kPa, and the carboxylic acid and NHS ester groups enabled strong adhesion to tissues. Besides, the swollen DST hydrogel integrated mechanisms for high stretchability and energy dissipation, achieving tough adhesion to wet and dynamic tissues.

In addition, hydrogel fiber-based optical light-guides have received interests for applications such as deep-tissue biosensors, optogenetic stimulation, and photomedicine due to their excellent biocompatibility and tissue-like modulus.^[295,296] For example, the core–sheath hydrogel fiber optical waveguide with an optimized composition reached transmittance of $\approx 90\%$ in most of the visible region, and exhibited tissue-like modulus of 0.61–2.58 MPa, and excellent biocompatibility.^[252] In the experiment of in vivo cancer therapy, the tumor irradiated with a 915 nm near-infrared laser via the hydrogel fibers exhibited fast temperature increase to 48 °C, confirming that they could serve as an effective

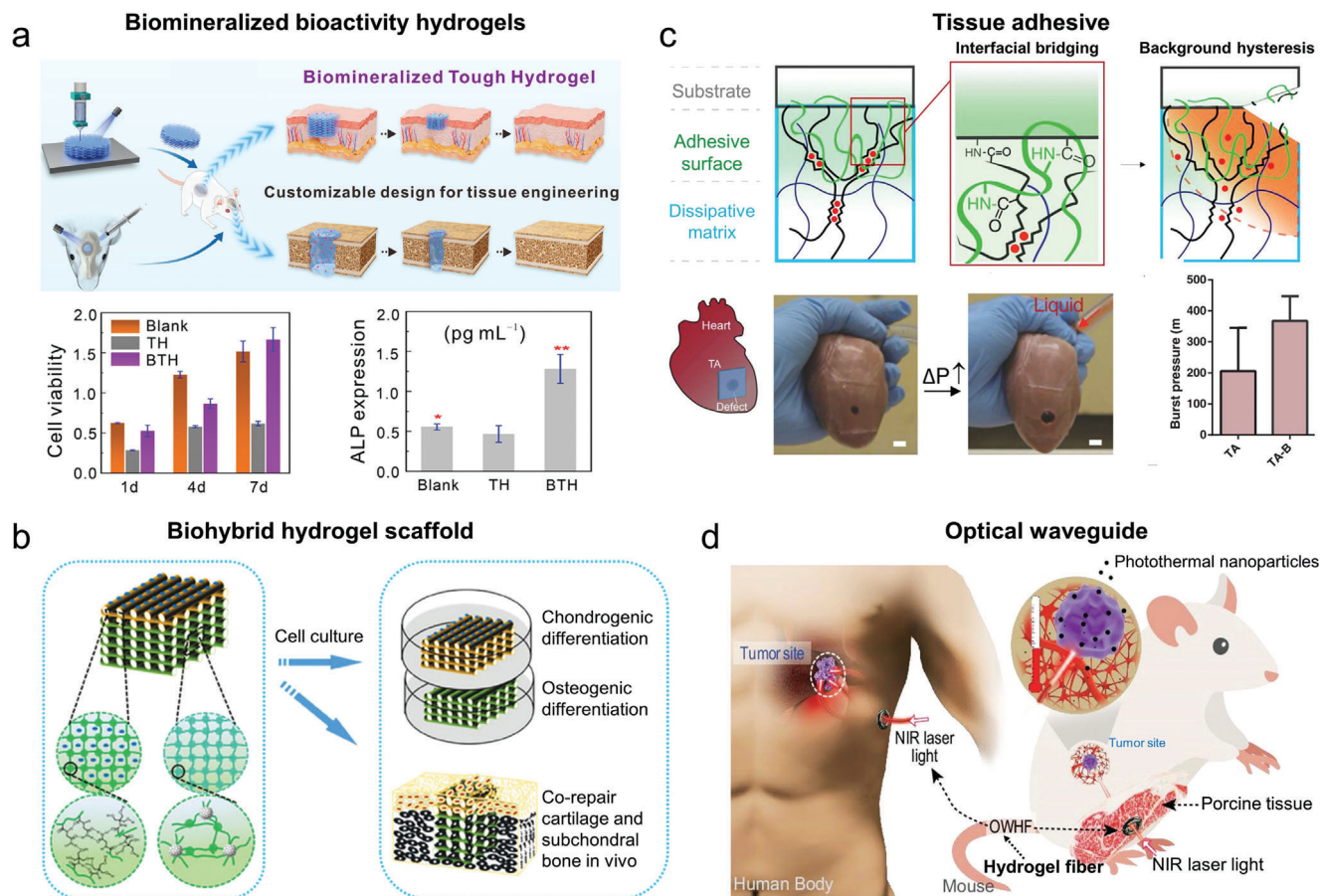


Figure 10. Biomedical applications of mechanically robust and functional hydrogels. a) Biomaterialized tough hydrogel constructs for tissue engineering, showing high bioactivity and enhanced expression of vital osteogenic markers. Reproduced with permission.^[284] Copyright 2022, American Chemical Society. b) A bilayer biohybrid gradient hydrogel scaffold that facilitates in vivo corepair of cartilage and subchondral bone. Reproduced with permission.^[290] Copyright 2018, Wiley-VCH. c) A tough myocardium adhesive hydrogel composed of an adhesive surface and an energy dissipative matrix, capable of withstanding repetitive inflation–deflation cycles without leakage. Reproduced with permission.^[264] Copyright 2017, AAAS. d) An optical waveguide hydrogel fiber delivering laser signals for in vivo photothermal therapy. Reproduced with permission.^[252] Copyright 2020, Oxford University Press.

vehicle for the delivery of laser signals and energy deep into the organisms for deep-tissue photomedicine such as photothermal therapy (Figure 10d).

4.2. Bioelectronics

In recent years, hydrogels have aroused great interests in developing a new generation of soft bioelectronic devices that are established on human skins or inside the bodies, owing to their similarities to biological tissues and versatility in electrical, mechanical, and biofunctional properties.^[8,297–300] Wearable on-skin bioelectronics are capable of real-time, noninvasive monitoring of physiological signals including physical, electrical, and chemical signals that reflect the overall health and fitness conditions.^[301–303] However, one of the most common challenge for on-skin bioelectronics is device fatigue, fracture, and detachment due to body motions, resulting in deterioration and failure of device functions. Recent progress in tough and mechanically functional hydrogels provide potential solutions to this challenge, and diverse shaping of tough hydrogels further en-

ables enhanced properties such as high stretchability, high permeability, and compliance to curved surfaces that are highly desirable for wearable functions.^[304–308] Zhao and co-workers recently developed a conductive polymerizable rotaxane hydrogel (PR-Gel), in which polymerizable pseudorotaxane composed of acrylated β -cyclodextrin and bile acid via host–guest interactions was copolymerized with acrylamide.^[18] The pseudorotaxane generated a large number of mobile junctions in the hydrogel similar to that of slide-ring hydrogels. Therefore, the hydrogel exhibited high stretchability up to 830%, and no significant hysteresis was observed under cycled strains of 300%. The high stretchability and fatigue resistance facilitated its usage for long-term and stable monitoring of large strains (Figure 11a). Meanwhile, 3D printed PR-Gel based on-skin electrodes could detect human electrocardiogram (ECG) signals in real time with high stability (Figure 11b). Facile fabrication of thin-film tough hydrogels with controlled thickness in the micrometer scale is highly desirable as it provides permeable and low-impedance substrates for on-skin electronics. Kim and co-workers fabricated an ultra-thin PAAm hydrogel film ($\approx 150 \mu\text{m}$), which worked as a tissue-like skin–device interface with high mass-permeability and

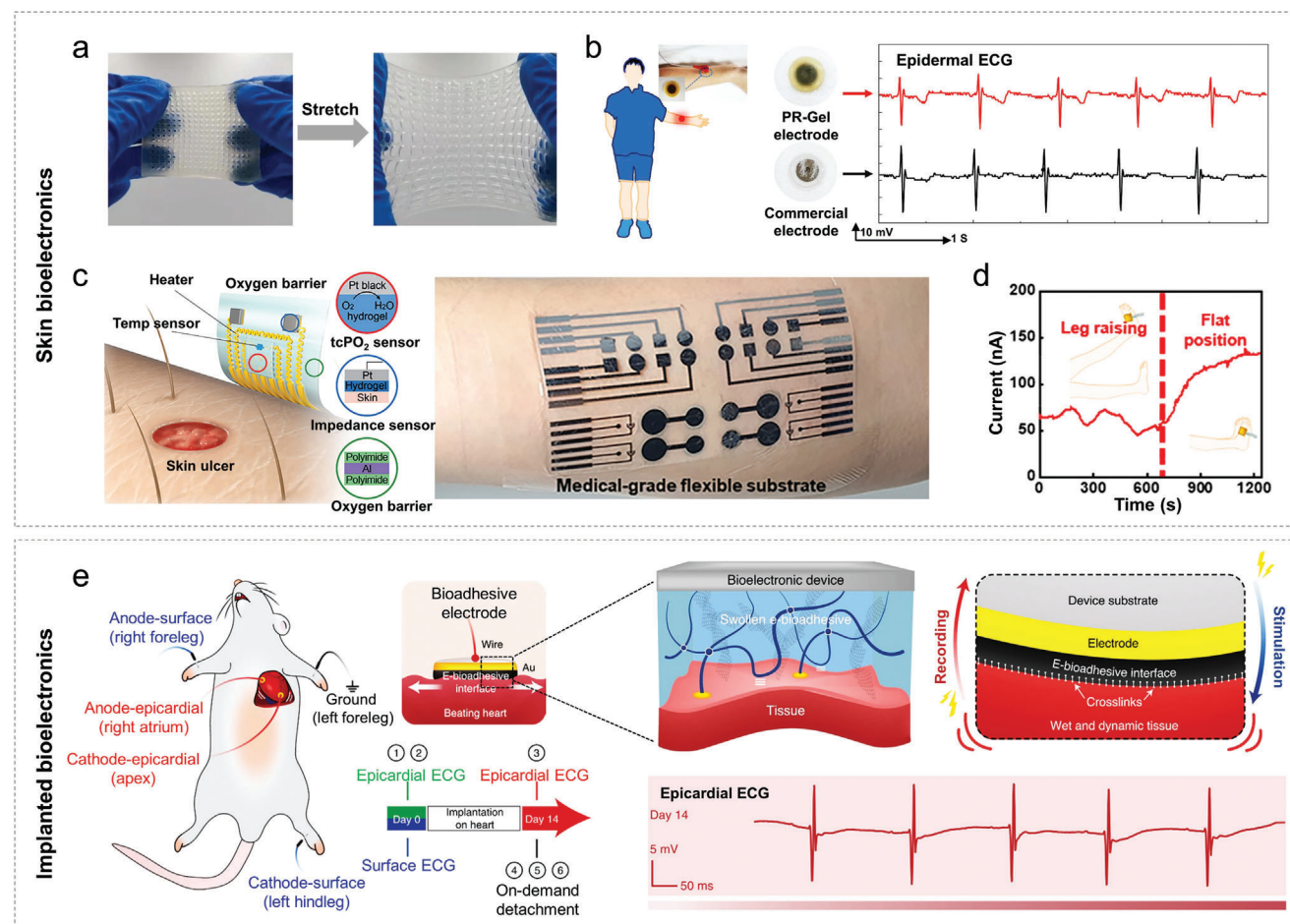


Figure 11. Mechanically robust and functional bioelectronic hydrogel devices. a, b) A 3D printed highly stretchable and resilient PR-Gel based on-skin electrode that stably detects epidermal ECG. Reproduced with permission.^[18] Copyright 2023, Springer Nature. c) Illustration of wearable transcutaneous biosensors for the measurement of tcPO₂ and local tissue impedance, and a photo of the integrated device on human skin. d) In vivo tcPO₂ measurement for various leg positions. (c,d) Reproduced with permission.^[307] Copyright 2021, AAAS. e) An implanted bioelectrode based on an electrical bioadhesive hydrogel interface that monitors epicardial ECG of a rat heart. Reproduced with permission.^[314] Copyright 2020, Springer Nature.

conformity with the skin (Figure 11c). The ultrathin structure of the hydrogel film enabled fast diffusion of oxygen molecules from the warm skin surface to the electrode in a tcPO₂ sensor, and fast transport of drug ions through the hydrogel film for transdermal drug delivery was also demonstrated. Various leg positions that affected the blood flow could be monitored via the tcPO₂ sensor attached on the foot (Figure 11d). Functionalization with conductive polymers aided in decreasing the impedance of the hydrogel interface, beneficial for tissue impedance monitoring and transcutaneous electrical nerve stimulation. Recently, a PAAm–alginate hydrogel film with sub-10 μm thickness synthesized via a cold-lamination method was reported,^[308] and the ultrathin hydrogel-interfaced on-skin electronics featured long-term wearability and device stability. Integration of self-healing properties made on-skin devices mechanically and electrically robust against unexpected damages.^[309–311] For example, a nanocomposite hydrogel composed of polyzwitterions crosslinked by nanoclays through reversible adsorption was highly stretchable and self-healable.^[312] The polar zwitterion groups provided active sites to form noncovalent bond-

ing with various substrates, and thus the nanocomposite hydrogel exhibited pressure-sensitive adhesiveness on target substrates. An on-skin nanocomposite hydrogel film was used as a touch pad for human–machine interaction with self-healable input functions. Wu and co-workers recently developed an artificial ionic skin by introducing a zwitterionic network consisting of weakly complexed zwitterions to a hydrogen-bonded polycarboxylic acid network. Subsequent debonding of the two networks in response to stretching led to a skin-like strain-stiffening behavior, which resolved the conflict between elasticity, strength, and self-healability. Such a molecular design paved the way for developing hydrogel-based bioelectronic devices with skin-like sophisticated mechanical and sensory properties.^[311]

In implantable bioelectronic applications, tough hydrogels are especially pertinent in providing a robust and conductive interface with the biological wet tissue, thereby improving tissue–device integration and enhancing the performance of biointegrated electronic devices.^[313–316] An adhesive hydrogel interface provides robust adhesion between wet tissues and electronic devices with high interfacial toughness, supporting the

stability of bioelectronic functions in dynamic physiological conditions. The high conductivity can also minimize unfavorable increase of electrical impedance at the tissue–device interface. A graphene nanocomposite was developed, capable of tough bonding with wet tissues by quick removal of water from the wet surface by hydration and then forming covalent bonds with tissues (Figure 11e). The formed tough hydrogel served as an electrical bioadhesive interface on tissues, and the bioadhesive electrode could maintain stable recording of epicardial ECG during 14 days of in vivo implantation.^[314]

4.3. Artificial Muscles and Soft Robots

Compared with conventional materials such as polymer fibers, elastomers, and shape memory alloys used for artificial muscles and soft robots, hydrogels are especially advantageous for their tissue-like softness, good biocompatibility, responsiveness to various stimuli, and capability of large volume deformation.^[10,317,318] The function of soft actuation based on hydrogel materials are closely related to their capability of controllable deformations, i.e., shape morphing. Common hydrogels without specific structural design are isotropic with omnidirectional activity, exhibiting isotropic volume change under a uniform stimulus. Thus, the design and fabrication of heterogeneous structures is fundamental for the development of morphing hydrogels.^[319] Heterogeneous structures can be built through the thickness of a thin sheet or along the in-plane dimension of a 2D sheet. In a thin sheet with heterogeneity along the thickness direction, a modest difference in swelling/shrinking in response to an external stimulus can drive macroscopic bending/folding deformation.^[320] Accordingly, bilayer hydrogel structures with distinct materials,^[321] different crosslinking densities^[322] or different filler orientations,^[323] and gradient hydrogel structures with gradient distribution of polymer chains^[324] or crosslinking^[325] are developed. In a planar-patterned hydrogel, the localized swelling is confined by the surrounding low-swelling region upon an external stimulus, resulting in out-of-plane buckling that reduces the in-plane compression/stretching energy.^[326] In-plane heterogeneity are usually implemented by introducing different crosslinking densities,^[326] compositions^[327] or filler orientations.^[328,329] Based on these heterogeneous structures, various shape morphing modes such as bending, folding, rolling, twisting, contraction, and expansion can be programmed. In addition, advanced processing techniques such as photolithography and 3D printing can serve as powerful strategies for fabricating heterogeneous hydrogels with programmed distribution of materials and geometries, thereby generating more sophisticated 2D-to-3D shape morphing. The existing morphing hydrogels usually exhibit low actuation forces and slow responses,^[330] hence, the development of dynamic shape morphing toward high-performance artificial muscles and robots calls for hydrogels with large actuation forces and fast responsiveness.

Emerging responsive hydrogels with toughening mechanisms such as double networks,^[228,331] covalent-noncovalent dual networks,^[332,333] and multiple physically crosslinked networks^[246,334] have greatly improved the mechanical strength of hydrogel actuators and led to enhanced actuation forces.^[330]

At the same time, response speeds can be improved by strategies such as developing nonosmotic mechanisms for actuation and fabricating fiber-based hydrogel structures. Inspired by the superior leap ability of frogs, He and co-workers developed a high-power-density strong contractile hydrogel material based on a mechanism of storing and releasing elastic potential energy, and the hydrogel exhibited a large force (40 kPa) and high work density (15.3 kJ m^{-3}), outperforming biological muscles (8 kJ m^{-3}).^[333] An elastic poly(AAm-co-AAc) hydrogel was stretched and immersed in an iron(III) chloride solution, which facilitated the formation of coordination bonds between Fe^{3+} and carboxylic groups, locking the deformation and thus storing of the mechanical energy. The dual-crosslinked network led to much enhanced mechanical strength. The stored energy in the hydrogel could then be released by stimuli such as UV light illumination and an acid solution, which destabilized the coordination bonds by photoreduction (Fe^{3+} to Fe^{2+}) or protonation (COO^- to COOH), triggering the return of the hydrogel to its original length along the stretched direction and generating large contraction force (Figure 12a). Recently, highly aligned block copolymer hydrogel fibers with alternating crystalline and amorphous domains were reported, resembling the structure of mammalian skeletal muscles.^[246] The process of strain-programmed crystallization enabled mechanical toughness up to 121.2 MJ m^{-3} comparable to natural spider silk, and the fiber strained with an elongation ratio of 5 exhibited crystallinity of 77% and polymer alignment along the elongation direction. A stimulation of heating or hydration would induce a change of the crystallization domains to amorphous states, resulting in actuation strains of up to 80% and energy density up to 506 J kg^{-1} (Figure 12b).

Tough hydrogel-based actuators and soft robots can be integrated with human bodies for diverse functionalities^[11,335] such as smart wearables,^[20,184,336] medical devices for surgery or drug delivery inside human bodies,^[235,337,338] and artificial organs.^[223,233,339] For example, thermally responsive fibers were prepared by uniformly coating PAAc-CS-calcium acetate hydrogel skins onto commercial fibers. The functionalized fibers were then woven into a wearable textile, which was soft and deformable at room temperature. When the temperature was increased to $70 \text{ }^\circ\text{C}$, the modulus increased by 30 883%, achieving good load-bearing capacity (Figure 12c),^[184] and demonstrating potential applications in the field of thermal protective clothing. Wang and co-workers printed a thermal shape memory poly(*N*-acryloylsemicarbazide-co-acrylic acid) hydrogel stent that could change in size in adaptation to different vessels.^[338] The hydrogel stent was squeezed into a compact shape and fixed at $5 \text{ }^\circ\text{C}$, which was then delivered to a simulated vascular stenosis. The stent would then expand and recover its shape in a physiological environment at $37 \text{ }^\circ\text{C}$ and open the stenosis, achieving active expansion in the smart intervention process (Figure 12d). In addition, our group developed a robotic heart based on double network hydrogels, which demonstrated continuous and stable heartbeat-like motions when cyclic pneumatic pumping was implemented.^[228] Water-soluble biomaterials such as Cl^- and glucose could be transported from a hydrogel vessel inside the robotic heart to the external deionized water environment through the porous hydrogel network, demonstrating an effective biomaterial transport function (Figure 12e).

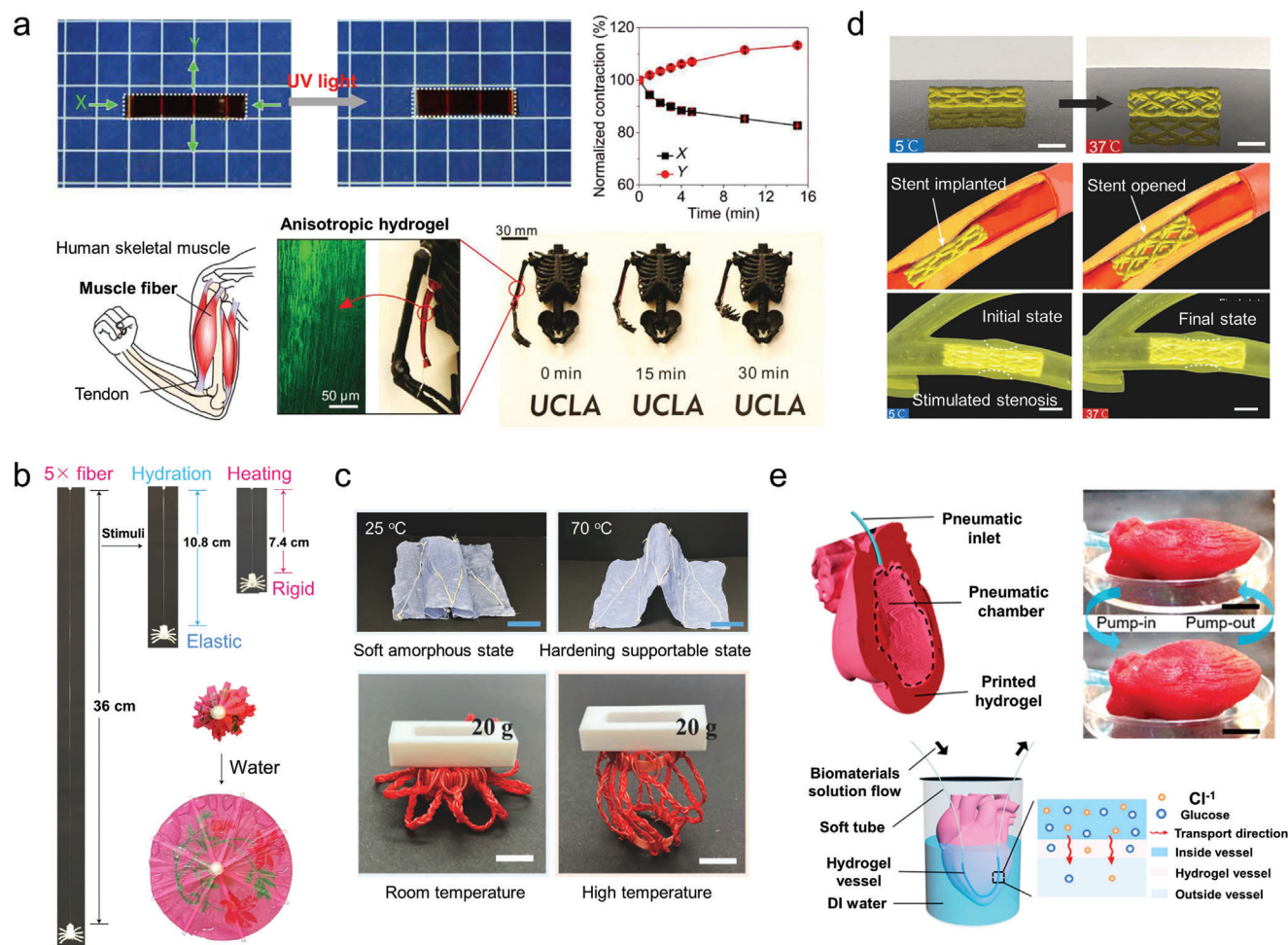


Figure 12. Artificial muscle and soft robotic hydrogel devices. a) Anisotropic actuation deformation of a poly(AAm-co-AAc)-Fe³⁺ hydrogel based on UV light induced releasing of elastic potential energy, generating strong contraction with high similarity to natural muscles. Reproduced with permission.^[333] Copyright 2020, AAAS. b) Hydration or heating induced strong contraction of a block copolymer hydrogel fiber. Reproduced with permission.^[246] Copyright 2022, Springer Nature. c) Thermal stiffening textiles consisting of commercial fibers coated with a PAAc-CS-calcium acetate hydrogel skin. Reproduced with permission.^[184] Copyright 2022, Wiley-VCH. d) A thermally shape memory hydrogel stent that can be delivered to a simulated vessel and open the stenosis. Reproduced with permission.^[338] Copyright 2022, Wiley-VCH. e) A double network hydrogel based robotic heart that exhibits stable pneumatic heartbeat-like motion and biomaterial transport. Reproduced with permission.^[228] Copyright 2019, American Chemical Society.

5. Conclusions and Perspective

The remarkable similarities of hydrogels to biological living tissues make them key players for the integration of humans and machines. Common hydrogels suffer from low strength and toughness, limiting their mechanical reliability for use as biointegrated hydrogel machines, including wearable and implantable devices. However, recent progress in polymer science has produced mechanically enhanced and functional hydrogels, while new processing technologies have emerged for the shaping and patterning of hydrogels, stimulating the development of hydrogel devices that are applicable to various biointegrated applications. In this review, the relationship between the polymer network and mechanical performance of hydrogels are discussed in detail. To improve mechanical properties of hydrogels, toughening mechanisms based on increasing homogeneities of polymer networks, introducing energy dissipation interactions, or improving

functionalities of crosslinking points are exploited, which regulate polymer network structures at the micro/nano and molecular scales. Representative examples such as the slide-ring hydrogel, the B-DN hydrogel, the ion-doped SiO₂-PAAc hydrogel, and the aligned micro/nanofibrous PVA hydrogel, exhibited extraordinary toughness or strength comparable to or even outperforming natural tough materials. On this basis, some seemingly contradicting but combined mechanical properties that exist in biological materials are replicated in synthetic hydrogels, including high toughness and resilience, high toughness and stiffness, self-healing and high strength, and stimuli-responsive stiffening/softening. Those distinct mechanical functionalities are adaptive to different biointegrated applications. In addition, recent processing technologies such as 3D printing, spinning, and coating combined with compatible toughening mechanisms, enable macro/microscale shaping and patterning of hydrogels and creation of diverse mechanically robust constructs. The

mechanically robust and functional hydrogels with customizable shapes have shown wide applications in wearable and implantable devices for biomedical, bioelectronic, and robotic applications.

Despite the booming development of tough and functional hydrogels for fabrication of biointegrated hydrogel devices, extra efforts should be made to further broaden this field and promote their practical applications. For the mechanical engineering of tough hydrogels, research on the polymer structural design principles for engineering distinct mechanical behaviors is still in progress. In-depth understanding on mechanical properties of hydrogels, such as toughness, resilience, modulus, maximum strain, fatigue, and nonlinearity, are crucial to devising diverse mechanically functional hydrogel devices that interact closely with human bodies for long-term usage. In respect of processing of tough hydrogels, toughening mechanisms that are compatible with the processing techniques are still limited, owing to the requirements for both delicate polymer network engineering procedures and different shaping conditions. Therefore, some of the extreme mechanical properties developed in bulky hydrogels can still hardly be achieved in shaped and patterned hydrogels. Further research focused on processing hydrogels into patterned bioelectronic devices with desired mechanical functionalities is highly demanded, and it requires careful consideration and regulation of the multiscale engineering process for both delicate polymer network structuring and high-resolution hydrogel shaping/patterning. For practical use of hydrogel devices, distinct properties of hydrogels in addition to mechanical functionalities are required for specific biointegrated applications. For implanted devices, biocompatibility, bioactivity, physiological stability, and biodegradability are the major requirements, which are still rarely observed in reported tough hydrogels. The hydrogels utilized in tissue engineering are mostly acellular scaffolds, as tough hydrogels often restrict cell activities. To this end, orthogonal design implemented on multiscale structures of hydrogels is a promising approach to achieve multiple properties combined in a synergistic manner. For wearable and on-skin applications, current smart stimuli-responsive hydrogel devices usually need to work in aqueous environments. Although encapsulation of functional hydrogel devices can alleviate the dehydration and loss of water under an external stimulus in air, novel material systems should be explored, such as devising hygroscopic hydrogels capable of self-retaining moisture on the surface of human skins, and developing stimulus-responsive functionalities based on reversible water redistribution within the hydrogel networks. The pursuit for further polymer science and technological innovations for improved properties of hydrogels and adaptive, reliable functionalities of biointegrated hydrogel devices, requires continuous and collective efforts from researchers in multiple disciplines.

Acknowledgements

This work was supported by the National Natural Science Foundation of China (Grant Nos. 52303321, 51873134, and 22308236), the Natural Science Foundation of the Jiangsu Higher Education Institutions of China (Grant No. 23KJA430012), the National Natural Science Foundation of Jiangsu Province, China (Grant No. BK20230501), the PPM Institute of Functional Materials, Poly Plastic Masterbatch (Suzhou) Co., Ltd. (No.

2023004), the Opening Project of the Key Laboratory of Bionic Engineering (Ministry of Education), Jilin University (KF2023002), and the Soochow University Start-up Fund (NH11500323).

Conflict of Interest

The authors declare no conflict of interest.

Keywords

bioelectronics, biomedical, mechanical functions, shaping, soft robots, tough hydrogels

Received: September 25, 2023

Revised: February 16, 2024

Published online: March 5, 2024

- [1] E. M. Ahmed, *J. Adv. Res.* **2015**, *6*, 105.
- [2] X. Zhao, X. Chen, H. Yuk, S. Lin, X. Liu, G. Parada, *Chem. Rev.* **2021**, *121*, 4309.
- [3] K. Y. Lee, D. J. Mooney, *Chem. Rev.* **2001**, *101*, 1869.
- [4] S. Nam, D. Mooney, *Chem. Rev.* **2021**, *121*, 11336.
- [5] C. Cui, W. Liu, *Prog. Polym. Sci.* **2021**, *116*, 101388.
- [6] C. Yang, Z. Suo, *Nat. Rev. Mater.* **2018**, *3*, 125.
- [7] T. R. Ray, J. Choi, A. J. Bandodkar, S. Krishnan, P. Gutruf, L. Tian, R. Ghaffari, J. A. Rogers, *Chem. Rev.* **2019**, *119*, 5461.
- [8] H. Yuk, B. Lu, X. Zhao, *Chem. Soc. Rev.* **2019**, *48*, 1642.
- [9] Y. Cong, J. Fu, *Langmuir* **2022**, *38*, 11503.
- [10] S. M. Mirvakili, I. W. Hunter, *Adv. Mater.* **2018**, *30*, 1704407.
- [11] M. Cianchetti, C. Laschi, A. Menciassi, P. Dario, *Nat. Rev. Mater.* **2018**, *3*, 143.
- [12] C. Storm, J. J. Pastore, F. C. MacKintosh, T. C. Lubensky, P. A. Janmey, *Nature* **2005**, *435*, 191.
- [13] J. Kang, J. B. H. Tok, Z. Bao, *Nat. Electron.* **2019**, *2*, 144.
- [14] C. J. Little, N. K. Bawolin, X. Chen, *Tissue Eng., Part B* **2011**, *17*, 213.
- [15] G. A. Johnson, D. M. Tramaglino, R. E. Levine, K. Ohno, N.-Y. Choi, S. L.-Y. Woo, *J. Orthop. Res.* **1994**, *12*, 796.
- [16] B. P. Chan, K. W. Leong, *Eur. Spine J.* **2008**, *17*, 467.
- [17] C. Liu, N. Morimoto, L. Jiang, S. Kawahara, T. Noritomi, H. Yokoyama, K. Mayumi, K. Ito, *Science* **2021**, *372*, 1078.
- [18] X. Xiong, Y. Chen, Z. Wang, H. Liu, M. Le, C. Lin, G. Wu, L. Wang, X. Shi, Y.-G. Jia, Y. Zhao, *Nat. Commun.* **2023**, *14*, 1331.
- [19] M. Kanik, S. Orguc, G. Varnavides, J. Kim, T. Benavides, D. Gonzalez, T. Akitilto, C. C. Tasan, A. P. Chandrakasan, Y. Fink, P. Anikeeva, *Science* **2019**, *365*, 145.
- [20] S. Nam, B. R. Seo, A. J. Najibi, S. L. McNamara, D. J. Mooney, *Nat. Mater.* **2023**, *22*, 249.
- [21] J. P. Gong, *Soft Matter* **2010**, *6*, 2583.
- [22] X. Zhao, *Soft Matter* **2014**, *10*, 672.
- [23] W. Wang, Y. Zhang, W. Liu, *Prog. Polym. Sci.* **2017**, *71*, 1.
- [24] A. M. S. Costa, J. F. Mano, *Eur. Polym. J.* **2015**, *72*, 344.
- [25] T. Sakai, T. Matsunaga, Y. Yamamoto, C. Ito, R. Yoshida, S. Suzuki, N. Sasaki, M. Shibayama, U.-i. Chung, *Macromolecules* **2008**, *41*, 5379.
- [26] Y. Akagi, T. Matsunaga, M. Shibayama, U.-i. Chung, T. Sakai, *Macromolecules* **2010**, *43*, 488.
- [27] T. Matsunaga, T. Sakai, Y. Akagi, U.-i. Chung, M. Shibayama, *Macromolecules* **2009**, *42*, 6245.
- [28] T. Sakai, *Polym. J.* **2014**, *46*, 517.
- [29] T. Sakai, Y. Akagi, T. Matsunaga, M. Kurakazu, U.-i. Chung, M. Shibayama, *Macromol. Rapid Commun.* **2010**, *31*, 1954.
- [30] M. Shibayama, X. Li, T. Sakai, *Colloid Polym. Sci.* **2019**, *297*, 1.

- [31] M. Kurakazu, T. Katashima, M. Chijiishi, K. Nishi, Y. Akagi, T. Matsunaga, M. Shibayama, U.-i. Chung, T. Sakai, *Macromolecules* **2010**, *43*, 3935.
- [32] X. Li, S. Nakagawa, Y. Tsuji, N. Watanabe, M. Shibayama, *Sci. Adv.* **2019**, *5*, 8647.
- [33] K. Hayashi, F. Okamoto, S. Hoshi, T. Katashima, D. C. Zujur, X. Li, M. Shibayama, E. P. Gilbert, U.-i. Chung, S. Ohba, T. Oshika, T. Sakai, *Nat. Biomed. Eng.* **2017**, *1*, 0044.
- [34] T. Fujiyabu, X. Li, M. Shibayama, U.-i. Chung, T. Sakai, *Macromolecules* **2017**, *50*, 9411.
- [35] G. A. Parada, X. Zhao, *Soft Matter* **2018**, *14*, 5186.
- [36] B. Marco-Dufort, R. Iten, M. W. Tibbitt, *J. Am. Chem. Soc.* **2020**, *142*, 15371.
- [37] H. Kamata, Y. Akagi, Y. Kayasuga-Kariya, U.-i. Chung, T. Sakai, *Science* **2014**, *343*, 873.
- [38] V. Yesilyurt, M. J. Webber, E. A. Appel, C. Godwin, R. Langer, D. G. Anderson, *Adv. Mater.* **2016**, *28*, 86.
- [39] Y. Bu, L. Zhang, G. Sun, F. Sun, J. Liu, F. Yang, P. Tang, D. Wu, *Adv. Mater.* **2019**, *31*, 1901580.
- [40] Y. Okumura, K. Ito, *Adv. Mater.* **2001**, *13*, 485.
- [41] K. Mayumi, K. Ito, *Polymer* **2010**, *51*, 959.
- [42] K. Ito, *Polym. J.* **2007**, *39*, 489.
- [43] S. Loethen, J. M. Kim, D. H. Thompson, *Polym. Rev.* **2007**, *47*, 383.
- [44] G. Wenz, B.-H. Han, A. Müller, *Chem. Rev.* **2006**, *106*, 782.
- [45] G. Liu, Q. Yuan, G. Hollett, W. Zhao, Y. Kang, J. Wu, *Polym. Chem.* **2018**, *9*, 3436.
- [46] A. Bin Imran, K. Esaki, H. Gotoh, T. Seki, K. Ito, Y. Sakai, Y. Takeoka, *Nat. Commun.* **2014**, *5*, 5124.
- [47] L. Feng, S.-S. Jia, Y. Chen, Y. Liu, *Chem. Eur. J.* **2020**, *26*, 14080.
- [48] C. Norioka, Y. Inamoto, C. Hajime, A. Kawamura, T. Miyata, *NPG Asia Mater.* **2021**, *13*, 34.
- [49] J. Kim, G. Zhang, M. Shi, Z. Suo, *Science* **2021**, *374*, 212.
- [50] G. Nian, J. Kim, X. Bao, Z. Suo, *Adv. Mater.* **2022**, *34*, 2206577.
- [51] L. Fu, L. Li, Q. Bian, B. Xue, J. Jin, J. Li, Y. Cao, Q. Jiang, H. Li, *Nature* **2023**, *618*, 740.
- [52] M. Rubinstein, S. Panyukov, *Macromolecules* **2002**, *35*, 6670.
- [53] M. E. De Rosa, H. H. Winter, *Rheol. Acta* **1994**, *33*, 220.
- [54] X.-Q. Wang, K. H. Chan, W. Lu, T. Ding, S. W. L. Ng, Y. Cheng, T. Li, M. Hong, B. C. K. Tee, G. W. Ho, *Nat. Commun.* **2022**, *13*, 3369.
- [55] C. Lang, J. A. LaNasa, N. Utomo, Y. Xu, M. J. Nelson, W. Song, M. A. Hickner, R. H. Colby, M. Kumar, R. J. Hickey, *Nat. Commun.* **2019**, *10*, 3855.
- [56] J. P. Gong, Y. Katsuyama, T. Kurokawa, Y. Osada, *Adv. Mater.* **2003**, *15*, 1155.
- [57] J.-Y. Sun, X. Zhao, W. R. K. Illeperuma, O. Chaudhuri, K. H. Oh, D. J. Mooney, J. J. Vlassak, Z. Suo, *Nature* **2012**, *489*, 133.
- [58] S. Hong, D. Sycks, H. F. Chan, S. Lin, G. P. Lopez, F. Guilak, K. W. Leong, X. Zhao, *Adv. Mater.* **2015**, *27*, 4035.
- [59] L. Stevens, P. Calvert, G. G. Wallace, M. i. h. Panhuis, *Soft Matter* **2013**, *9*, 3009.
- [60] H. Li, H. Zheng, Y. J. Tan, S. B. Tor, K. Zhou, *ACS Appl. Mater. Interfaces* **2021**, *13*, 12814.
- [61] Y. Yang, X. Wang, F. Yang, L. Wang, D. Wu, *Adv. Mater.* **2018**, *30*, 1707071.
- [62] H. J. Zhang, T. L. Sun, A. K. Zhang, Y. Ikura, T. Nakajima, T. Nonoyama, T. Kurokawa, O. Ito, H. Ishitobi, J. P. Gong, *Adv. Mater.* **2016**, *28*, 4884.
- [63] Q. Chen, L. Zhu, H. Chen, H. Yan, L. Huang, J. Yang, J. Zheng, *Adv. Funct. Mater.* **2015**, *25*, 1598.
- [64] M. A. Haque, T. Kurokawa, G. Kamita, J. P. Gong, *Macromolecules* **2011**, *44*, 8916.
- [65] Q. Chen, L. Zhu, C. Zhao, Q. Wang, J. Zheng, *Adv. Mater.* **2013**, *25*, 4171.
- [66] Y. Yang, X. Wang, F. Yang, H. Shen, D. Wu, *Adv. Mater.* **2016**, *28*, 7178.
- [67] J. Li, Z. Suo, J. J. Vlassak, *J. Mater. Chem. B* **2014**, *2*, 6708.
- [68] Y. Zhao, B. H. Xia, L. Wang, R. J. Wang, D. N. Meng, Y. Liu, J. W. Zhou, H. Q. Lian, L. Zu, X. G. Cui, Y. R. Liang, M. F. Zhu, *Macromol. Mater. Eng.* **2018**, *303*, 1700527.
- [69] E. S. Dragan, *Chem. Eng. J.* **2014**, *243*, 572.
- [70] R. Takahashi, T. L. Sun, Y. Saruwatari, T. Kurokawa, D. R. King, J. P. Gong, *Adv. Mater.* **2018**, *30*, 1706885.
- [71] K. Fukao, K. Tanaka, R. Kiyama, T. Nonoyama, J. P. Gong, *J. Mater. Chem. B* **2020**, *8*, 5184.
- [72] F. Zhu, L. Cheng, Z. J. Wang, W. Hong, Z. L. Wu, J. Yin, J. Qian, Q. Zheng, *ACS Appl. Mater. Interfaces* **2017**, *9*, 11363.
- [73] S. Z. Bonyadi, C. J. Demott, M. A. Grunlan, A. C. Dunn, *J. Mech. Behav. Biomed. Mater.* **2021**, *114*, 104202.
- [74] L. Wang, X. Zhang, K. Yang, Y. V. Fu, T. Xu, S. Li, D. Zhang, L.-N. Wang, C.-S. Lee, *Adv. Funct. Mater.* **2020**, *30*, 1904156.
- [75] X.-H. Wang, F. Song, D. Qian, Y.-D. He, W.-C. Nie, X.-L. Wang, Y.-Z. Wang, *Chem. Eng. J.* **2018**, *349*, 588.
- [76] T. Matsuda, R. Kawakami, R. Namba, T. Nakajima, J. P. Gong, *Science* **2019**, *363*, 504.
- [77] Z. Wang, X. Zheng, T. Ouchi, T. B. Kouznetsova, H. K. Beech, S. Avron, T. Matsuda, B. H. Bowser, S. Wang, J. A. Johnson, J. A. Kalow, B. D. Olsen, J. P. Gong, M. Rubinstein, S. L. Craig, *Science* **2021**, *374*, 193.
- [78] P. Lin, S. Ma, X. Wang, F. Zhou, *Adv. Mater.* **2015**, *27*, 2054.
- [79] H. C. Yu, S. Y. Zheng, L. Fang, Z. Ying, M. Du, J. Wang, K.-F. Ren, Z. L. Wu, Q. Zheng, *Adv. Mater.* **2020**, *32*, 2005171.
- [80] S. Y. Zheng, S. Mao, J. Yuan, S. Wang, X. He, X. Zhang, C. Du, D. Zhang, Z. L. Wu, J. Yang, *Chem. Mater.* **2021**, *33*, 8418.
- [81] X. N. Zhang, Y. J. Wang, S. Sun, L. Hou, P. Wu, Z. L. Wu, Q. Zheng, *Macromolecules* **2018**, *51*, 8136.
- [82] D. Zhao, J. Huang, Y. Zhong, K. Li, L. Zhang, J. Cai, *Adv. Funct. Mater.* **2016**, *26*, 6279.
- [83] D. Xu, J. Huang, D. Zhao, B. Ding, L. Zhang, J. Cai, *Adv. Mater.* **2016**, *28*, 5844.
- [84] Y. Zhang, Y. Li, W. Liu, *Adv. Funct. Mater.* **2015**, *25*, 471.
- [85] J. Cao, J. Li, Y. Chen, L. Zhang, J. Zhou, *Adv. Funct. Mater.* **2018**, *28*, 1800739.
- [86] Z. Qin, R. Niu, C. Tang, J. Xia, F. Ji, D. Dong, H. Zhang, S. Zhang, J. Li, F. Yao, *Macromol. Mater. Eng.* **2018**, *303*, 1700396.
- [87] Y. Hu, Z. Du, X. Deng, T. Wang, Z. Yang, W. Zhou, C. Wang, *Macromolecules* **2016**, *49*, 5660.
- [88] Y. Li, J. Yan, Y. Liu, X.-M. Xie, *ACS Nano* **2022**, *16*, 1567.
- [89] D. Hu, Y. Cui, K. Mo, J. Wang, Y. Huang, X. Miao, J. Lin, C. Chang, *Composites, Part B* **2020**, *197*, 108118.
- [90] M. T. I. Mredha, Y. Z. Guo, T. Nonoyama, T. Nakajima, T. Kurokawa, J. P. Gong, *Adv. Mater.* **2018**, *30*, 1704937.
- [91] W. Kong, C. Wang, C. Jia, Y. Kuang, G. Pastel, C. Chen, G. Chen, S. He, H. Huang, J. Zhang, S. Wang, L. Hu, *Adv. Mater.* **2018**, *30*, 1801934.
- [92] L. Xu, X. Zhao, C. Xu, N. A. Kotov, *Adv. Mater.* **2018**, *30*, 1703343.
- [93] S. Lin, J. Liu, X. Liu, X. Zhao, *Proc. Natl. Acad. Sci. USA* **2019**, *116*, 10244.
- [94] J. Zhao, H. Tong, A. Kirillova, W. J. Koshut, A. Malek, N. C. Brigham, M. L. Becker, K. Gall, B. J. Wiley, *Adv. Funct. Mater.* **2022**, *32*, 2205662.
- [95] M. Hua, S. Wu, Y. Ma, Y. Zhao, Z. Chen, I. Frenkel, J. Strzalka, H. Zhou, X. Zhu, X. He, *Nature* **2021**, *590*, 594.
- [96] J. Visser, F. P. W. Melchels, J. E. Jeon, E. M. van Bussel, L. S. Kimpton, H. M. Byrne, W. J. A. Dhert, P. D. Dalton, D. W. Hutmacher, J. Malda, *Nat. Commun.* **2015**, *6*, 6933.
- [97] A. Agrawal, N. Rahbar, P. D. Calvert, *Acta Biomater.* **2013**, *9*, 5313.

- [98] S. Lin, C. Cao, Q. Wang, M. Gonzalez, J. E. Dolbow, X. Zhao, *Soft Matter* **2014**, *10*, 7519.
- [99] F. T. Moutos, L. E. Freed, F. Guilak, *Nat. Mater.* **2007**, *6*, 162.
- [100] C. Xiang, Z. Wang, C. Yang, X. Yao, Y. Wang, Z. Suo, *Mater. Today* **2020**, *34*, 7.
- [101] Y. Huang, D. R. King, T. L. Sun, T. Nonoyama, T. Kurokawa, T. Nakajima, J. P. Gong, *Adv. Funct. Mater.* **2017**, *27*, 1605350.
- [102] K. Haraguchi, T. Takehisa, *Adv. Mater.* **2002**, *14*, 1120.
- [103] Q. Wang, J. L. Mynar, M. Yoshida, E. Lee, M. Lee, K. Okuro, K. Kinbara, T. Aida, *Nature* **2010**, *463*, 339.
- [104] K. Haraguchi, H.-J. Li, *Macromolecules* **2006**, *39*, 1898.
- [105] K. Haraguchi, T. Takehisa, S. Fan, *Macromolecules* **2002**, *35*, 10162.
- [106] T. Huang, H. G. Xu, K. X. Jiao, L. P. Zhu, H. R. Brown, H. L. Wang, *Adv. Mater.* **2007**, *19*, 1622.
- [107] F.-K. Shi, X.-P. Wang, R.-H. Guo, M. Zhong, X.-M. Xie, *J. Mater. Chem. B* **2015**, *3*, 1187.
- [108] S. Xia, Q. Zhang, S. Song, L. Duan, G. Gao, *Chem. Mater.* **2019**, *31*, 9522.
- [109] Y. Wu, D. U. Shah, C. Liu, Z. Yu, J. Liu, X. Ren, M. J. Rowland, C. Abell, M. H. Ramage, O. A. Scherman, *Proc. Natl. Acad. Sci. USA* **2017**, *114*, 8163.
- [110] R. Liu, S. Liang, X.-Z. Tang, D. Yan, X. Li, Z.-Z. Yu, *J. Mater. Chem.* **2012**, *22*, 14160.
- [111] B. Bao, Q. Zeng, K. Li, J. Wen, Y. Zhang, Y. Zheng, R. Zhou, C. Shi, T. Chen, C. Xiao, B. Chen, T. Wang, K. Yu, Y. Sun, Q. Lin, Y. He, S. Tu, L. Zhu, *Nat. Mater.* **2023**, *22*, 1253.
- [112] S. Rose, A. Dizeux, T. Narita, D. Hourdet, A. Marcellan, *Macromolecules* **2013**, *46*, 4095.
- [113] L.-W. Xia, R. Xie, X.-J. Ju, W. Wang, Q. Chen, L.-Y. Chu, *Nat. Commun.* **2013**, *4*, 2226.
- [114] M. Morimura, S. Ida, M. Oyama, H. Takeshita, S. Kanaoka, *Macromolecules* **2021**, *54*, 1732.
- [115] J. Hu, T. Kurokawa, K. Hiwatashi, T. Nakajima, Z. L. Wu, S. M. Liang, J. P. Gong, *Macromolecules* **2012**, *45*, 5218.
- [116] C. Li, X. Zhou, L. Zhu, Z. Xu, P. Tan, H. Wang, G. Chen, X. Zhou, *Soft Matter* **2021**, *17*, 1566.
- [117] W. Li, S. Zheng, X. Zou, Y. Ren, Z. Liu, W. Peng, X. Wang, D. Liu, Z. Shen, Y. Hu, J. Guo, Z. Sun, F. Yan, *Adv. Funct. Mater.* **2022**, *32*, 2207348.
- [118] J. Cui, J. Chen, Z. Ni, W. Dong, M. Chen, D. Shi, *ACS Appl. Mater. Interfaces* **2022**, *14*, 47148.
- [119] J. Hu, T. Kurokawa, T. Nakajima, T. L. Sun, T. Suekama, Z. L. Wu, S. M. Liang, J. P. Gong, *Macromolecules* **2012**, *45*, 9445.
- [120] J. Hu, K. Hiwatashi, T. Kurokawa, S. M. Liang, Z. L. Wu, J. P. Gong, *Macromolecules* **2011**, *44*, 7775.
- [121] J. Hu, T. Kurokawa, T. Nakajima, Z. L. Wu, S. M. Liang, J. P. Gong, *Macromolecules* **2014**, *47*, 3587.
- [122] L. Zhang, J. Zhao, J. Zhu, C. He, H. Wang, *Soft Matter* **2012**, *8*, 10439.
- [123] S. Lin, X. Liu, J. Liu, H. Yuk, H.-C. Loh, G. A. Parada, C. Settens, J. Song, A. Masic, G. H. McKinley, X. Zhao, *Sci. Adv.* **2019**, *5*, 8528.
- [124] X. Liang, G. Chen, S. Lin, J. Zhang, L. Wang, P. Zhang, Z. Wang, Z. Wang, Y. Lan, Q. Ge, J. Liu, *Adv. Mater.* **2021**, *33*, 2102011.
- [125] Y. Wu, Y. Zhang, H. Wu, J. Wen, S. Zhang, W. Xing, H. Zhang, H. Xue, J. Gao, Y. Mai, *Adv. Mater.* **2023**, *35*, 2210624.
- [126] L. Xu, S. Gao, Q. Guo, C. Wang, Y. Qiao, D. Qiu, *Adv. Mater.* **2020**, *32*, 2004579.
- [127] S. Wu, M. Hua, Y. Alsaïd, Y. Du, Y. Ma, Y. Zhao, C. Y. Lo, C. Wang, D. Wu, B. Yao, J. Strzalka, H. Zhou, X. Zhu, X. He, *Adv. Mater.* **2021**, *33*, 2007829.
- [128] S. Wu, M. Hua, Y. Alsaïd, Y. Du, Y. Ma, Y. Zhao, C.-Y. Lo, C. Wang, D. Wu, B. Yao, J. Strzalka, H. Zhou, X. Zhu, X. He, *Adv. Mater.* **2021**, *33*, 2007829.
- [129] Y. Yang, Y. Ru, T. Zhao, M. Liu, *Chem* **2023**, *9*, 3113.
- [130] J. Xu, X. Ren, G. Gao, *Polymer* **2018**, *150*, 194.
- [131] S. Wang, M. Liu, L. Gao, G. Guo, Y. Huo, *ACS Appl. Mater. Interfaces* **2019**, *11*, 19554.
- [132] J. Pan, H. Zeng, L. Gao, Q. Zhang, H. Luo, X. Shi, H. Zhang, *Adv. Funct. Mater.* **2022**, *32*, 2110277.
- [133] Q. He, Y. Huang, S. Wang, *Adv. Funct. Mater.* **2018**, *28*, 1705069.
- [134] K. Cui, T. L. Sun, X. Liang, K. Nakajima, Y. N. Ye, L. Chen, T. Kurokawa, J. P. Gong, *Phys. Rev. Lett.* **2018**, *121*, 185501.
- [135] K. Cui, Y. N. Ye, T. L. Sun, C. Yu, X. Li, T. Kurokawa, J. P. Gong, *Macromolecules* **2020**, *53*, 5116.
- [136] T. Yuan, X. Cui, X. Liu, X. Qu, J. Sun, *Macromolecules* **2019**, *52*, 3141.
- [137] F. Luo, T. L. Sun, T. Nakajima, T. Kurokawa, Y. Zhao, K. Sato, A. B. Ihsan, X. Li, H. Guo, J. P. Gong, *Adv. Mater.* **2015**, *27*, 2722.
- [138] F. Luo, T. L. Sun, T. Nakajima, D. R. King, T. Kurokawa, Y. Zhao, A. B. Ihsan, X. Li, H. Guo, J. P. Gong, *Macromolecules* **2016**, *49*, 2750.
- [139] T. L. Sun, T. Kurokawa, S. Kuroda, A. B. Ihsan, T. Akasaki, K. Sato, M. A. Haque, T. Nakajima, J. P. Gong, *Nat. Mater.* **2013**, *12*, 932.
- [140] X. Hu, M. Vatankhah-Varnoosfaderani, J. Zhou, Q. Li, S. S. Sheiko, *Adv. Mater.* **2015**, *27*, 6899.
- [141] Y. J. Wang, X. N. Zhang, Y. Song, Y. Zhao, L. Chen, F. Su, L. Li, Z. L. Wu, Q. Zheng, *Chem. Mater.* **2019**, *31*, 1430.
- [142] X. N. Zhang, C. Du, Y. J. Wang, L. X. Hou, M. Du, Q. Zheng, Z. L. Wu, *Macromolecules* **2022**, *55*, 7512.
- [143] H. J. Zhang, X. Wang, Y. Yang, T. L. Sun, A. Zhang, X. You, *Macromolecules* **2022**, *55*, 7401.
- [144] X. Dai, Y. Zhang, L. Gao, T. Bai, W. Wang, Y. Cui, W. Liu, *Adv. Mater.* **2015**, *27*, 3566.
- [145] A. Ní Annaidh, K. Bruyère, M. Destrade, M. D. Gilchrist, M. Otténio, *J. Mech. Behav. Biomed. Mater.* **2012**, *5*, 139.
- [146] P. H. Corkhill, A. S. Trevett, B. J. Tighe, *Proc. Inst. Mech. Eng., Part H* **1990**, *204*, 147.
- [147] M. V. Chin-Purcell, J. L. Lewis, *J. Biomech. Eng.* **1996**, *118*, 545.
- [148] A. Race, A. A. Amis, *J. Biomech.* **1994**, *27*, 13.
- [149] J. Li, S. Li, J. Huang, A. Q. Khan, B. An, X. Zhou, Z. Liu, M. Zhu, *Adv. Sci.* **2022**, *9*, 2103965.
- [150] F. Burla, Y. Mulla, B. E. Vos, A. Aufderhorst-Roberts, G. H. Koenderink, *Nat. Rev. Phys.* **2019**, *1*, 249.
- [151] S. S. Sheiko, A. V. Dobrynin, *Macromolecules* **2019**, *52*, 7531.
- [152] H. Lei, L. Dong, Y. Li, J. Zhang, H. Chen, J. Wu, Y. Zhang, Q. Fan, B. Xue, M. Qin, B. Chen, Y. Cao, W. Wang, *Nat. Commun.* **2020**, *11*, 4032.
- [153] R. Liu, H. Wang, W. Lu, L. Cui, S. Wang, Y. Wang, Q. Chen, Y. Guan, Y. Zhang, *Chem. Eng. J.* **2021**, *415*, 128839.
- [154] X. Liu, J. Wu, K. Qiao, G. Liu, Z. Wang, T. Lu, Z. Suo, J. Hu, *Nat. Commun.* **2022**, *13*, 1622.
- [155] J. Zou, X. Jing, Z. Chen, S.-J. Wang, X.-S. Hu, P.-Y. Feng, Y.-J. Liu, *Adv. Funct. Mater.* **2023**, *33*, 2213895.
- [156] W. Li, X. Wang, Z. Liu, X. Zou, Z. Shen, D. Liu, L. Li, Y. Guo, F. Yan, *Nat. Mater.* **2024**, *23*, 131.
- [157] J. Wang, F. Tang, C. Yao, L. Li, *Adv. Funct. Mater.* **2023**, *33*, 2214935.
- [158] D. Ji, J. Kim, *Adv. NanoBiomed Res.* **2021**, *1*, 2100026.
- [159] W. R. K. Illeperuma, J.-Y. Sun, Z. Suo, J. J. Vlassak, *Extreme Mech. Lett.* **2014**, *1*, 90.
- [160] P. Xi, F. Quan, J. Yao, Y. Xia, K. Fang, Y. Jiang, *ACS Nano* **2021**, *15*, 16478.
- [161] Y. Yu, Y. He, Z. Mu, Y. Zhao, K. Kong, Z. Liu, R. Tang, *Adv. Funct. Mater.* **2020**, *30*, 1908556.
- [162] B. Xu, P. Zheng, F. Gao, W. Wang, H. Zhang, X. Zhang, X. Feng, W. Liu, *Adv. Funct. Mater.* **2017**, *27*, 1604327.
- [163] N. Rauner, M. Meuris, M. Zoric, J. C. Tiller, *Nature* **2017**, *543*, 407.
- [164] Y. Dou, Z.-P. Wang, W. He, T. Jia, Z. Liu, P. Sun, K. Wen, E. Gao, X. Zhou, X. Hu, J. Li, S. Fang, D. Qian, Z. Liu, *Nat. Commun.* **2019**, *10*, 5293.
- [165] Y. Shi, B. Wu, S. Sun, P. Wu, *Nat. Commun.* **2023**, *14*, 1370.
- [166] L. Xu, Y. Qiao, D. Qiu, *Adv. Mater.* **2023**, *35*, 2209913.

- [167] C. Creton, O. Okay, in *Advances in Polymer Science*, Vol. 285 (Eds: C. Creton, O. Okay), Springer International Publishing, Berlin 2020.
- [168] D. L. Taylor, M. in het Panhuis, *Adv. Mater.* **2016**, *28*, 9060.
- [169] P. Wang, G. Deng, L. Zhou, Z. Li, Y. Chen, *ACS Macro Lett.* **2017**, *6*, 881.
- [170] Z. Guo, H. Gu, Y. He, Y. Zhang, W. Xu, J. Zhang, Y. Liu, L. Xiong, A. Chen, Y. Feng, *Chem. Eng. J.* **2020**, *388*, 124282.
- [171] Z. Jiang, B. Diggle, I. C. G. Shackelford, L. A. Connal, *Adv. Mater.* **2019**, *31*, 1904956.
- [172] L. Xu, Y. Chen, M. Yu, M. Hou, G. Gong, H. Tan, N. Li, J. Xu, *Nano Energy* **2023**, *107*, 108119.
- [173] E. Su, M. Yurtsever, O. Okay, *Macromolecules* **2019**, *52*, 3257.
- [174] H. Fan, J. Wang, Z. Jin, *Macromolecules* **2018**, *51*, 1696.
- [175] C. Shao, H. Chang, M. Wang, F. Xu, J. Yang, *ACS Appl. Mater. Interfaces* **2017**, *9*, 28305.
- [176] S. Li, H. Pan, Y. Wang, J. Sun, *J. Mater. Chem. A* **2020**, *8*, 3667.
- [177] U. Gulyuz, O. Okay, *Macromolecules* **2014**, *47*, 6889.
- [178] M. M. Perera, N. Ayres, *Polym. Chem.* **2020**, *11*, 1410.
- [179] J. Ye, S. Fu, S. Zhou, M. Li, K. Li, W. Sun, Y. Zhai, *Eur. Polym. J.* **2020**, *139*, 110024.
- [180] T. Long, Y. Li, X. Fang, J. Sun, *Adv. Funct. Mater.* **2018**, *28*, 1804416.
- [181] J. R. Capadona, K. Shanmuganathan, D. J. Tyler, S. J. Rowan, C. Weder, *Science* **2008**, *319*, 1370.
- [182] X. Lin, X. Wang, L. Zeng, Z. L. Wu, H. Guo, D. Hourdet, *Chem. Mater.* **2021**, *33*, 7633.
- [183] T. Nonoyama, Y. W. Lee, K. Ota, K. Fujioka, W. Hong, J. P. Gong, *Adv. Mater.* **2020**, *32*, 1905878.
- [184] C. Sun, J. Luo, S. Yan, K. Li, Y. Li, H. Wang, C. Hou, Q. Zhang, *Adv. Funct. Mater.* **2023**, *33*, 2211035.
- [185] Y. Zhang, H. Gao, H. Wang, Z. Xu, X. Chen, B. Liu, Y. Shi, Y. Lu, L. Wen, Y. Li, Z. Li, Y. Men, X. Feng, W. Liu, *Adv. Funct. Mater.* **2018**, *28*, 1705962.
- [186] J.-F. Lutz, Ö. Akdemir, A. Hoth, *J. Am. Chem. Soc.* **2006**, *128*, 13046.
- [187] T. Takigawa, T. Yamawaki, K. Takahashi, T. Masuda, *Polym. Gels Networks* **1998**, *5*, 585.
- [188] T. R. Matzelle, G. Geuskens, N. Kruse, *Macromolecules* **2003**, *36*, 2926.
- [189] H. Guo, N. Sanson, D. Hourdet, A. Marcellan, *Adv. Mater.* **2016**, *28*, 5857.
- [190] H. Guo, N. Sanson, A. Marcellan, D. Hourdet, *Macromolecules* **2016**, *49*, 9568.
- [191] S. Ida, M. Morimura, H. Kitanaka, Y. Hirokawa, S. Kanaoka, *Polym. Chem.* **2019**, *10*, 6122.
- [192] Y.-N. Chen, L. Peng, T. Liu, Y. Wang, S. Shi, H. Wang, *ACS Appl. Mater. Interfaces* **2016**, *8*, 27199.
- [193] L. X. Hou, H. Ju, X. P. Hao, H. Zhang, L. Zhang, Z. He, J. Wang, Q. Zheng, Z. L. Wu, *Adv. Mater.* **2023**, *35*, 2300244.
- [194] R. Liang, H. Yu, L. Wang, L. Lin, N. Wang, K.-u.-R. Naveed, *ACS Appl. Mater. Interfaces* **2019**, *11*, 43563.
- [195] M. T. I. Mredha, S. K. Pathak, V. T. Tran, J. Cui, I. Jeon, *Chem. Eng. J.* **2019**, *362*, 325.
- [196] L. Li, J. M. Scheiger, P. A. Levkin, *Adv. Mater.* **2019**, *31*, 1807333.
- [197] J. M. Dennis, A. M. Savage, R. A. Mrozek, J. L. Lenhart, *Polym. Int.* **2021**, *70*, 720.
- [198] Z. Tao, H. Fan, J. Huang, T. Sun, T. Kurokawa, J. P. Gong, *ACS Appl. Mater. Interfaces* **2019**, *11*, 37139.
- [199] A. Liu, X. Gao, X. Xie, W. Ma, M. Xie, R. Sun, *Dyes Pigment.* **2020**, *177*, 108288.
- [200] S. Kawano, K. Nakano, H. Sato, M. Muraoka, M. Shizuma, *Polym. Chem.* **2022**, *13*, 5820.
- [201] A. M. Rosales, K. M. Mabry, E. M. Nehls, K. S. Anseth, *Biomacromolecules* **2015**, *16*, 798.
- [202] J. Sun, C. Ma, S. Maity, F. Wang, Y. Zhou, G. Portale, R. Göstl, W. H. Roos, H. Zhang, K. Liu, A. Herrmann, *Angew. Chem., Int. Ed.* **2021**, *60*, 3222.
- [203] J. Huang, L. Zhao, T. Wang, W. Sun, Z. Tong, *ACS Appl. Mater. Interfaces* **2016**, *8*, 12384.
- [204] B. Yan, J. Huang, L. Han, L. Gong, L. Li, J. N. Israelachvili, H. Zeng, *ACS Nano* **2017**, *11*, 11074.
- [205] J. K. Mouw, G. Ou, V. M. Weaver, *Nat. Rev. Mol. Cell Biol.* **2014**, *15*, 771.
- [206] P. H. J. Kouwer, M. Koepf, V. A. A. Le Sage, M. Jaspers, A. M. van Buul, Z. H. Eksteen-Akeroyd, T. Woltinge, E. Schwartz, H. J. Kitto, R. Hoogenboom, S. J. Picken, R. J. M. Nolte, E. Mendes, A. E. Rowan, *Nature* **2013**, *493*, 651.
- [207] M. Fernandez-Castano Romera, R. P. M. Lafleur, C. Guibert, I. K. Voets, C. Storm, R. P. Sijbesma, *Angew. Chem., Int. Ed.* **2017**, *56*, 8771.
- [208] L. Martikainen, K. Bertula, M. Turunen, O. Ikkala, *Macromolecules* **2020**, *53*, 9983.
- [209] J. Luo, S. Li, J. Xu, M. Chai, L. Gao, C. Yang, X. Shi, *Adv. Funct. Mater.* **2021**, *31*, 2104139.
- [210] J. Wang, B. Wu, P. Wei, S. Sun, P. Wu, *Nat. Commun.* **2022**, *13*, 4411.
- [211] C. Lian, Z. Lin, T. Wang, W. Sun, X. Liu, Z. Tong, *Macromolecules* **2012**, *45*, 7220.
- [212] X. Yu, Y. Wang, H. Zhang, Z. Li, Y. Zheng, X. Fan, Y. Lv, X. Zhang, T. Liu, *Chem. Mater.* **2023**, *35*, 9287.
- [213] J. Cui, R. Xu, W. Dong, T. Kaneko, M. Chen, D. Shi, *ACS Appl. Mater. Interfaces* **2023**, *15*, 48736.
- [214] Y. Li, J. Wang, Y. Wang, W. Cui, *Composites, Part B* **2021**, *223*, 109101.
- [215] J. Li, C. Wu, P. K. Chu, M. Gelinsky, *Mater. Sci. Eng., R* **2020**, *140*, 100543.
- [216] C. Y. Li, X. P. Hao, Z. L. Wu, Q. Zheng, *Chem. Asian J.* **2019**, *14*, 94.
- [217] A. C. Daly, L. Riley, T. Segura, J. A. Burdick, *Nat. Rev. Mater.* **2020**, *5*, 20.
- [218] A. Schwab, R. Levato, M. D'Este, S. Piluso, D. Eglin, J. Malda, *Chem. Rev.* **2020**, *120*, 11028.
- [219] X. N. Zhang, Q. Zheng, Z. L. Wu, *Composites, Part B* **2022**, *238*, 109895.
- [220] G. Ge, Q. Wang, Y.-Z. Zhang, H. N. Alshareef, X. Dong, *Adv. Funct. Mater.* **2021**, *31*, 2107437.
- [221] P. Heidarian, A. Z. Kouzani, A. Kaynak, M. Paulino, B. Nasri-Nasrabadi, *ACS Biomater. Sci. Eng.* **2019**, *5*, 2688.
- [222] R. J. Mondschein, A. Kanitkar, C. B. Williams, S. S. Verbridge, T. E. Long, *Biomaterials* **2017**, *140*, 170.
- [223] Y. Cheng, K. H. Chan, X. Q. Wang, T. Ding, T. Li, X. Lu, G. W. Ho, *ACS Nano* **2019**, *13*, 13176.
- [224] M. Hirsch, A. Charlet, E. Amstad, *Adv. Funct. Mater.* **2021**, *31*, 2005929.
- [225] C. Wang, P. Zhang, W. Xiao, J. Zhao, M. Shi, H. Wei, Z. Deng, B. Guo, Z. Zheng, Y. Yu, *Nat. Commun.* **2020**, *11*, 4694.
- [226] P. Jiang, P. Lin, C. Yang, H. Qin, X. Wang, F. Zhou, *Chem. Mater.* **2020**, *32*, 9983.
- [227] H. C. Yu, C. Y. Li, M. Du, Y. Song, Z. L. Wu, Q. Zheng, *Macromolecules* **2019**, *52*, 629.
- [228] Y. Cheng, K. H. Chan, X.-Q. Wang, T. Ding, T. Li, X. Lu, G. W. Ho, *ACS Nano* **2019**, *13*, 13176.
- [229] Z. Xu, C. Fan, Q. Zhang, Y. Liu, C. Cui, B. Liu, T. Wu, X. Zhang, W. Liu, *Adv. Funct. Mater.* **2021**, *31*, 2100462.
- [230] Q. Zhang, Z. Xu, X. Zhang, C. Liu, R. Yang, Y. Sun, Y. Zhang, W. Liu, *Adv. Funct. Mater.* **2022**, *32*, 2200360.
- [231] F. Zhu, L. Cheng, J. Yin, Z. L. Wu, J. Qian, J. Fu, Q. Zheng, *ACS Appl. Mater. Interfaces* **2016**, *8*, 31304.
- [232] F. Zhu, X. Y. Lin, Z. L. Wu, L. Cheng, J. Yin, Y. Song, J. Qian, Q. Zheng, *Polymer* **2016**, *95*, 9.

- [233] H. Yang, M. Ji, M. Yang, M. Shi, Y. Pan, Y. Zhou, H. J. Qi, Z. Suo, J. Tang, *Matter* **2021**, *4*, 1935.
- [234] D. R. King, T. Okumura, R. Takahashi, T. Kurokawa, J. P. Gong, *ACS Appl. Mater. Interfaces* **2019**, *11*, 35343.
- [235] Q. Ge, Z. Chen, J. Cheng, B. Zhang, Y.-F. Zhang, H. Li, X. He, C. Yuan, J. Liu, S. Magdassi, S. Qu, *Sci. Adv.* **2021**, *7*, 4261.
- [236] C. Chen, J. Feng, J. Li, Y. Guo, X. Shi, H. Peng, *Chem. Rev.* **2023**, *123*, 613.
- [237] W. Weng, J. Yang, Y. Zhang, Y. Li, S. Yang, L. Zhu, M. Zhu, *Adv. Mater.* **2020**, *32*, 1902301.
- [238] X. Zhao, F. Chen, Y. Li, H. Lu, N. Zhang, M. Ma, *Nat. Commun.* **2018**, *9*, 3579.
- [239] M. Ju, B. Wu, S. Sun, P. Wu, *Adv. Funct. Mater.* **2020**, *30*, 1910387.
- [240] P. Wei, K. Hou, T. Chen, G. Chen, I. T. Mugaanire, M. Zhu, *Mater. Horiz.* **2020**, *7*, 811.
- [241] L. Gu, Y. Jiang, J. Hu, *Adv. Mater.* **2019**, *31*, 1904311.
- [242] Y. Wu, D. U. Shah, B. Wang, J. Liu, X. Ren, M. H. Ramage, O. A. Scherman, *Adv. Mater.* **2018**, *30*, 1707169.
- [243] C. K. Chu, A. J. Joseph, M. D. Limjoco, J. Yang, S. Bose, L. S. Thapa, R. Langer, D. G. Anderson, *J. Am. Chem. Soc.* **2020**, *142*, 19715.
- [244] T. Chen, X. Qiao, P. Wei, G. Chen, I. T. Mugaanire, K. Hou, M. Zhu, *Chem. Mater.* **2020**, *32*, 9675.
- [245] S. Zhang, Y. Zhou, A. Libanori, Y. Deng, M. Liu, M. Zhou, H. Qu, X. Zhao, P. Zheng, Y.-L. Zhu, J. Chen, S. C. Tan, *Nat. Electron.* **2023**, *6*, 338.
- [246] C. Lang, E. C. Lloyd, K. E. Matuszewski, Y. Xu, V. Ganesan, R. Huang, M. Kumar, R. J. Hickey, *Nat. Nanotechnol.* **2022**, *17*, 752.
- [247] J. Song, S. Chen, L. Sun, Y. Guo, L. Zhang, S. Wang, H. Xuan, Q. Guan, Z. You, *Adv. Mater.* **2020**, *32*, 1906994.
- [248] L. Shuai, Z. H. Guo, P. Zhang, J. Wan, X. Pu, Z. L. Wang, *Nano Energy* **2020**, *78*, 105389.
- [249] Y. Yuan, Q. Yu, J. Wen, C. Li, Z. Guo, X. Wang, N. Wang, *Angew. Chem., Int. Ed.* **2019**, *58*, 11785.
- [250] M. Zhang, S. Chen, N. Sheng, B. Wang, Z. Wu, Q. Liang, Z. Han, H. Wang, *J. Mater. Chem. A* **2021**, *9*, 12574.
- [251] M. Li, X. Chen, X. Li, J. Dong, X. Zhao, Q. Zhang, *ACS Appl. Mater. Interfaces* **2021**, *13*, 43323.
- [252] G. Chen, G. Wang, X. Tan, K. Hou, Q. Meng, P. Zhao, S. Wang, J. Zhang, Z. Zhou, T. Chen, Y. Cheng, B. S. Hsiao, E. Reichmanis, M. Zhu, *Natl. Sci. Rev.* **2020**, *8*, 209.
- [253] X.-Y. Du, Q. Li, G. Wu, S. Chen, *Adv. Mater.* **2019**, *31*, 1903733.
- [254] R. Costa-Almeida, L. Gasperini, J. Borges, P. S. Babo, M. T. Rodrigues, J. F. Mano, R. L. Reis, M. E. Gomes, *ACS Biomater. Sci. Eng.* **2017**, *3*, 1322.
- [255] X. Duan, J. Yu, Y. Zhu, Z. Zheng, Q. Liao, Y. Xiao, Y. Li, Z. He, Y. Zhao, H. Wang, L. Qu, *ACS Nano* **2020**, *14*, 14929.
- [256] J. Ni, S. Lin, Z. Qin, D. Veysset, X. Liu, Y. Sun, A. J. Hsieh, R. Radovitzky, K. A. Nelson, X. Zhao, *Matter* **2021**, *4*, 1919.
- [257] Q. Zhou, J. Lyu, G. Wang, M. Robertson, Z. Qiang, B. Sun, C. Ye, M. Zhu, *Adv. Funct. Mater.* **2021**, *31*, 2104536.
- [258] C. Chen, J. Tang, Y. Gu, L. Liu, X. Liu, L. Deng, C. Martins, B. Sarmiento, W. Cui, L. Chen, *Adv. Funct. Mater.* **2019**, *29*, 1806899.
- [259] Y. Yang, C. Wang, C. G. Wiener, J. Hao, S. Shatas, R. A. Weiss, B. D. Vogt, *ACS Appl. Mater. Interfaces* **2016**, *8*, 22774.
- [260] Q. Mu, Q. Zhang, W. Yu, M. Su, Z. Cai, K. Cui, Y. Ye, X. Liu, L. Deng, B. Chen, N. Yang, L. Chen, L. Tao, Y. Wei, *ACS Appl. Mater. Interfaces* **2020**, *12*, 33152.
- [261] N. Yang, H. Yang, Z. Shao, M. Guo, *Macromol. Rapid Commun.* **2017**, *38*, 1700275.
- [262] J. Liu, S. Qu, Z. Suo, W. Yang, *Natl. Sci. Rev.* **2020**, *8*, 254.
- [263] H. Yuk, T. Zhang, S. Lin, G. A. Parada, X. Zhao, *Nat. Mater.* **2016**, *15*, 190.
- [264] J. Li, A. D. Celiz, J. Yang, Q. Yang, I. Wamala, W. Whyte, B. R. Seo, N. V. Vasilev, J. J. Vlassak, Z. Suo, D. J. Mooney, *Science* **2017**, *357*, 378.
- [265] Q. Liu, G. Nian, C. Yang, S. Qu, Z. Suo, *Nat. Commun.* **2018**, *9*, 846.
- [266] X. Yao, J. Liu, C. Yang, X. Yang, J. Wei, Y. Xia, X. Gong, Z. Suo, *Adv. Mater.* **2019**, *31*, 1903062.
- [267] H. Yuk, C. E. Varela, C. S. Nabzdyk, X. Mao, R. F. Padera, E. T. Roche, X. Zhao, *Nature* **2019**, *575*, 169.
- [268] Y. Yu, H. Yuk, G. A. Parada, Y. Wu, X. Liu, C. S. Nabzdyk, K. Youcef-Toumi, J. Zang, X. Zhao, *Adv. Mater.* **2019**, *31*, 1807101.
- [269] M.-H. Bai, B. Zhao, Z.-Y.-T. Liu, Z.-L. Zheng, X. Wei, L. Li, K. Li, X. Song, J.-Z. Xu, Z.-M. Li, *Adv. Mater.* **2022**, *34*, 2108848.
- [270] J. Yang, R. Bai, Z. Suo, *Adv. Mater.* **2018**, *30*, 1800671.
- [271] F. Zhang, C. Hu, L. Yang, K. Liu, Y. Ge, Y. Wei, J. Wang, R. Luo, Y. Wang, *J. Mater. Chem. B* **2021**, *9*, 2697.
- [272] D. Wirthl, R. Pichler, M. Drack, G. Kettlhuber, R. Moser, R. Gerstmayr, F. Hartmann, E. Bradt, R. Kaltseis, C. M. Siket, S. E. Schausberger, S. Hild, S. Bauer, M. Kaltenbrunner, *Sci. Adv.* **2017**, *3*, 1700053.
- [273] R. Xu, Y. Zhang, S. Ma, Z. Ma, B. Yu, M. Cai, F. Zhou, *Adv. Mater.* **2022**, *34*, 2108889.
- [274] Z. Yang, Y. He, Y. Ma, L. Li, Y. Wang, *Adv. Funct. Mater.* **2023**, *33*, 2213150.
- [275] Z. Yang, Y. He, S. Liao, Y. Ma, X. Tao, Y. Wang, *Sci. Adv.* **2021**, *7*, 9117.
- [276] X. Yang, C. Yang, J. Liu, X. Yao, Z. Suo, *Sci. China: Technol. Sci.* **2020**, *63*, 1314.
- [277] S. Fuchs, K. Shariati, M. Ma, *Adv. Healthcare Mater.* **2020**, *9*, 1901396.
- [278] Y. Liu, W. He, Z. Zhang, B. P. Lee, *Gels* **2018**, *4*, 46.
- [279] Y. Tanabe, K. Yasuda, C. Azuma, H. Taniguro, S. Onodera, A. Suzuki, Y. M. Chen, J. P. Gong, Y. Osada, *J. Mater. Sci.: Mater. Med.* **2008**, *19*, 1379.
- [280] K. Arakaki, N. Kitamura, H. Fujiki, T. Kurokawa, M. Iwamoto, M. Ueno, F. Kanaya, Y. Osada, J. P. Gong, K. Yasuda, *J. Biomed. Mater. Res., Part A* **2010**, *93A*, 1160.
- [281] K. Yasuda, N. Kitamura, J. P. Gong, K. Arakaki, H. J. Kwon, S. Onodera, Y. M. Chen, T. Kurokawa, F. Kanaya, Y. Ohmiya, Y. Osada, *Macromol. Biosci.* **2009**, *9*, 307.
- [282] D. Chimene, R. Kaunas, A. K. Gaharwar, *Adv. Mater.* **2020**, *32*, 1902026.
- [283] M. Costantini, S. Testa, P. Mozetic, A. Barbetta, C. Fuoco, E. Fornetti, F. Tamiro, S. Bernardini, J. Jaroszewicz, W. Świąszkowski, M. Trombetta, L. Castagnoli, D. Seliktar, P. Garstecki, G. Cesareni, S. Cannata, A. Rainer, C. Gargioli, *Biomaterials* **2017**, *131*, 98.
- [284] H. Wei, B. Zhang, M. Lei, Z. Lu, J. Liu, B. Guo, Y. Yu, *ACS Nano* **2022**, *16*, 4734.
- [285] K. W. M. Boere, J. Visser, H. Seyednejad, S. Rahimian, D. Gawlitta, M. J. van Steenbergen, W. J. A. Dhert, W. E. Hennink, T. Vermonden, J. Malda, *Acta Biomater.* **2014**, *10*, 2602.
- [286] F. Gao, Z. Xu, Q. Liang, H. Li, L. Peng, M. Wu, X. Zhao, X. Cui, C. Ruan, W. Liu, *Adv. Sci.* **2019**, *6*, 1900867.
- [287] C. Antich, J. de Vicente, G. Jiménez, C. Chocarro, E. Carrillo, E. Montañez, P. Gálvez-Martín, J. A. Marchal, *Acta Biomater.* **2020**, *106*, 114.
- [288] Q. Li, S. Xu, Q. Feng, Q. Dai, L. Yao, Y. Zhang, H. Gao, H. Dong, D. Chen, X. Cao, *Bioact. Mater.* **2021**, *6*, 3396.
- [289] Y. B. Kim, H. Lee, G. H. Kim, *ACS Appl. Mater. Interfaces* **2016**, *8*, 32230.
- [290] F. Gao, Z. Xu, Q. Liang, B. Liu, H. Li, Y. Wu, Y. Zhang, Z. Lin, M. Wu, C. Ruan, W. Liu, *Adv. Funct. Mater.* **2018**, *28*, 1706644.
- [291] Z. Luo, G. Tang, H. Ravanbakhsh, W. Li, M. Wang, X. Kuang, C. E. Garciamendez-Mijares, L. Lian, S. Yi, J. Liao, M. Xie, J. Guo, Z. Zhou, Y. S. Zhang, *Adv. Mater.* **2022**, *34*, 2108931.

- [292] D. Gan, W. Xing, L. Jiang, J. Fang, C. Zhao, F. Ren, L. Fang, K. Wang, X. Lu, *Nat. Commun.* **2019**, *10*, 1487.
- [293] K. Zhang, X. Chen, Y. Xue, J. Lin, X. Liang, J. Zhang, J. Zhang, G. Chen, C. Cai, J. Liu, *Adv. Funct. Mater.* **2022**, *32*, 2111465.
- [294] Z. Yang, R. Huang, B. Zheng, W. Guo, C. Li, W. He, Y. Wei, Y. Du, H. Wang, D. Wu, H. Wang, *Adv. Sci.* **2021**, *8*, 2003627.
- [295] S. Shabahang, S. Kim, S.-H. Yun, *Adv. Funct. Mater.* **2018**, *28*, 1706635.
- [296] J. Guo, X. Liu, N. Jiang, A. K. Yetisen, H. Yuk, C. Yang, A. Khademhosseini, X. Zhao, S.-H. Yun, *Adv. Mater.* **2016**, *28*, 10244.
- [297] R. Vo, H.-H. Hsu, X. Jiang, *Biomater. Sci.* **2021**, *9*, 23.
- [298] C. Wang, T. Yokota, T. Someya, *Chem. Rev.* **2021**, *121*, 2109.
- [299] D. Gao, K. Parida, P. S. Lee, *Adv. Funct. Mater.* **2020**, *30*, 1907184.
- [300] Y. Lu, G. Yang, S. Wang, Y. Zhang, Y. Jian, L. He, T. Yu, H. Luo, D. Kong, Y. Xianyu, B. Liang, T. Liu, X. Ouyang, J. Yu, X. Hu, H. Yang, Z. Gu, W. Huang, K. Xu, *Nat. Electron.* **2024**, *7*, 51.
- [301] Y. Wang, H. Haick, S. Guo, C. Wang, S. Lee, T. Yokota, T. Someya, *Chem. Soc. Rev.* **2022**, *51*, 3759.
- [302] D. Gan, Z. Huang, X. Wang, L. Jiang, C. Wang, M. Zhu, F. Ren, L. Fang, K. Wang, C. Xie, X. Lu, *Adv. Funct. Mater.* **2020**, *30*, 1907678.
- [303] S. J. K. O'Neill, Z. Huang, M. H. Ahmed, A. J. Boys, S. Velasco-Bosom, J. Li, R. M. Owens, J. A. McCune, G. G. Malliaras, O. A. Scherman, *Adv. Mater.* **2023**, *35*, 2207634.
- [304] X. P. Hao, C. Y. Li, C. W. Zhang, M. Du, Z. Ying, Q. Zheng, Z. L. Wu, *Adv. Funct. Mater.* **2021**, *31*, 2105481.
- [305] H. C. Yu, X. P. Hao, C. W. Zhang, S. Y. Zheng, M. Du, S. Liang, Z. L. Wu, Q. Zheng, *Small* **2021**, *17*, 2103836.
- [306] R. Zhao, S. Lin, H. Yuk, X. Zhao, *Soft Matter* **2018**, *14*, 2515.
- [307] C. Lim, Y. J. Hong, J. Jung, Y. Shin, S.-H. Sunwoo, S. Baik, O. K. Park, S. H. Choi, T. Hyeon, J. H. Kim, S. Lee, D.-H. Kim, *Sci. Adv.* **2021**, *7*, 3716.
- [308] S. Cheng, Z. Lou, L. Zhang, H. Guo, Z. Wang, C. Guo, K. Fukuda, S. Ma, G. Wang, T. Someya, H.-M. Cheng, X. Xu, *Adv. Mater.* **2023**, *35*, 2206793.
- [309] Y. Zhao, Y. Ohm, J. Liao, Y. Luo, H.-Y. Cheng, P. Won, P. Roberts, M. R. Carneiro, M. F. Islam, J. H. Ahn, L. M. Walker, C. Majidi, *Nat. Electron.* **2023**, *6*, 206.
- [310] M. Qi, R. Yang, Z. Wang, Y. Liu, Q. Zhang, B. He, K. Li, Q. Yang, L. Wei, C. Pan, M. Chen, *Adv. Funct. Mater.* **2023**, *33*, 2214479.
- [311] W. Zhang, B. Wu, S. Sun, P. Wu, *Nat. Commun.* **2021**, *12*, 4082.
- [312] G. Gao, F. Yang, F. Zhou, J. He, W. Lu, P. Xiao, H. Yan, C. Pan, T. Chen, Z. L. Wang, *Adv. Mater.* **2020**, *32*, 2004290.
- [313] L. Han, X. Lu, M. Wang, D. Gan, W. Deng, K. Wang, L. Fang, K. Liu, C. W. Chan, Y. Tang, L.-T. Weng, H. Yuan, *Small* **2017**, *13*, 1601916.
- [314] J. Deng, H. Yuk, J. Wu, C. E. Varela, X. Chen, E. T. Roche, C. F. Guo, X. Zhao, *Nat. Mater.* **2021**, *20*, 229.
- [315] G. Li, K. Huang, J. Deng, M. Guo, M. Cai, Y. Zhang, C. F. Guo, *Adv. Mater.* **2022**, *34*, 2200261.
- [316] X. Xia, Q. Liang, X. Sun, D. Yu, X. Huang, S. M. Mugo, W. Chen, D. Wang, Q. Zhang, *Adv. Funct. Mater.* **2022**, *32*, 2208024.
- [317] N. Park, J. Kim, *Adv. Intell. Syst.* **2020**, *2*, 1900135.
- [318] Y. Ouyang, G. Huang, J. Cui, H. Zhu, G. Yan, Y. Mei, *Chem. Mater.* **2022**, *34*, 9307.
- [319] D. Jiao, Q. L. Zhu, C. Y. Li, Q. Zheng, Z. L. Wu, *Acc. Chem. Res.* **2022**, *55*, 1533.
- [320] S. Timoshenko, *J. Opt. Soc. Am.* **1925**, *11*, 233.
- [321] H. Yang, C. Li, M. Yang, Y. Pan, Q. Yin, J. Tang, H. J. Qi, Z. Suo, *Adv. Funct. Mater.* **2019**, *29*, 1901721.
- [322] T.-Y. Huang, H.-W. Huang, D. D. Jin, Q. Y. Chen, J. Y. Huang, L. Zhang, H. L. Duan, *Sci. Adv.* **2020**, *6*, 8219.
- [323] R. M. Erb, J. S. Sander, R. Grisch, A. R. Studart, *Nat. Commun.* **2013**, *4*, 1712.
- [324] H. Cui, N. Pan, W. Fan, C. Liu, Y. Li, Y. Xia, K. Sui, *Adv. Funct. Mater.* **2019**, *29*, 1807692.
- [325] H. Hu, C. Huang, M. Galluzzi, Q. Ye, R. Xiao, X. Yu, X. Du, *Research* **2021**, *2021*, 9786128.
- [326] J. Kim, J. A. Hanna, M. Byun, C. D. Santangelo, R. C. Hayward, *Science* **2012**, *335*, 1201.
- [327] Z. J. Wang, W. Hong, Z. L. Wu, Q. Zheng, *Angew. Chem., Int. Ed.* **2017**, *56*, 15974.
- [328] Y. S. Kim, M. Liu, Y. Ishida, Y. Ebina, M. Osada, T. Sasaki, T. Hikima, M. Takata, T. Aida, *Nat. Mater.* **2015**, *14*, 1002.
- [329] Q. L. Zhu, C. Du, Y. Dai, M. Daab, M. Matejdes, J. Brey, W. Hong, Q. Zheng, Z. L. Wu, *Nat. Commun.* **2020**, *11*, 5166.
- [330] Z. Jiang, P. Song, *Science* **2022**, *376*, 245.
- [331] H. Yuk, S. Lin, C. Ma, M. Takaffoli, N. X. Fang, X. Zhao, *Nat. Commun.* **2017**, *8*, 14230.
- [332] S. Y. Zheng, Y. Shen, F. Zhu, J. Yin, J. Qian, J. Fu, Z. L. Wu, Q. Zheng, *Adv. Funct. Mater.* **2018**, *28*, 1803366.
- [333] Y. Ma, M. Hua, S. Wu, Y. Du, X. Pei, X. Zhu, F. Zhou, X. He, *Sci. Adv.* **2020**, *6*, 2520.
- [334] M. Hua, D. Wu, S. Wu, Y. Ma, Y. Alsaied, X. He, *ACS Appl. Mater. Interfaces* **2021**, *13*, 12689.
- [335] W. Li, Q. Guan, M. Li, E. Saiz, X. Hou, *Prog. Polym. Sci.* **2023**, *140*, 101665.
- [336] W. Wang, L. Yao, C.-Y. Cheng, T. Zhang, H. Atsumi, L. Wang, G. Wang, O. Anilionyte, H. Steiner, J. Ou, K. Zhou, C. Wawrousek, K. Petrecca, A. M. Belcher, R. Karnik, X. Zhao, D. I. C. Wang, H. Ishii, *Sci. Adv.* **2017**, *3*, 1601984.
- [337] L. K. Rivera-Tarazona, T. Shukla, K. A. Singh, A. K. Gaharwar, Z. T. Campbell, T. H. Ware, *Adv. Funct. Mater.* **2022**, *32*, 2106843.
- [338] J. Wu, Z. Zhang, Z. Wu, D. Liu, X. Yang, Y. Wang, X. Jia, X. Xu, P. Jiang, X. Wang, *Adv. Funct. Mater.* **2023**, *33*, 2210395.
- [339] M. Baumgartner, F. Hartmann, M. Drack, D. Preninger, D. Wirthl, R. Gerstmayr, L. Lehner, G. Mao, R. Pruckner, S. Demchysyn, L. Reiter, M. Strobel, T. Stockinger, D. Schiller, S. Kimeswenger, F. Greibich, G. Buchberger, E. Bradt, S. Hild, S. Bauer, M. Kaltenbrunner, *Nat. Mater.* **2020**, *19*, 1102.



Xiao-Qiao Wang received her Ph.D. degree in material chemical engineering at Nanjing Tech University, China, in 2016. From 2016 to 2022, she worked as a postdoctoral research fellow at the National University of Singapore (NUS). She is currently a professor of the Department of College of Textile and Clothing Engineering at the Soochow University. Her research interest focuses on soft/flexible materials and their engineering for smart wearables and robots.



Ke-Qin Zhang has been a professor in National Engineering Laboratory for Modern Silk and College of Textile and Clothing Engineering of Soochow University since 2009. He received his Ph.D. degree from Nanjing University in 2000. His research interests include fabrication, modification, and functionalization of fibers in different scales, as well as the applications of fiber materials in wearable devices.



Ghim Wei Ho received her Ph.D. degree in semiconductor nanostructures at the Nanoscience Centre, University of Cambridge in 2006. She is a professor of the Department of Electrical and Computer Engineering at the National University of Singapore (NUS). She leads the Sustainable Smart Solar System research group working on fundamental and applied research on nanosystems with emerging low-dimensional nanomaterials, interfacial interactions, and hybridized functionalities for energy, environment, electronics, and healthcare.